OPEN ACCESS

ORIGINAL ARTICLE

miR-574-5p negatively regulates *Qki6/7* to impact *β-catenin*/Wnt signalling and the development of colorectal cancer

Shunlong Ji,[1] Gengtai Ye,[2] Jun Zhang,[1] Linpei Wang,[2] Tao Wang,[1] Zhen Wang,[1] Tiantian Zhang,[1] Guanghui Wang,[1] Zongsheng Guo,[1] Yu Luo,[3] Jianchun Cai,[2] James Y Yang[1,4]

► Additional materials are published online only. To view these files please visit the journal online (http://dx.doi.org/10.1136/gutjnl-2011-301083).

[1]State Key Laboratory of Cellular Stress Biology and Department of Biomedical Sciences, School of Life Sciences, Xiamen University, Xiamen, People's Republic of China
[2]Department of Surgical Oncology the First Affiliated Hospital of Xiamen University and Xiamen Cancer Center, Xiamen, People's Republic of China
[3]School of Nursing, the Third Military Medical University, Chongqing, People's Republic of China
[4]Fujian Provincial Transgenic Core, Xiamen University Laboratory Animal Center, Xiamen, People's Republic of China

Correspondence to
Dr James Y Yang, Department of Biomedical Sciences, School of Life Sciences, Xiamen University, Xiamen, China 361005; jyqy2008@gmail.com
or
Dr Jianchun Cai, Department of Surgical Oncology, the First Affiliated Hospital of Xiamen University and Xiamen Cancer Center, Xiamen, China 361003; jianchunfh2@sina.com

SJ, GY and JZ contributed equally to the work.

Revised 16 January 2012
Accepted 2 February 2012
Published Online First 5 April 2012

Open Access Scan to access more free content

ABSTRACT

Objective Deficiency or reduced expression of signal transduction and activation of RNA family protein *Quaking* (*Qki*) is associated with developmental defects in neural and vascular tissues and the development of debilitating human diseases including colorectal cancer (CRC). However, the mechanisms underlying the aberrant downregulation or deficiency of *Qki* were uncertain.

Design Expression of miR-574-5p, *Qki5/6/7/7b* splicing variants, *β-catenin* and $p27^{Kip1}$ was determined in mouse and human CRC cells and tissues to investigate the post-transcriptional regulation of *Qki* isoforms by miR-574-5p and its impact on *β-catenin*/$p27^{Kip1}$ signalling, cell cycle progression, proliferation, migration, invasion and tumour growth.

Results In the CRC tissues of C57BL/6-$Apc^{min/+}$ mice, miR-574-5p was found to be significantly upregulated and negatively correlated with the expression of *Qki* but positively correlated with the expression of *β-catenin*. In mouse and human CRC cells, miR-574-5p was shown to regulate *Qki* isoforms (*Qki6/7* in particular) post-transcriptionally and caused altered expression in *β-catenin* and $p27^{Kip1}$, increased proliferation, migration and invasion and decreased differentiation and cell cycle exit. Furthermore, in clinical CRC tissues, miR-574-5p was shown to be greatly upregulated and inversely correlated with the expression of *Qki*s. Finally, inhibition of miR-574-5p was shown to suppress the growth of tumours in the nude mice.

Conclusions Together, these novel findings suggest that miR-574-5p is a potent ribo-regulator for *Qkis* and that aberrant miR-574-5p upregulation can be oncogenic.

Significance of this study

What is already known on this subject?

- Downregulation of QKI5 and QKI6 was shown to be associated with the development of colorectal cancer (CRC).
- QKI5/6 might contribute to the development of CRC by controlling *β-catenin* and $p27^{Kip1}$ signalling.
- DNA methylation in the promoter region of *Qki* was suggested to contribute in part to *Qki's* aberrant down regulation in CRC.

What are the new findings?

- miR-574-5p regulates *Qki6/7* negatively and post-transcriptionally.
- QKI7 is the most predominant isoform in human CRC cells. QKI5/6/7 proteins all regulate *β-catenin* post-transcriptionally.
- miR-574-5p expression correlates inversely with that of *Qki*s in CRC cells and tissues.
- Aberrant upregulation of miR-574-5p can be oncogenic and its inhibition is beneficial.

How might it impact on clinical practice in the foreseeable future?

- The discovery of this miR-574-5p-QKI-*β-catenin*/$p27^{Kip1}$ axis of signal transduction will enable better understanding of the pathogenic mechanisms in human diseases associated with the abnormal expression of miR-574-5p, QKI and QKI-regulated genes.
- miR-574-5p and *Qki*s might serve as diagnostic or therapeutic targets for CRC.

INTRODUCTION

Quaking (QKI) is a RNA binding protein belonging to the signal transduction and activation of RNA (STAR) protein family that has been implicated in the regulation of cellular processes such as cell cycle and differentiation,[1] apoptosis,[2] cell fate decision and development[3–5] and angiogenesis.[6 7] Aberrant expression of the STAR proteins has been associated with a number of developmental defects and human diseases.[8 9] Studies have shown that Src associated in mitosis, of 68 kDa (Sam68), a prototype of the STAR proteins, is a multifunctional player in human cancers.[10–14] Genetic deletion in the *Qki* locus, on the other hand, was found to be associated with human glioblastoma or astrocytic glioma[15–17] mental retardation and autism.[18] Haploinsufficiency of *Qki* has also been linked with the 6q terminal deletion syndrome.[19] Furthermore, reduced *Qki* expression has been implicated in the pathogenesis of human disorders such as schizophrenia[20 21] and major depressive disorders.[22] Yang *et al* found that QKI5 and QKI6 were greatly reduced or even absent in colorectal cancer (CRC) cells and tissues and that downregulation of QKI5/6 was associated with abnormal regulation of

β-catenin and *p27^{Kip1}* signalling.[23] More recently, QKI expression was found to be significantly reduced in several types of tumours, including testis, lung, breast, bladder, cervix, ovary and colon cancer, which was shown to be associated with an abnormal decrease in the histone variant macroH2A1.1.[24]

Despite the potentially dire biological consequences of dysregulation in the expression of *Qki*, the exact genetic and epigenetic mechanisms governing *Qki* expression are poorly understood.[8 25] Klempan *et al* studied the effects of genetic and epigenetic variation on the promoter function and expression of *Qki* in the human brains of the suicide victims with major depressive disorders.[22] While significant reductions in *Qki* expression were found in the cortical regions, the hippocampus and the amygdala of suicide victims, analysis of variations in and methylation state of the promoter sequence did not identify differences at genetic and epigenetic levels between depressed suicide victims and controls. In a later study with 288 individuals diagnosed with schizophrenia and 288 controls, no association was found between seven genetic markers (including single-nucleotide polymorphism and haplotype) around the promoter region of the *Qki* gene and schizophrenia.[26] In the study conducted by Yang *et al*,[23] while characterisations of the *Qki* promoter region in a few CRC cell lines suggested enhanced promoter DNA methylation, increased methylation was found in only 4 out of 10 CRC tissue samples tested. Moreover, methylation was often detected in both CRC tissues and the neighbouring normal tissues from the same patient. Furthermore, DNA methylation is unlikely to be the major mechanism responsible for the downregulation of *Qki* as it cannot adequately explain the temporal, spatial and isoform-specific regulation of *Qki* in many cases of cell development and diseases. Collectively these observations suggest that genetic variations and epigenetic modifications in the *Qki* promoter region might not be the major determinants responsible for reduced *Qki* expression that is associated with human diseases such as schizophrenia, depression and cancers.

MicroRNAs (miRNAs) are non-coding small RNAs that serve as important regulators of gene expression by targeting the 3′ untranslated region (UTR) of messenger RNA (mRNA) and inducing mRNA degradation and suppression of translation.[27 28] The 3′UTRs of *Qki* mRNAs are evolutionally conserved and thus may be important to *Qki*'s post-transcriptional regulation.[29–31] In this current study, we found that miR-574-5p negatively regulates *Qki6/7/7b* through interactions with miRNA recognition elements (MREs) on the corresponding 3′UTRs. In mouse and human CRC tissues, very significant upregulation of miR-574-5p is correlated with substantial reductions in *Qki6/7/7b*, which might contribute significantly to the aberrant regulation of *β-catenin* and *p27^{Kip1}* and to the pathogenesis or progression of CRC. These results unravel a novel and important mechanism for the regulation of *Qki*s and the development of CRC.

MATERIALS AND METHODS

For details of the following, please see the supplemental materials and methods section in online supplementary information: plasmid construction, cell culture, transient transfections, western blot, immunohistochemistry, immunofluorescence staining, in situ hybridisation analyses; cell cycle, proliferation, migration, colony formation and invasion assays; luciferase reporter assays, intestinal alkaline phosphatase (IAP) enzyme assays and real-time quantitative RT-PCR (qPCR) analyses of mRNAs and miRNAs.

Animal experiments

All experimental procedures involving animals were performed in accordance with animal protocols approved by the Institutional Animal Use and Care Committee of Xiamen University. C57BL/6-*Apc$^{min/+}$* mice and controls were generous gifts from Dr Boan Li, Xiamen University. Five-week-old male athymic BALB/c nude mice were obtained from the SLAC Laboratory Animals Co Ltd (Shanghai, China).

For xenograft tumour growth, 5×10^6 SW480 cells pre-infected with control lentiviruses or lentiviruses carrying shRNA for miR-574-5p were injected subcutaneously into the dorsal flanks of mice. Beginning from the 10th day after the injection, the size of the tumour was measured every 3 days by a Vernier calliper along two perpendicular axes. The volume of the tumour was calculated with the formula: volume (mm^3) = length (mm) × width $(mm)^2\times0.52$. Twenty-eight days after the injection, the mice were sacrificed and the tumours were dissected for further analyses.

For bioluminescence imaging of tumour growth in live animals, see supplemental materials and methods section in online supplementary information.

Clinical samples

All clinical samples were collected with the informed consent of the patients and study protocols that were in accordance with the ethical guidelines of the Declaration of Helsinki (1975) and were approved by the Institutional Medical Ethics Committee of Xiamen University. CRC pathological diagnosis was verified by at least two pathologists. Sixty human CRC specimens and paired adjacent epithelial tissues and serum samples from seven patients with CRC and seven normal controls were obtained from the First Affiliated Hospital of Xiamen University from 25 January 2010 to December 2011. Tumour and non-cancerous tissues were confirmed histologically by haematoxylin and eosin (H&E) staining.

Bioinformatics, data acquisition, image processing and statistical analyses

See supplemental materials and methods section in online supplementary information.

RESULTS

Negative correlation between miR-574-5p and *Qki* expression and positive correlation between miR-574-5p and *β-catenin* in the CRC tissues of C57BL/6-*Apc$^{min/+}$* mice

Our bioinformatics analyses suggested the presence of multiple MREs on the 3′UTR of mouse or human *Qki5/6/7/7b* mRNAs, including those for miR-574-5p, miR-17 and miR-20a (figure S1, online supplementary information). We therefore performed qPCR and western blotting to analyse the expression levels of *Qki* mRNAs and proteins and miRNAs in the CRC tissues from C57BL/6-*Apc$^{min/+}$* (*Apc*-mutant) mice and in colorectal tissues from normal control mice. Compared with the expression levels in the normal tissues, total *Qki* mRNA/protein (pan-*Qki*/pan-QKI) and *Qki5/6/7* mRNA/protein isoforms were all greatly downregulated while *β-catenin* was greatly upregulated in the CRC tissues of the *Apc*-mutant mice (figure 1A–C). Analyses of miRNA expression indicated that miR-574-5p, miR-717 and miR-20a were significantly upregulated in mouse CRC tissues but miR-200b, miR-466g and miR-17 were not (figure 1D). Among the three significantly upregulated miRNAs, miR-574-5p had the highest fold change (~3.7-fold, $p<0.001$). Interestingly, MREs for miR-574-5p were found on the 3′UTRs of mouse

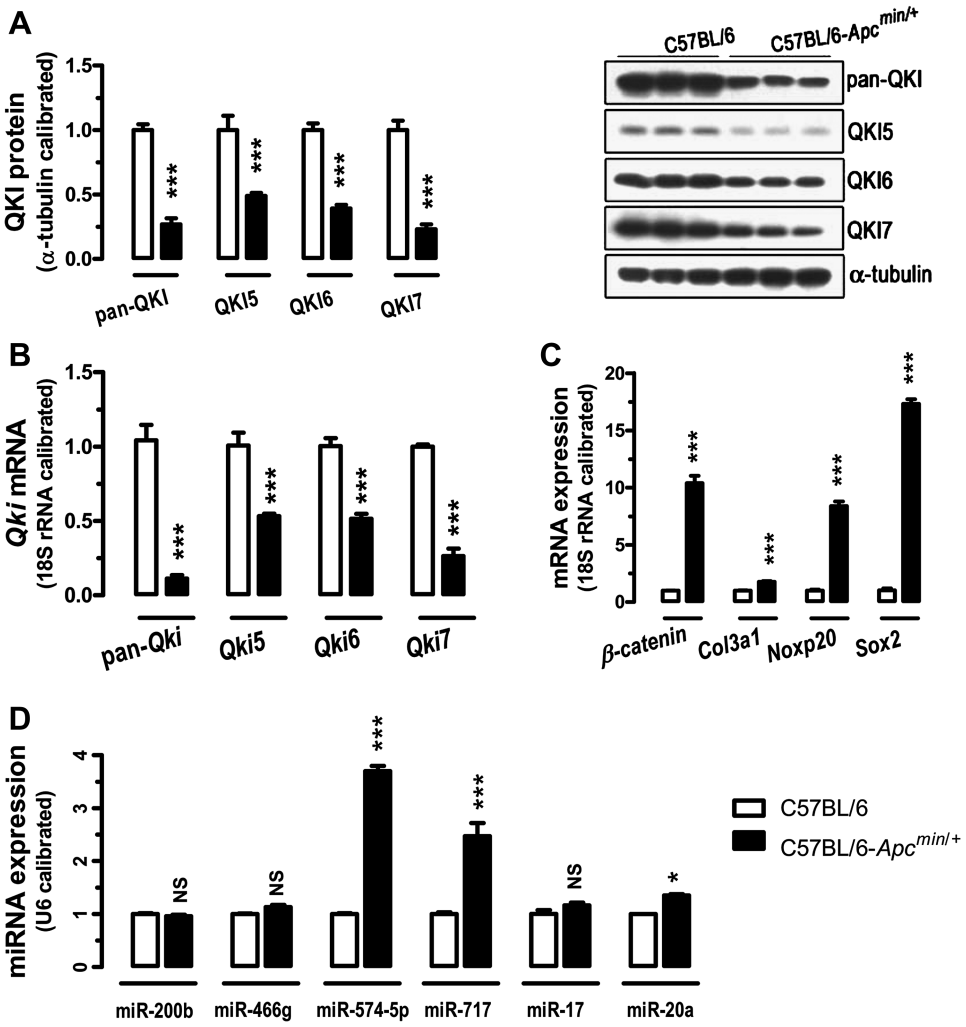

Figure 1 miR-574-5p expression correlates negatively with the expression of *Qki* but correlates positively with *β-catenin* in C57BL/6-*Apc*$^{min/+}$ mice (16-week old males, n=3). Data are represented as mean ± SEM. *p<0.05; ***p<0.001. (A) Total QKI and QKI5/6/7 protein expression levels were greatly downregulated in mouse colorectal cancer (CRC) tissues. (B) Total *Qki* and *Qki5/6/7* messenger RNA (mRNA) expression levels were significantly downregulated in mouse CRC tissues. (C) The expression levels of *β-catenin*, *Noxp20*, *Col3a1* and *Sox2* mRNAs were greatly increased in mouse CRC tissues. *Col3a1*, procollagen type III, α-1; *Noxp20*, nervous system overexpressed protein-20; *Sox2*, SRY-like HMG box-2. (D) The expression levels of miR-574-5p, miR-717 and miR-20a were significantly upregulated in mouse CRC tissues, whereas that of miR-200b, miR-466g and miR-17 were not. See also online figure S1. miRNA, microRNA; NS, not significant.

Qki6/7 but not on that of *Qki5* mRNA (online figure S1), suggesting that miR-574-5p might be involved in the negative regulation of *Qki6/7* in mouse colorectal tissues. Remarkably, the expression levels of two putative intronic miR-574-5p-hosting genes, nervous system overexpressed protein-20 (*Noxp20*,[32] and miRBase) and procollagen type III, α-1 (*Col3a1*)[33] and the level of a transcription factor SRY-like HMG box-2 (*Sox2*) were also significantly upregulated in mouse CRC tissues (figure 1C). This result suggests that miR-574-5p might be co-regulated with *Noxp20* or *Col3a1* in the mouse tissues.

miR-574-5p represses the expression of *Qki6/7/7b* through a post-transcriptional mechanism

To demonstrate the silencing effects of miR-574-5p on *Qki*s, we performed transient transfection studies in cultured CRC cells (figure 2). Our qPCR analyses indicated that, compared with the control group, transfection of CT26 cells with a plasmid over-expressing miR-574 precursor (pmiR-574) or with chemically synthesised mimics for miR-574-5p (see supplemental materials and methods section in online supplementary information) led to a 49–59% reduction in total *Qki* mRNA expression (p<0.001, figure 2A). Conversely, inhibition of miR-574-5p with an anti-sense inhibitor (see supplemental materials and methods section in online supplementary information) resulted in a 92% increase in *Qki* mRNA expression (p<0.001). Similar effects were found for *Qki5/6/7* mRNA isoforms. Parallelling the increase in *Qki* mRNAs following the inhibition of miR-574-5p, total QKI and QKI5/6/7 proteins were all significantly increased as indicated by western blots (p<0.001, figure 2B). Moreover, similar effects were observed for human HCT116, SW480 and SW620 cells (figure S2, online supplementary information).

To determine whether miR-574-5p regulates *Qki*s by targeting *Qki*-3′UTR, we constructed mouse *Qki*-3′UTR-luciferase reporter plasmids (see supplemental materials and methods section in online supplementary information) and used them for CRC cell transfections. Plasmid pmQki7-3′UTR-luc carries the 3′UTR for *Qki7* mRNA that contains a putative miR-574-5p MRE, which is also shared by *Qki6*-3′UTR and *Qki7b*-3′UTR (figure S1, online supplementary information). In contrast, plasmid pmQki5-3′UTR-luc carries the *Qki5*-3′UTR that does not contain any MRE for miR-574-5p. Consistent with the bioinformatics prediction, however, increased miR-574-5p or inhibition of miR-574-5p did not lead to significant changes in *Qki5*-3′UTR activity, suggesting that miR-574-5p does not regulate *Qki5* mRNA through 3′UTR-mediated mechanisms (figure 2C). As anticipated, however, increased miR-574-5p led to significant suppression of *Qki7*-3′UTR activity in CT26 cells. Conversely, inhibition of miR-574-5p led to significant activation of *Qki7*-3′UTR (figure 2C), suggesting that *Qki6/7/7b* mRNAs are all under the post-transcriptional control of miR-574-5p. Mutational analyses of the miR-574-5p MRE on *Qki7*-3′UTR (pMT-miR-574-5p-MRE-luc (mutated MRE)

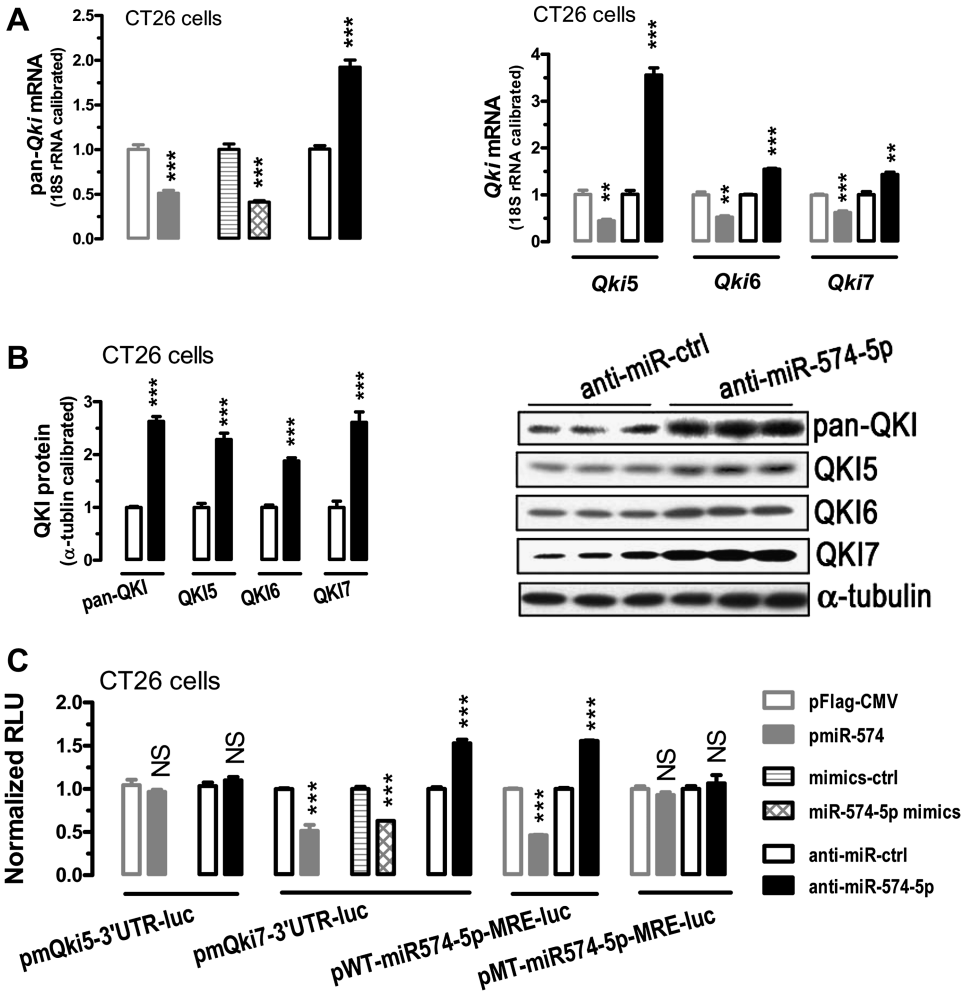

Figure 2 miR-574-5p represses *Qki6/7/7b*. CT26 cells were transfected with a microRNA (miRNA)-overexpressing plasmid or a miRNA mimics or a miRNA inhibitor, in the absence or presence of a luciferase reporter together with pSV40-β-galactosidase (4:3:1). Cells were harvested for quantitative PCR (qPCR), western blotting and luciferase activity assays 24 h after the transfections. For qPCR and the luciferase reporter assays, $n=3-4$. Statistical comparisons were made between a control (pFlag-CMV, mimics control, or inhibitor control)-transfected cells and a particular treatment. Data are represented as mean ± SEM. $^{**}p<0.01$; $^{***}p<0.001$. (A) Overexpression of miR-574-5p or transfection with its mimics caused significant downregulation of total *Qki* messenger RNA (mRNA) and *Qki5/6/7* mRNA isoforms, whereas inhibition of miR-574-5p significantly increased the level of total *Qki* and *Qki5/6/7* mRNA isoforms as determined by qPCR. (B) Inhibition of miR-574-5p significantly increased the levels of total QKI and QKI5/6/7 protein as determined by western blots. (C) miR-574-5p regulates *Qki6/7/7b* (but not *Qki5*) by interacting with the 3′ untranslated region of *Qki6/7/7b*. β-galactosidase activity was determined and used for the calibration of luciferase reporter activity. NS, not significant. See also online figure S2. RLU, relative light units.

versus pWT-miR-574-5p-MRE-luc (wildtype MRE)) further confirmed the specific interaction between miR-574-5p and *Qki6/7/7b*-3′UTR (figure 2C).

QKI5/6/7 represses *β-catenin* expression and activity in CRC cells

β-catenin is one of the predicted targets of QKI proteins,[34] with two putative QREs on its mRNA (figure S3, online supplementary information). However, a previous study suggested that QKI5/6 suppressed the expression of β-catenin protein but not that of mRNA.[23] We therefore wanted to further determine how QKI5/6/7 would affect the expression of *β-catenin* mRNA and protein and the *β-catenin*/Wnt signalling activity in CRC cells. To this end, we first transiently transfected CT26 cells with three plasmids overexpressing mouse *Qki5/6/7* respectively (see supplemental materials and methods section in online supplementary information). Overexpression of each QKI caused significant downregulation of *β-catenin* mRNA and protein expression (figure 3A,C). To determine whether QKIs regulate *β-catenin* through post-transcriptional silencing, we constructed a mouse *β-catenin*-3′UTR-luciferase reporter (pmCtnnb1-3′UTR-luc) that contains two putative QREs (figure S3 and supplemental materials and methods section in online supplementary information). Co-transfection studies indicated that overexpression of QKI5/6/7 all dose dependently reduced the reporter activity (figure 3B), suggesting that these QKIs are all capable of silencing *β-catenin* expression post-transcriptionally. Consistent with QKI-mediated downregulation of *β-catenin*, the TOP/FOP-Flash analyses indicated that these three QKIs could all suppress the activity of TOP-Flash reporter but not the FOP-Flash reporter (figure 3D), suggesting that *β-catenin*/Wnt signalling is regulated in part by the STAR family proteins QKI5/6/7.

miR-574-5p positively regulates *β-catenin* but negatively regulates *p27^{Kip1}*

To determine how miR-574-5p might affect *β-catenin* and *p27^{Kip1}*, two putative targets for QKIs, we performed qPCR and western blot analyses with CRC cells. In CT26 and SW480 cells, overexpression of miR-574-5p caused significant upregulation of mRNA and protein levels in *β-catenin*, whereas inhibition of miR-574-5p caused significant downregulation (figure 4A–C). In contrast, overexpression of miR-574-5p caused downregulation of *p27^{Kip1}* and inhibition of miR-574-5p caused upregulation of *p27^{Kip1}* mRNA and protein (figure 4D–F). These results suggest that miR-574-5p positively regulates *β-catenin* but negatively regulates *p27^{Kip1}*, both largely through downregulating the QKIs.

Effects of miR-574-5p on CRC cell proliferation, differentiation, invasion, migration and colony formation

To evaluate the impact of miR-574-mediated regulation of QKIs, *β-catenin* and *p27^{Kip1}*, we inhibited or overexpressed miR-574-5p in CT26 cells or SW480 cells. In human and mouse cells, inhibition of miR-574-5p greatly reduced cell proliferation as determined by the MTT assays (figure 5A). In SW480 cells, the G1

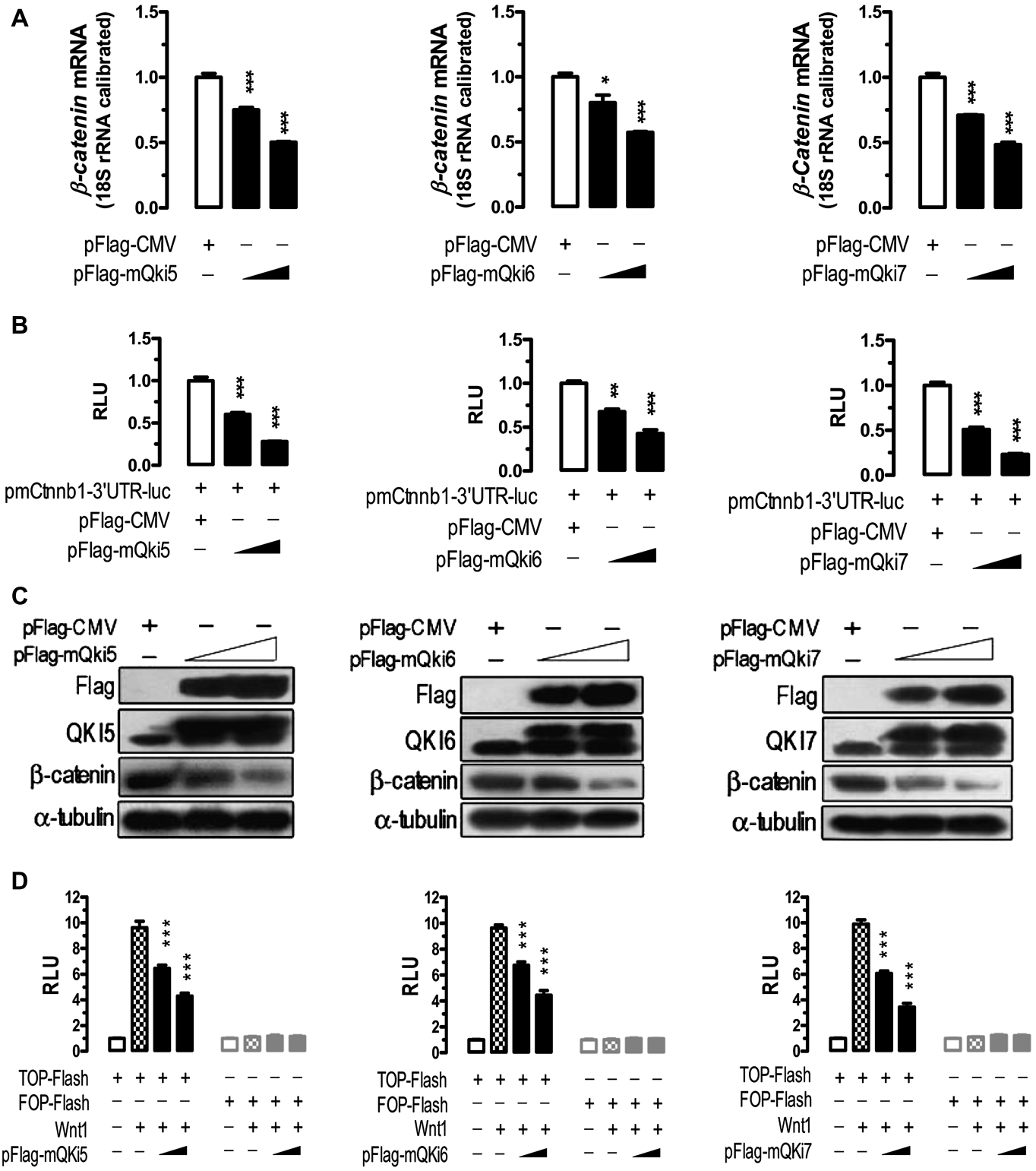

Figure 3 QKI5, QKI6 and QKI7 negatively regulate *β-catenin* expression and activity. For western blots, CT26 cells were transfected with pFlag-CMV or QKI overexpressing plasmids (pFlag-mQki5 or pFlag-mQki6 or pFlag-mQki7). For luciferase reporter assays, cells were co-transfected with a *Qki*-overexpressing plasmid (pFlag-mQki5 or pFlag-mQki6 or pFlag-mQki7), a luciferase reporter plasmid (pmCtnnb1-3′UTR-luc or TOP-Flash or FOP-Flash), Wnt1, together with pSV40-β-galactosidase (3:2:2:1). Cells were harvested for analyses 24 h after the transfections. α-Tubulin expression and β-galactosidase activity were determined and used for the calibration of western blots and luciferase reporter assay respectively. For the luciferase reporter assays, $n=3$. Data are represented as mean ± SEM. *$p<0.05$; **$p<0.01$; ***$p<0.001$. (A) QKI5/6/7 repress the expression of *β-catenin* messenger (mRNA) in CT26 cells dose dependently. (B) QKI5/6/7 dose-dependently repress the expression of *β-catenin* by interacting with *β-catenin*-3′ untranslated region. (C) QKI5/6/7 repress β-catenin protein expression dose dependently. Plasmid-derived proteins and endogenous proteins appeared to be resolved as two separate bands. (D) QKI5/6/7 suppress *β-catenin*/Wnt signalling dose dependently. See also online figure S3. RLU, relative light units.

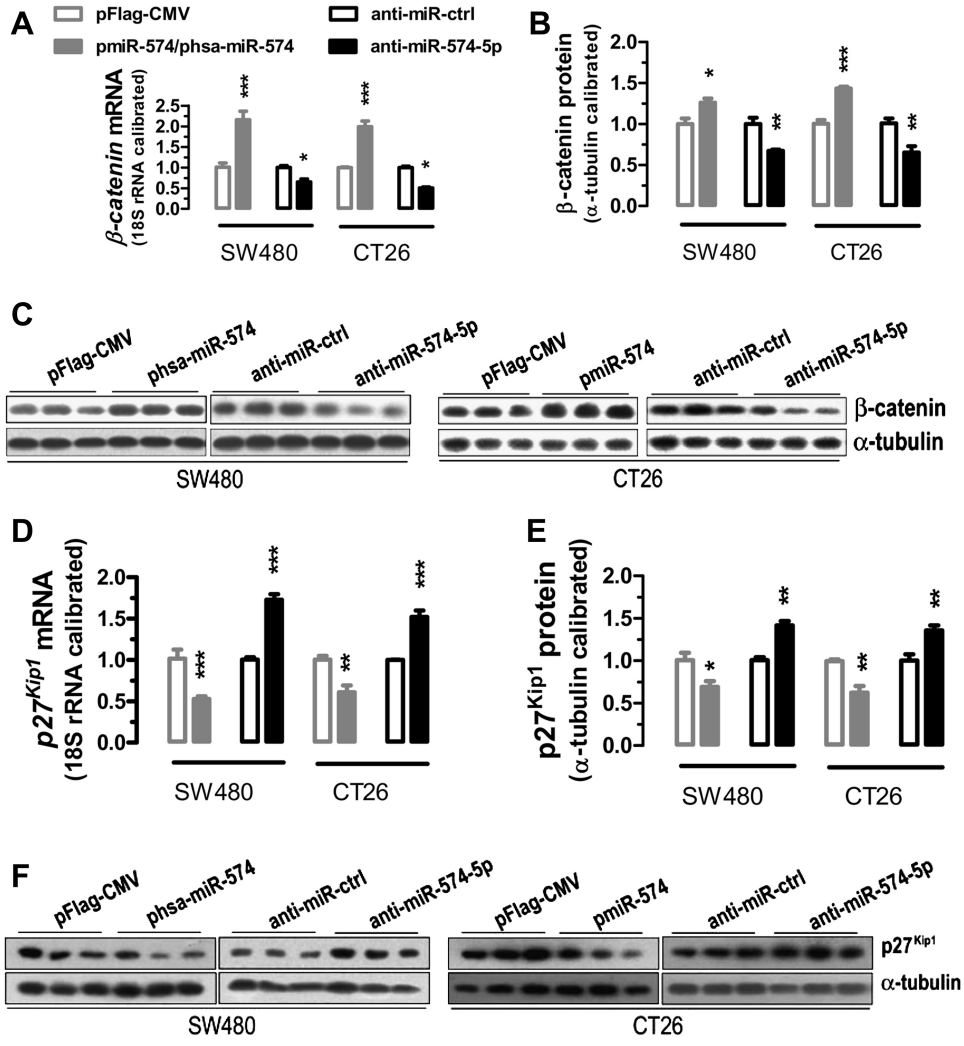

Figure 4 miR-574-5p positively regulates β-catenin but negatively regulates *p27^{Kip1}*. SW480 and CT26 cells were transfected with a miRNA-overexpressing plasmid or a microRNA (miRNA) inhibitor. Cells were harvested for quantitative PCR and western blot assays 24 h after the transfections (n=3). Statistical comparisons were made between a control ((pFlag-CMV or inhibitor control)-transfected cells) and a particular treatment. Data are represented as mean ± SEM. *p<0.05; **p<0.01; ***p<0.001. (A, B) Overexpression of miR-574-5p significantly increased messenger RNA (mRNA) or protein expression of *β-catenin*, whereas inhibition of miR-574-5p significantly reduced the levels of *β-catenin* mRNA or protein in SW480 and CT26 cells. (C) Western blots for β-catenin in SW480 and CT26 cells. (D, E) Overexpression of miR-574-5p significantly decreased mRNA or protein expression of *p27^{Kip1}* in SW480 and CT26 cells, whereas inhibition of miR-574-5p significantly increased the levels of *p27^{Kip1}* mRNA or protein in SW480 and CT26 cells. (F) Western blots for p27^{Kip1} in SW480 and CT26 cells.

cells were significantly increased while the S cells were significantly decreased 72 h after miR-574-5p inhibition, suggesting G1/S arrest (figure 5B). We analysed the expression of *Lactase* mRNA and the enzyme activity of intestinal alkaline phosphatase (IAP), two important markers of intestinal differentiation. In CT26 cells, overexpression of miR-574-5p significantly reduced the expression of *Lactase* mRNA and the activity of IAP, whereas inhibition of miR-574-5p increased both (figure 5C,D). Meanwhile, overexpression of miR-574-5p significantly increased invasion likelihood in CT26 cells, whereas inhibition of miR-574-5p decreased invasion likelihood (figure 5E). Furthermore, overexpression of miR574-5p in SW480 cells greatly enhanced cell migration, whereas inhibition of miR-574-5p suppressed the migration (figure 5F). Additionally, specific inhibition of miR-574-5p also greatly decreased the ability of colony formation in SW480 cells (figure 6B). Together these data suggest that when overexpressed, miR-574-5p might be oncogenic.

To verify that miR-574-5p-mediated repression of QKIs is important for the oncogenic function of miR-574-5p, we co-expressed one of the three mouse QKIs (QKI5/6/7) with miR-574-5p in CT26 cells (online figure S4). In comparison with cells overexpressing miR-574-5p only, cells co-overexpressing miR-574-5p and QKI5/6/7 in general all appeared to lead to increased mRNA expression of *p27^{Kip1}*, reduced mRNA expression of *β-catenin*, reduced ability in cell invasion and slightly reduced cell proliferation, although the re-introduction of QKI5 only caused relatively minor and in some cases not significant effects. These results confirm that the miR-574-5p-mediated repression of *Qki*s contributes significantly to its oncogenic function.

Inverse correlation between the expression of miR-574-5p and the expression of total *Qki* mRNA/protein in CRC clinical samples

To explore the relationship between the expression of miR-574-5p and the expression of total *Qki* mRNA/protein, we performed qPCR and western blots with 60 pairs of clinical samples. In about 76.7% of human CRC tissues (46 out of 60), miR-574-5p was found to be significantly upregulated in comparison with the controls, while total *Qki* mRNA and protein expression levels were greatly reduced (figure 7A–E). These results were further confirmed by immunohistochemistry analyses of QKI protein and in situ hybridisation analyses of miR-574-5p (figure 7F). Largely consistent with the down-regulation in total *Qki*, *Qki5/6/7/7b* mRNA and protein isoforms were all significantly downregulated in most CRC tissues (online figure S5). Pearson's correlation analyses demonstrated significant inverse correlations between the expression of miR-574-5p and the expression of total *Qki* mRNA (Pearson r=−0.4082, p<0.05) or QKI protein (Pearson r=−0.4406, p<0.05) in the 60 pairs of CRC samples tested (figure 7D,E). No apparent association, however, was found between miR-574-5p

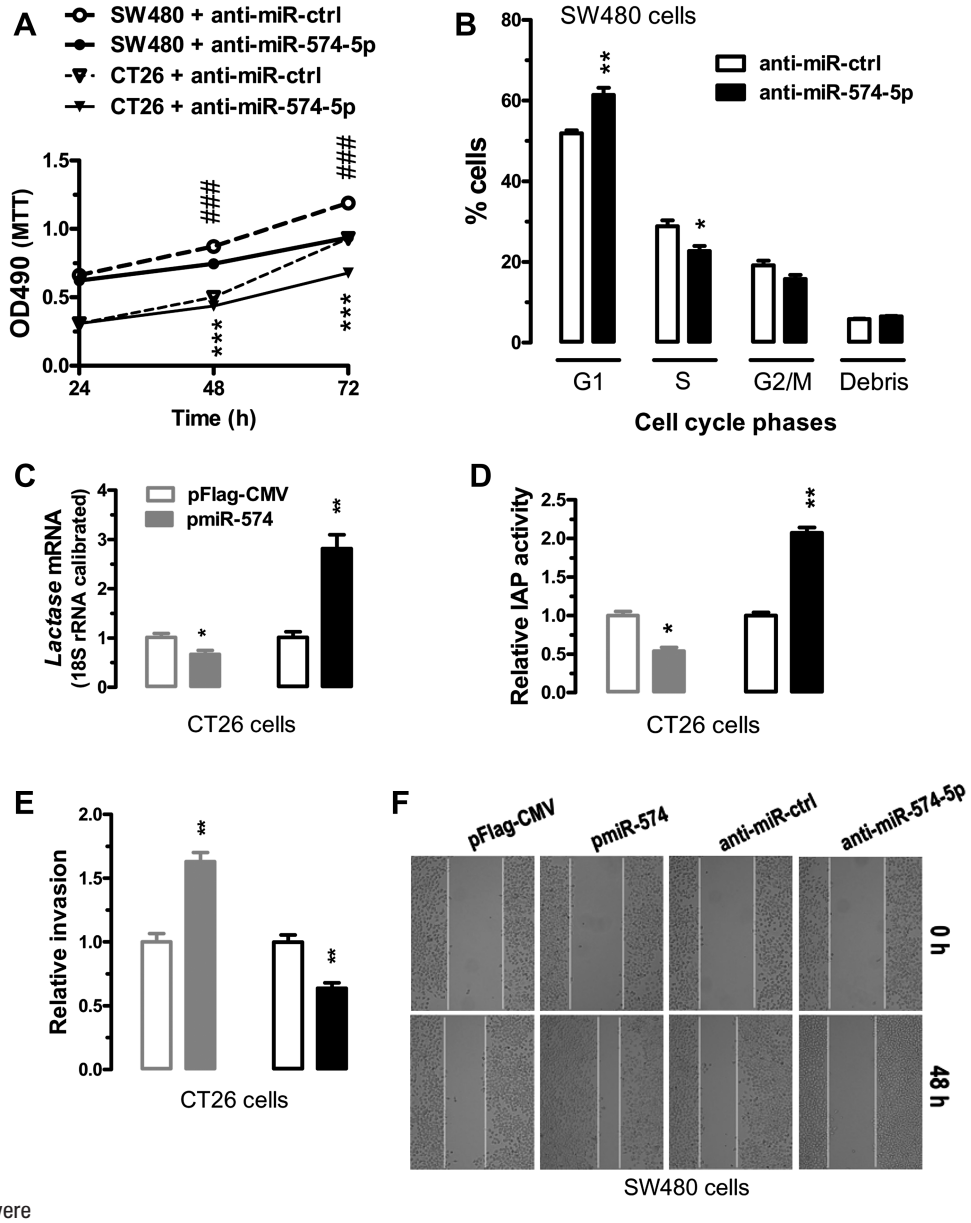

Figure 5 Effects of miR-574-5p on cell cycle, proliferation, differentiation, invasion and migration. SW480 or CT26 cells were transfected with a microRNA (miRNA)-overexpressing plasmid or a miRNA inhibitor (see supplemental materials and methods section in online supplementary information). Cells were harvested for analyses 24 h after the transfections (n=3). Statistical comparisons were made between a control ((pFlag-CMV or inhibitor control)-transfected cells) and a particular treatment. Data are represented as mean ± SEM. *p<0.05; **p<0.01; *** or ###, p<0.001. (A) Inhibition of miR-574-5p significantly reduced the rate of proliferation in CT26 and SW480 cells. ### represents comparisons among SW480 cells whereas *** represents comparisons among CT26 cells. (B) Inhibition of miR-574-5p caused G1/S arrest in SW480 cells. (C) Overexpression of miR-574-5p significantly decreased messenger RNA (mRNA) of *Lactase*, whereas inhibition of miR-574-5p significantly increased the mRNA level of *Lactase* in CT26 cells. (D) Overexpression of miR-574-5p significantly decreased the activity of intestinal alkaline phosphatase (IAP), whereas inhibition of miR-574-5p significantly increased IAP activity in CT26 cells. (E) Overexpression of miR-574-5p significantly enhanced cell invasion, whereas inhibition of miR-574-5p significantly suppressed invasion in CT26 cells as determined by the Matrigel invasion assays. (F) Overexpression of miR-574-5p significantly enhanced migration in SW480 cells, whereas inhibition of miR-574-5p suppressed cell migration as determined by wound-healing assays. Results are typical for three independent experiments. Similar results were obtained for CT26 cells but not included. Original magnification, ×100.

expression and patient gender, patient age, tumour location, TNM staging or lymph node status (online table S1). As a matter of fact, the highest levels (5.737±2.546-fold of the normal level) of miR-574-5p expression were detected for TNM stage I cancers that decreased subsequently but maintained at moderate levels (2.4–2.6-fold) for TNM stages II, III and IV cancers. A similar trend was observed for lymph node status.

Remarkably, serum miR-574-5p was also found to be significantly elevated in patients with CRC with respect to the controls (2.11±0.39 for patients with CRC vs 1.00±0.22 for controls, p<0.05, figure 7G).

Qki isoform subcellular localisation and relative expression levels in CRC cells and tissues

We performed western blot and immunofluorescence analyses to determine the subcellular localisation of QKI isoforms in the CRC cells. Largely consistent with previous studies in neural cells[35] and HeLa cells,[2 36] QKI5 was found to be present in the nucleus and cytoplasm of CT26 and SW620 cells, whereas QKI6/7 proteins were exclusively localised in the cytoplasm (online figure S6A,B). To determine the relative expression levels of *Qki* mRNA isoforms, we performed qPCR analyses for mouse CT26, human HCT116, SW480 and SW620 cells (online figure S6C), CRC tissues and normal adjacent epithelial tissues from 10 patients with CRC (online figure S6D). In cultured CT26 cells, *Qki6* mRNA was 210-fold higher than that of *Qki5* mRNA while *Qki7* was 308 times higher. In three lines of cultured human CRC cells and most of the human tissues (CRC and normal colorectal tissues), *Qki7* mRNA was consistently more than 100-fold higher than that of any other isoforms (including *Qki5/6/7b*), with only a few exceptions. These results highlight that *Qki6* and *Qki7* are the predominant isoforms in mouse CRC cells but in human CRC cells and tissues, *Qki7* is the most abundant splicing variant.

To evaluate the effects of increased miR-574-5p on the expression and subcellular distribution of β-catenin, we

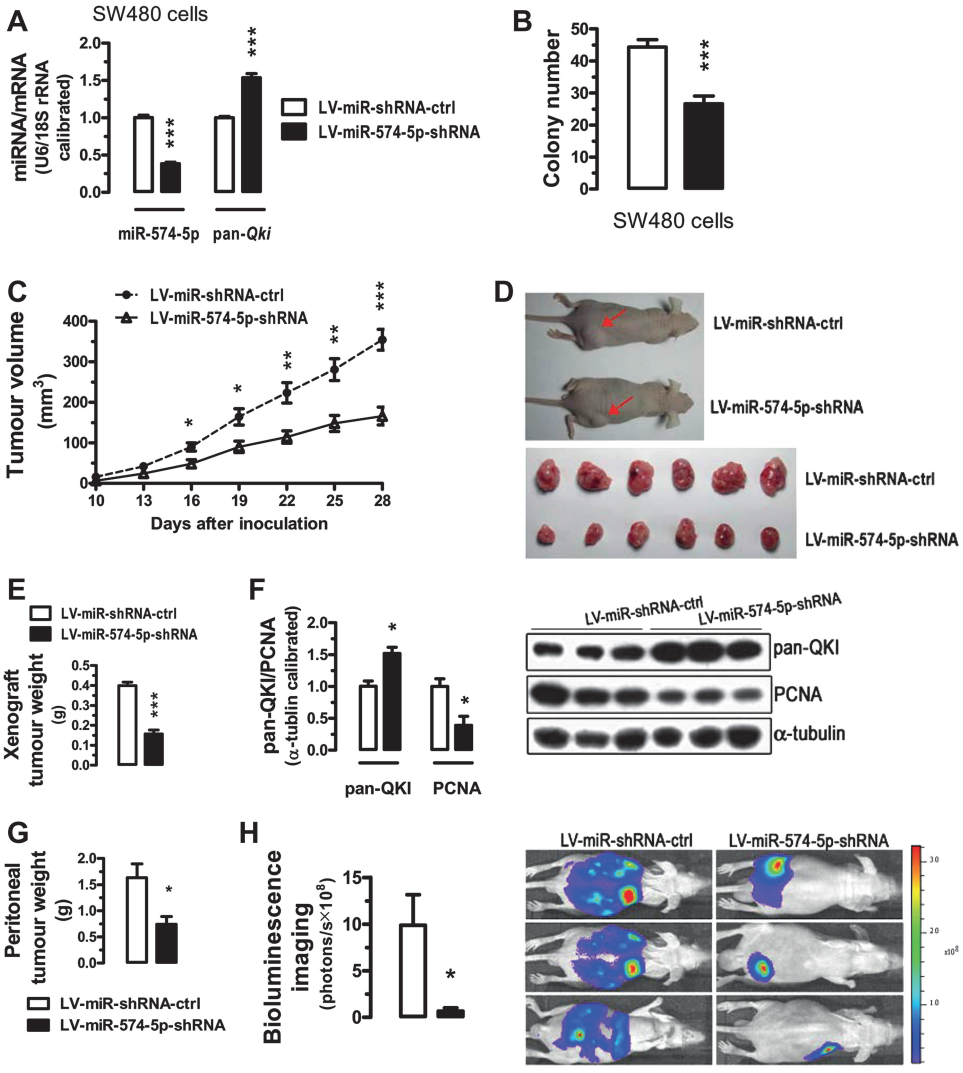

Figure 6 Inhibition of miR-574-5p suppresses tumour growth in the nude mice. For a xenograft tumour model, SW480 cells were pre-infected with LV-miR-shRNA-ctrl or LV-miR-574-5p-shRNA (see supplemental materials and methods section in online supplementary information). Subsequently, the LV-infected cells were harvested and suspended in phosphate-buffered saline and then inoculated subcutaneously ($\sim 5\times10^6$ cells/mouse) into the right side of the posterior flank of 5-week-old nude mice. For bioluminescence imaging of tumour growth in live animals, CT26 cells stably overexrpressing luciferase or its controls were injected into the nude mice intraperitoneally (5×10^5 cells/mouse). Starting from the third day after CT26 cell inoculation, each mouse was injected with 2×10^7 transducing units of control lentiviruses or lentiviruses carrying short hairpin RNA (shRNA) for miR-574-5p once a week for 2 weeks. Peritoneal tumour growth was monitored by bioluminescence imaging (described in supplemental materials and methods section in online supplementary information). Data are represented as mean ± SEM. *p<0.05; **p<0.01; ***p<0.001. (A) Downregulation of miR-574-5p and upregulation of total *Qki* messenger RNA (mRNA) 96 h after lentiviral infection (n=3). (B) Lentivirus-miR-shRNA-mediated inhibition of miR-574-5p significantly decreased colony formation in SW480 cells. SW480 cells were transfected with LV-miR-shRNA-ctrl or LV-miR-574-5p-shRNA. Ninety-six hours after the transfection, 50 transfected cells were seeded on six-well plates and maintained in DMEM containing 10% FBS for 2 weeks before colony counting (n=3). (C) Time-dependent growth of xenograft tumour tissues in the nude mice (n=6). (D, E) Tumour tissues dissected 28 days after the inoculation and the comparison of the tumour weights (n=6). (F) Altered expression of total QKI and proliferating cell nuclear antigen in the dissected tumour tissues (n=3). (G) Weights of visible and dissected peritoneal tumours following gene therapy with lentiviruses carrying shRNA for miR-574-5p or its controls for 24 days (n=3). (H) Intraperitoneal tumour growth as demonstrated by bioluminescence imaging in the live nude mice inoculated with CT26 cells stably overexpressing a luciferase reporter gene 24 days after treatment with lentiviruses carrying shRNA for miR-574-5p or its control (n=3). miRNA, microRNA. DMEM, Dulbecco's Modified Eagle Medium; FBS, fetal bovine serum; PCNA, proliferating cell nuclear antigen.

performed both the western blots and immunofluorescent staining in CT26 cells overexpressing miR-574-5p (online figure S7). Our western blots indicated that following miR-574-5p overexpression, β-catenin protein was significantly increased in the nuclear and membrane fractions while not much increase was found in the cytoplasm. Immunofluorescent staining also confirmed significant increases in β-catenin in the nucleus.

Inhibition of miR-574-5p suppresses tumour growth in the nude mice

To further investigate the role of miR-574-5p in tumour growth, we assessed the effects of inhibition of miR-574-5p on the growth of xenograft tumours in nude mice. Mice were injected with SW480 cells that were pre-infected with control lentiviruses or lentiviruses carrying shRNA for miR-574-5p. Lentivirus-mediated knockdown of miR-574-5p caused significant upregulation in total *Qki* (figure 6A). Probably as a consequence, the ability to form colonies was significantly reduced in miR-574-5p knockdown cells (figure 6B). In nude mice, tumour growth with miR-574-5p-knockdown cells was much slower than that with the control SW480 cells (figure 6C). When dissected at the end of the study (day 28), the average tumour weight of the miR-574-5p knockdown group was only 39% of that of the control group (p<0.001) (figure 6D,E). In the miR-574-5p knockdown tumour tissues, total QKI protein was greatly increased whereas the proliferating cell nuclear antigen expression was significantly decreased (figure 6F). In a more systemic in vivo miR-574-5p inhibition experiment, CT26 cells stably overexpressing luciferase were injected into the nude mice intraperitoneally. The mice were then treated with control lentiviruses or lentiviruses carrying shRNA for miR-574-5p. As shown in figure 6G,H, miR-574-5p inhibition greatly reduced peritoneal tumour growth in the nude mice as monitored by bioluminescent imaging on the 24th day. Together these results suggest that in vivo inhibition of miR-574-5p suppresses CRC tumour growth and this effect is largely due to the increased expression in QKI proteins.

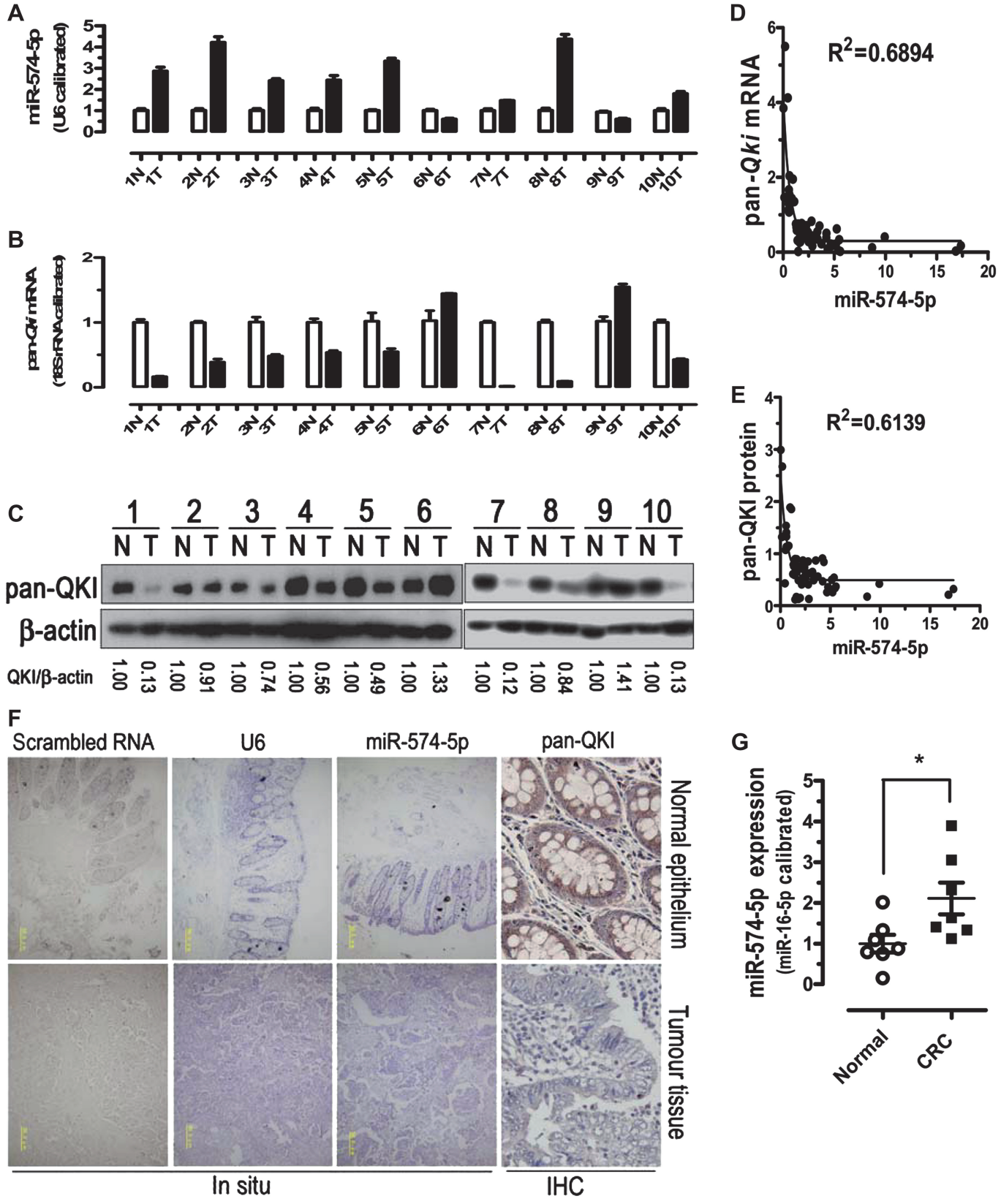

Figure 7 Expression of miR-574-5p and total *Qki* messenger RNA (mRNA)/protein levels in control and colorectal cancer (CRC) samples. Arabic numbers indicate individual sample pairs. (A) miR-574-5p expression was significantly upregulated in human CRC tissues. (B, C) Total *Qki* mRNA and protein were significantly downregulated in human CRC tissues. N, normal adjacent epithelial tissue; T, tumour tissue. (D, E) Inverse correlation between the expression of miR-574-5p and the expression of *Qki* mRNA/protein in 60 pairs of clinical samples. Nonlinear regression (exponential) was indicated. (F) Typical expression patterns of pan-QKI protein in human CRC tissues and normal adjacent epithelial tissues as determined by immunohistochemistry (IHC, original magnification, ×1000) and miR-574-5p expression patterns in human CRC tissues and normal adjacent epithelial tissues as determined by in situ hybridisation (original magnification, ×100; yellow bars represent 50.0 μm). See also online figure S5. (G) miR-574-5p expression was significantly upregulated in serum samples from patients with CRC. Normal, normal controls, $n=7$; CRC, patients with CRC, $n=7$.

DISCUSSION

QKI is emerging as a major regulator for RNA metabolism and cell signalling.[37 38] Dysregulation of QKIs has been associated with a number of important human diseases such as schizophrenia, ataxia and cancers.[8 24] However, the regulatory mechanisms underlying the dysregulation of QKIs were elusive. We showed in this current study that miR-574-5p represses the expression of *Qki6/7/7b* mRNAs by interacting with the MREs on their 3′UTRs. As predicted by bioinformatics analyses, however, miR-574-5p did not regulate the expression of *Qki5* through this miR-574-5p-3′UTR interaction. Nevertheless, *Qki5* expression very often was downregulated when miR-574-5p was overexpressed but upregulated when miR-574-5p was inhibited. This suggests that other indirect and unknown mechanisms might be involved in the regulation of *Qki5* that require further investigation. Importantly, we demonstrated in human CRC cells that *Qki7* mRNA expression is usually more than 100-fold higher than any other isoform, with only rare exceptions (figure S6D). This is in contrast to *Qki6* being the most abundant isoforms in the brain[39] and probably has important physiological implications. Surprisingly, we did not find increased apoptosis in *Qki7*-overexpressing CT26 cells or human cells with abundant QKI7 protein, contrary to previous reported QKI7-induced apoptosis in fibroblast cells and oligodendrocytes.[2 40] QKI5 and QKI6 were previously shown to exert a suppressive effect on *β-catenin*/Wnt signalling by reducing the level of β-catenin protein and affecting its subcellular redistribution, but they did not appear to affect mRNA expression of *β-catenin*.[23] By contrast, we showed in our current study that QKI5/6/7 proteins are all capable of repressing mRNA and protein expression of *β-catenin* and suppressing *β-catenin*/Wnt signalling in CRC cells. The reason for the discrepancy in *β-catenin* mRNA expression between the previous study and our current study is not clear but might be related to the semi-quantitative real-time PCR used in the previous study[23] compared with the qPCR used in our current study. In light of the relative abundance of QKI7 and its ability to regulate *β-catenin*/$p27^{Kip1}$ expression and their signalling activity, however, our novel results suggest a prominent role for QKI7 in QKI-mediated signal transduction and activation of RNA and in colorectal cell differentiation and the development of CRC which to date had been missed from the research.

In human and mouse, the miR-574 gene is intronic. Initially, miR-574-5p was thought to be hosted by the first intron of the gene encoding *Noxp20*[32] on human chromosome 4 or mouse chromosome 5. A recent study, however, also suggested that miR-574-5p might be encoded by the first intron of *Col3a1*. Interestingly, alterations in the expression of miR-574-5p have been found to be associated with a variety of diseases, including many types of cancers (online table S2). Ranade *et al* found that miR-574-5p is one of a few miRNAs that were associated with chemoresistance and decreased survival in patients with small cell lung cancer.[41] In serum samples of patients with early stage non-small cell lung cancer, they also found that miR-1254 and miR-574-5p were significantly elevated in the patients with cancer compared with controls,[42] which suggests miR-574-5p might be used as a biomarker for non-small cell lung cancer. Very recently, Meyers-Needham *et al* also showed that miR-574-5p mediated the silencing of tumour suppressor ceramide synthase-1 (*CerS1*) in head and neck squamous cell carcinoma by selectively targeting one of its alternatively spliced mRNA variants, *CerS1-2*.[43] Moreover, inhibition of miR-574-5p was shown to reconstitute *CerS1-2* expression and C_{18}-cermide generation in multiple lines of cancer cells, which subsequently led to suppressed proliferation and anchorage-independent growth of cancer cells. Together these results strongly suggest that miR-574-5p is oncogenic and its inhibition might be beneficial.

We demonstrated in our current investigation that miR-574-5p was significantly elevated in colorectal tissues and serum samples from patients with CRC, especially for cancers at TNM stage I. Consistent with the lack of association between miR-92a and TNM stage in CRC,[44] the abnormal upregulation of miR-574-5p in the CRC tissues of our current study was not found to be associated with TNM stage or lymph node status. One possible explanation for the lack of association between miR-574-5p and TNM stage or lymph node status is that miR-574-5p probably promotes CRC tumourigenesis or progression primarily at the early stages. Moreover, it is probably not necessary for miR-574-5p to be continuously increased with CRC progression because a moderate twofold to threefold increase appeared to be sufficient to knockdown *Qki* significantly (figure 7D,E). Indeed, QKI protein expression was maintained at low levels for cancers at TNM stages II, III and IV. We further demonstrated that aberrantly upregulated miR-574-5p probably contributes to the development of CRC in part by selectively targeting tumour suppressors *Qki6/7/7b* post transcriptionally, leading to the dys-regulation of *β-catenin*/Wnt signalling. Whether miR-574-5p also regulates macroH2A1.1 and *CerS1-2* in the CRC cells to contribute to CRC development or not, however, remains to be determined. Despite this, findings from our current study have important implications for the elucidation of pathogenic mechanisms and for clinical practice. Theoretically, the identification of this novel regulatory mechanism of *Qki* isoforms mediated by miR-574-5p sheds lights on the elucidation of pathogenic mechanisms underlying the development of important human diseases associated with the aberrant expression of miR-574-5p, QKIs and more than 1400 putative QKI-regulated genes (online figure S8). From a clinical perspective, our demonstration that serum miR-574-5p is significantly elevated in most patients with CRC suggests that miR-574-5p might serve as a novel diagnostic biomarker for early detection of CRC. As importantly, our demonstration that inhibition of miR-574-5p ameliorated CRC development or progression suggests that miR-574-5p might be an important therapeutic target for the prevention or treatment of CRC and other miR-574-5p-associated cancers.

Acknowledgements The authors thank Dr Qiao Wu for the TOP/FOP-flash luciferase reporters, Dr Boan Li for the *Apc*-mutant mice and Dr Bixing Zhao and Mr Lianwei Yang at the National Institute of Diagnostic and Vaccine Development (Xiamen University) for technical assistance. We also thank Professor Longping Wen for critical reading of the manuscript.

Contributors SJ, GY, JZ, LW, TW, ZW, TZ and GW performed the experiments, collected and analysed the data; YL and ZG designed the experiments, analysed the data and revised the paper; JC designed and supervised the project, analysed the data and revised the paper; JYY conceived, designed and supervised the project, analysed the data, wrote and revised the paper.

Funding This work was supported in part by grants from the National Science Foundation of China (30970649), the 973 Program of China (2009CB941601), the Fujian Provincial Department of Science and Technology (2010L0002), and the 111 Project of Education of China (B06016).

Competing interests None.

Ethics approval Institutional Medical Ethics Committee of Xiamen University.

Provenance and peer review Not commissioned; externally peer reviewed.

REFERENCES

1. **Biedermann B,** Hotz HR, Ciosk R. The Quaking family of RNA-binding proteins: coordinators of the cell cycle and differentiation. *Cell Cycle* 2010;**9**:1929—33.
2. **Pilotte J,** Larocque D, Richard S. Nuclear translocation controlled by alternatively spliced isoforms inactivates the QUAKING apoptotic inducer. *Genes Dev* 2001;**15**:845—58.
3. **Larocque D,** Galarneau A, Liu HN, *et al*. Protection of p27(Kip1) mRNA by quaking RNA binding proteins promotes oligodendrocyte differentiation. *Nat Neurosci* 2005;**8**:27—33.
4. **Li Z,** Takakura N, Oike Y, *et al*. Defective smooth muscle development in qkI-deficient mice. *Dev Growth Differ* 2003;**45**:449—62.
5. **Lobbardi R,** Lambert G, Zhao J, *et al*. Fine-tuning of Hh signaling by the RNA-binding protein Quaking to control muscle development. *Development* 2011;**138**:1783—94.
6. **van MA,** Grundmann S, Goumans MJ, *et al*. MicroRNA-214 inhibits angiogenesis by targeting Quaking and reducing angiogenic growth factor release. *Cardiovasc Res*. Published Online First: 6 February 2012. doi:10.1093/cvr/cvs003
7. **Noveroske JK,** Lai L, Gaussin V, *et al*. Quaking is essential for blood vessel development. *Genesis* 2002;**32**:218—30.
8. **Chenard CA,** Richard S. New implications for the QUAKING RNA binding protein in human disease. *J Neurosci Res* 2008;**86**:233—42.
9. **Richard S.** Reaching for the stars: linking RNA binding proteins to diseases. *Adv Exp Med Biol* 2010;**693**:142—57.
10. **Bielli P,** Busa R, Paronetto MP, *et al*. The RNA-binding protein Sam68 is a multifunctional player in human cancer. *Endocr Relat Cancer* 2011;**18**:R91—102.
11. **Rajan P,** Gaughan L, Dalgliesh C, *et al*. Regulation of gene expression by the RNA-binding protein Sam68 in cancer. *Biochem Soc Trans* 2008;**36**:505—7.
12. **Lukong KE,** Richard S. Targeting the RNA-binding protein Sam68 as a treatment for cancer? *Future Oncol* 2007;**3**:539—44.
13. **Chen ZY,** Cai L, Zhu J, *et al*. Fyn requires HnRNPA2B1 and Sam68 to synergistically regulate apoptosis in pancreatic cancer. *Carcinogenesis* 2011;**32**:1419—26.
14. **Song L,** Wang L, Li Y, *et al*. Sam68 up-regulation correlates with, and its down-regulation inhibits, proliferation and tumourigenicity of breast cancer cells. *J Pathol* 2010;**222**:227—37.
15. **Li ZZ,** Kondo T, Murata T, *et al*. Expression of Hqk encoding a KH RNA binding protein is altered in human glioma. *Jpn J Cancer Res* 2002;**93**:167—77.
16. **Yin D,** Ogawa S, Kawamata N, *et al*. High-resolution genomic copy number profiling of glioblastoma multiforme by single nucleotide polymorphism DNA microarray. *Mol Cancer Res* 2009;**7**:665—77.
17. **Ichimura K,** Mungall AJ, Fiegler H, *et al*. Small regions of overlapping deletions on 6q26 in human astrocytic tumours identified using chromosome 6 tile path array-CGH. *Oncogene* 2006;**25**:1261—71.
18. **Sukumar S,** Wang S, Hoang K, *et al*. Subtle overlapping deletions in the terminal region of chromosome 6q24.2-q26: three cases studied using FISH. *Am J Med Genet* 1999;**87**:17—22.
19. **Backx L,** Fryns JP, Marcelis C, *et al*. Haploinsufficiency of the gene Quaking (QKI) is associated with the 6q terminal deletion syndrome. *Am J Med Genet A* 2010;**152A**:319—26.
20. **Aberg K,** Saetre P, Lindholm E, *et al*. Human QKI, a new candidate gene for schizophrenia involved in myelination. *Am J Med Genet B Neuropsychiatr Genet* 2006;**141B**:84—90.
21. **Aberg K,** Saetre P, Jareborg N, *et al*. Human QKI, a potential regulator of mRNA expression of human oligodendrocyte-related genes involved in schizophrenia. *Proc Natl Acad Sci U S A* 2006;**103**:7482—7.
22. **Klempan TA,** Ernst C, Deleva V, *et al*. Characterization of QKI gene expression, genetics, and epigenetics in suicide victims with major depressive disorder. *Biol Psychiatry* 2009;**66**:824—31.
23. **Yang G,** Fu H, Zhang J, *et al*. RNA-binding protein quaking, a critical regulator of colon epithelial differentiation and a suppressor of colon cancer. *Gastroenterology* 2010;**138**:231—40.
24. **Novikov L,** Park JW, Chen H, *et al*. QKI-mediated alternative splicing of the histone variant MacroH2A1 regulates cancer cell proliferation. *Mol Cell Biol* 2011;**31**:4244—55.
25. **Bockbrader K,** Feng Y. Essential function, sophisticated regulation and pathological impact of the selective RNA-binding protein QKI in CNS myelin development. *Future Neurol* 2008;**3**:655—68.
26. **Huang K,** Tang W, Xu Z, *et al*. No association found between the promoter variations of QKI and schizophrenia in the Chinese population. *Prog Neuropsychopharmacol Biol Psychiatry* 2009;**33**:33—6.
27. **Bartel DP.** MicroRNAs: genomics, biogenesis, mechanism, and function. *Cell* 2004;**116**:281—97.
28. **Bartel DP.** MicroRNAs: target recognition and regulatory functions. *Cell* 2009;**136**:215—33.
29. **Artzt K,** Wu JI. STAR trek: an introduction to STAR family proteins and review of quaking (QKI). *Adv Exp Med Biol* 2010;**693**:1—24.
30. **Zorn AM,** Grow M, Patterson KD, *et al*. Remarkable sequence conservation of transcripts encoding amphibian and mammalian homologues of quaking, a KH domain RNA-binding protein. *Gene* 1997;**188**:199—206.
31. **Kondo T,** Furuta T, Mitsunaga K, *et al*. Genomic organization and expression analysis of the mouse qkI locus. *Mamm Genome* 1999;**10**:662—9.
32. **Boucquey M,** De PE, Locker M, *et al*. Noxp20 and Noxp70, two new markers of early neuronal differentiation, detected in teratocarcinoma-derived neuroectodermic precursor cells. *J Neurochem* 2006;**99**:657—69.
33. **Sterling KM.** The procollagen type III, alpha 1 (COL3A1) gene first intron expresses poly-A+ RNA corresponding to multiple ESTs and putative miRNAs. *J Cell Biochem* 2011;**112**:541—7.
34. **Galarneau A,** Richard S. Target RNA motif and target mRNAs of the Quaking STAR protein. *Nat Struct Mol Biol* 2005;**12**:691—8.
35. **Hardy RJ,** Loushin CL, Friedrich VL Jr, *et al*. Neural cell type-specific expression of QKI proteins is altered in quaking viable mutant mice. *J Neurosci* 1996;**16**:7941—9.
36. **Wu J,** Zhou L, Tonissen K, *et al*. The quaking I-5 protein (QKI-5) has a novel nuclear localization signal and shuttles between the nucleus and the cytoplasm. *J Biol Chem* 1999;**274**:29202—10.
37. **Feng Y,** Bankston A. The star family member QKI and cell signaling. *Adv Exp Med Biol* 2010;**693**:25—36.
38. **Vernet C,** Artzt K. STAR, a gene family involved in signal transduction and activation of RNA. *Trends Genet* 1997;**13**:479—84.
39. **Zhao L,** Tian D, Xia M, *et al*. Rescuing qkV dysmyelination by a single isoform of the selective RNA-binding protein QKI. *J Neurosci* 2006;**26**:11278—86.
40. **Chen T,** Richard S. Structure—function analysis of Qk1: a lethal point mutation in mouse quaking prevents homodimerization. *Mol Cell Biol* 1998;**18**:4863—71.
41. **Ranade AR,** Cherba D, Sridhar S, *et al*. MicroRNA 92a-2*: a biomarker predictive for chemoresistance and prognostic for survival in patients with small cell lung cancer. *J Thorac Oncol* 2010;**5**:1273—8.
42. **Foss KM,** Sima C, Ugolini D, *et al*. miR-1254 and miR-574-5p: serum-based microRNA biomarkers for early-stage non-small cell lung cancer. *J Thorac Oncol* 2011;**6**:482—8.
43. **Meyers-Needham M,** Ponnusamy S, Gencer S, *et al*. Concerted functions of HDAC1 and microRNA-574-5p repress alternatively spliced ceramide synthase 1 expression in human cancer cells. *EMBO Mol Med* 2012;**4**:78—92.
44. **Huang Z,** Huang D, Ni S, *et al*. Plasma microRNAs are promising novel biomarkers for early detection of colorectal cancer. *Int J Cancer* 2010;**127**:118—26.

SUPPLEMENTARY INFORMATION

1. SUPPLEMENTAL DATA

Fig. S1 miR-574-5p MREs on human *Qki6/7/7b* mRNAs (related to Fig. 1). ***A***, Human *Qki* gene structure, major transcripts, protein isoforms and 3'UTRs. Located at 6q26-q27, the human *Qki* gene contains eight exons. Due to alternative splicing, at least 4 major transcripts, namely *Qki5*/*6*/*7*/*7b*, can be produced. Each of these transcript isoforms has its own unique 3'UTR derived from the alternatively-spliced exons. However, a long stretch of overlapping sequences is found in the 3'UTRs for *Qki6*/*7*/*7b* respectively. Furthermore, a putative MRE for miR-574-5p was found in the 3'UTRs of *Qki6/7*/*7b* but not that of *Qki5* mRNA. Four major QKI proteins (QKI5/6/7/7b) can be produced from the four mRNA isoforms, which differ in their carboxyl termini encoded for by the alternatively spliced exons. A common N-terminal 311amino acid peptide fragment encoded by the first six exons is shared by all four protein isoforms. This region contains a KH domain flanked by the QUA1 and the QUA2 motifs respectively. QUA1 is involved in protein homodimerization or heterodimerization while the KH and QUA2 domains might be responsible for RNA binding. The Y-motif is a tyrosine-rich region that serves as a site for tyrosine phosphorylation. In addition, there is a P-motif for the proline–rich region. The C-terminal of QKI5 (but not of the other three isoforms) contains a nuclear localization signal (NLS) that directs its entry into the nucleus. The figure was redrawn based on previous reports[1-3]. The putative MREs for miR-574-5p were indicated on the 3'UTRs for *Qki6/7/7b* respectively. ***B***, Alignment of putative miR-574-5p seed-binding sites of mouse *Qki6/7*-3'UTR and human *Qki6/7/7b*-3'UTR. Mature human miR-574-5p (hsa-miR-574-5p) and mouse miR-574-5p (mmu-miR-574-5p) share 100% sequence similarity, with the sequence being 5'-ugagugugugugugagugugu-3'. ***C***, MREs for miR-17, miR-20a and miR-200b on mouse *Qki5*-3'UTR as predicted by the miRanda algorithm (www.microrna.org). Data sets on www.microrna.org so far contain more complete 3'UTRs for specific genes and the miRanda algorithm distinguishes the 3'UTRs. ***D*** & ***E***, MREs for miR-17, miR-20a, miR-200b, miR-466g, miR-574-5p and miR-717 on mouse *Qki6/7*-3'UTRs as predicted by the miRanda algorithm. Surprisingly, no MRE for miR-574-3p was predicted in the 3'UTRs for mouse or human *Qki5* or *Qki6/7/7b* mRNA.

Fig. S2 Effects of miR-574-5p on *Qki* expression in human HCT116, SW480 and SW620 cells (related to Fig. 2). Human CRC cells were transfected with a miR-574 overexpressing plasmid, a miR-574-5p inhibitor. Cells were harvested for qPCR or western blot assays 24 hours after the transfections (n = 3-4). Statistical comparisons were made between a control (pFlag-CMV or inhibitor control)-transfected cells and a particular treatment. NS, not significant; **, $\boldsymbol{p} < 0.01$; ***, $\boldsymbol{p} < 0.001$. ***A***, Inhibition of miR-574-5p significantly increased the levels of *Qki5/6/7/7b* mRNA isoforms in SW480 and SW620 cells, but only *Qki6/7* were increased in HCT116 cells. ***B***, Overexpression of miR-574-5p significantly reduced the level of total QKI protein in SW480 cells. ***C,*** Inhibition of miR-574-5p significantly increased the levels of total QKI and QKI5/6/7 proteins in SW480 cells.

Fig. S3 Putative QREs on *β-catenin* mRNAs from a few mammals (related to Fig. 3). hsa, *Homo sapiens*; pab, *Pongo abelii*; mmu, *Mus, musculus*; bta, *Bos taurus*; ssc, *Sus scrofa*. Two putative QREs were indicated by QRE1 and QRE2 respectively. The distal QRE1 for *β-catenin* mRNAs from orangutans, mice, cows and pigs completely satisfies the bipartite consensus sequence of NACUAAY-$N_{1\text{-}20}$-UAAY (Galarneau and Richard, 2005; Hafner et al., 2010). With human *β-catenin* mRNAs, however, the number of the intervening nucleotides in the QRE1 between the core site NACUAAY and the half site UAAY is 22 rather than smaller than or equal to 20. Similarly, the proximal QRE2 might also be functional [4]. However, this putative QRE is also slightly different from the consensus sequence, with the half-site being "CAAY" rather than "TAAY" and 22 intervening nucleotides between the putative core site and the putative half site.

Fig. S4 Co-overexpression of *Qki5/6/7* significantly attenuated the oncogenic effects of miR-574-5p. CT26 cells were grown and transfected with pmiR-574 or pFlag-CMV in the presence or absence of pFlag-Qki5/6/7 for 24 hours. Cells were subsequently harvested for mRNA or MTT analyses. For invasion analysis, similar transfection was performed with CT26 cells for 12 hours. Subsequently, 5×10^4 transfected cells were seeded per upper chambers in serum-free RPMI 1640 medium whereas the lower chambers were loaded with RPMI 1640 medium containing 5% FBS. After 48 hours of incubation, cells were harvested for analysis. *, $\boldsymbol{p} < 0.05$; *, $\boldsymbol{p} < 0.01$; ****, $\boldsymbol{p} < 0.001$. ***A,*** Re-introduction of *Qki5/6/7* significantly decreased *β-catenin* and increased $p27^{kip1}$ mRNA expression in miR-574-5p-overexpressing cells (n = 3-4). ***B*** and ***C,*** Re-introduction of *Qki5/6/7* significantly reduced cell viability and cell invasion in miR-574-5p-overexpressing cells (n = 3-4).

Fig. S5 Expression levels of *Qki5/6/7/7b* mRNA and protein isoforms in the human CRC tissues and the adjacent normal epithelial tissues. T, tumor tissue； N, normal adjacent epithelial tissue. ***A***, *Qki5* expression from ten pairs of clinical samples (#11-20) as determined by qPCR. ***B***, *Qki6* expression from ten pairs of clinical samples (#11-20) as determined by qPCR. ***C***, *Qki7* expression from ten pairs of clinical samples (#11-20) as determined by qPCR. ***D***, *Qki7b* expression from ten pairs of clinical samples (#11-20) as determined by qPCR. ***E***, QKI5/6/7/7b protein isoform expression in five pairs of clinical samples (#16-20) as determined by western blotting. $n = 5$, ***, $\boldsymbol{p} < 0.001$.

Fig. S6 Subcellular localization of QKI5/6/7 proteins in human SW620 or mouse CT26 cells and the relative expression of *Qki5/6/7/7b* mRNAs in CRC cells, clinical CRC tissue samples and normal adjacent epithelial tissue samples. ***A***, Subcellular localization of QKI5/6/7 proteins in SW620 or CT26 cells as determined by western blotting. ***B***, Subcellular localization of QKI5/6/7 proteins in CT26 cells as determined by immunofluorescence assays. Original magnification, ×1,000. ***C***, Relative expression of *Qki* mRNA isoforms in CT26, HCT116, SW480 and SW620 cells. Total RNA samples were isolated and qPCR was performed (n = 3-4). All values were normalized with *Qki*5 expression. ***D***, Relative expression of *Qki* mRNA isoforms in clinical CRC and normal adjacent epithelial samples from 10 patients. Both the values for tumor tissues (T, black-colored) and corresponding adjacent noncancerous epithelial tissues from a particular patient (N, grey-colored) were normalized with the expression of *Qki*5 mRNA in normal adjacent epithelial tissue from the same patient.

Fig. S7 Effects of miR-574-5p overexpression on β-catenin subcellular localization as determined by western blots and immunofluorescent staining. For western blots, CT26 cells were transfected with a miR-574-5p overexpressing plasmid (pmiR-574) or its control (pFlag-CMV) for 24 hours and harvested for western blot analyses. For immunofluorescent staining, CT26 cells were seed on the coverslips and transfected with pmiR-574 or pFlag-CMV for 24 hours. Cells were then fixed for immunofluorescence analyses. ***A***, Subcellular distribution of β-catenin protein as determined by western blots; ***B***, Subcellular distribution of β-catenin protein as determined by immunofluorescent staining. Original magnification, ×1000.

Fig. S8 The miR-574-5p-QKI-β-catenin/$p27^{Kip1}$ axis of signal transduction in the development of CRC. miR-574-5p derived from the first intron of either *Col3a1* or *Noxp20* regulates the expression of *Qki6/7/7b*

directly and negatively. *Qki5* may also be regulated by miR-574-5p indirectly. Down-regulation of QKIs will cause the overactivation of β-catenin and the suppression of $p27^{Kip1}$. As a result, activities in colorectal epithelial cell proliferation, migration and invasion will be enhanced, whereas cell cycle arrest and differentiation will be suppressed. Additionally, miR-574-5p might also repress the expression of tumor suppressor ceramide synthase-1 isoform 2 (*CerS1-2*) posttranscriptionally.[5] QKIs, on the other hand, might also control the expression of macroH1A1.1 to impact tumorigenesis.[6] miR-574-5p thus appears to be oncogenic and may contribute to the dysregulation of colorectal epithelial cell differentiation and tumorigenesis or cancer progression through the suppression of tumor-suppressive QKIs. miR-574-5p expression might be co-regulated with its hosting-genes (either *Noxp20* or *Col3a1*), although this needs to be verified with further study. Additionally, Sox2 is a transcriptional factor implicated in the maintenance of the pluripotency of stem cells[7-9], neurogenesis[10-13] and development of cancers.[14-17] In glioblastoma multiforme cells, the knockdown of *Sox2* caused significant down-regulation of miR-574-5p.[18] Coincidentally or not, aberrant Sox2 up-regulation and miR-574-5p up-regulation are often co-detected in diseases such as CRC ([15] and current study), glioblastoma,[18] lung cancer,[19-21] esophageal squamous carcinoma [16;22] etc. Together these observations suggest that Sox2 might regulate miR-574-5p positively. The possible regulation of *Noxp20*, *Col3a1* and miR-574-5p and *Qki*s by Apc, however, is not clear and warrant further research. *Apc*, adenomatous polyposis coli; *Col3a1*, procollagen Type III, alpha-1; *Noxp20*, nervous system overexpressed protein-20; *Sox2*, SRY-like HMG box-2.

Fig. S9 Schematic graphs for twelve plasmids used in the current study. See the Materials and Methods section for more details. hGH-pA, poly-A for human growth hormone gene; Luc, luciferase; SV40-pA, SV40 poly-A.

Table S1 The expression of miR-574-5p and pan-*Qki* mRNA and protein and the clinicopathological features of 60 CRC patients.

Table S2 Alterations of miR-574-5p expression in diseases.

Fig. S1

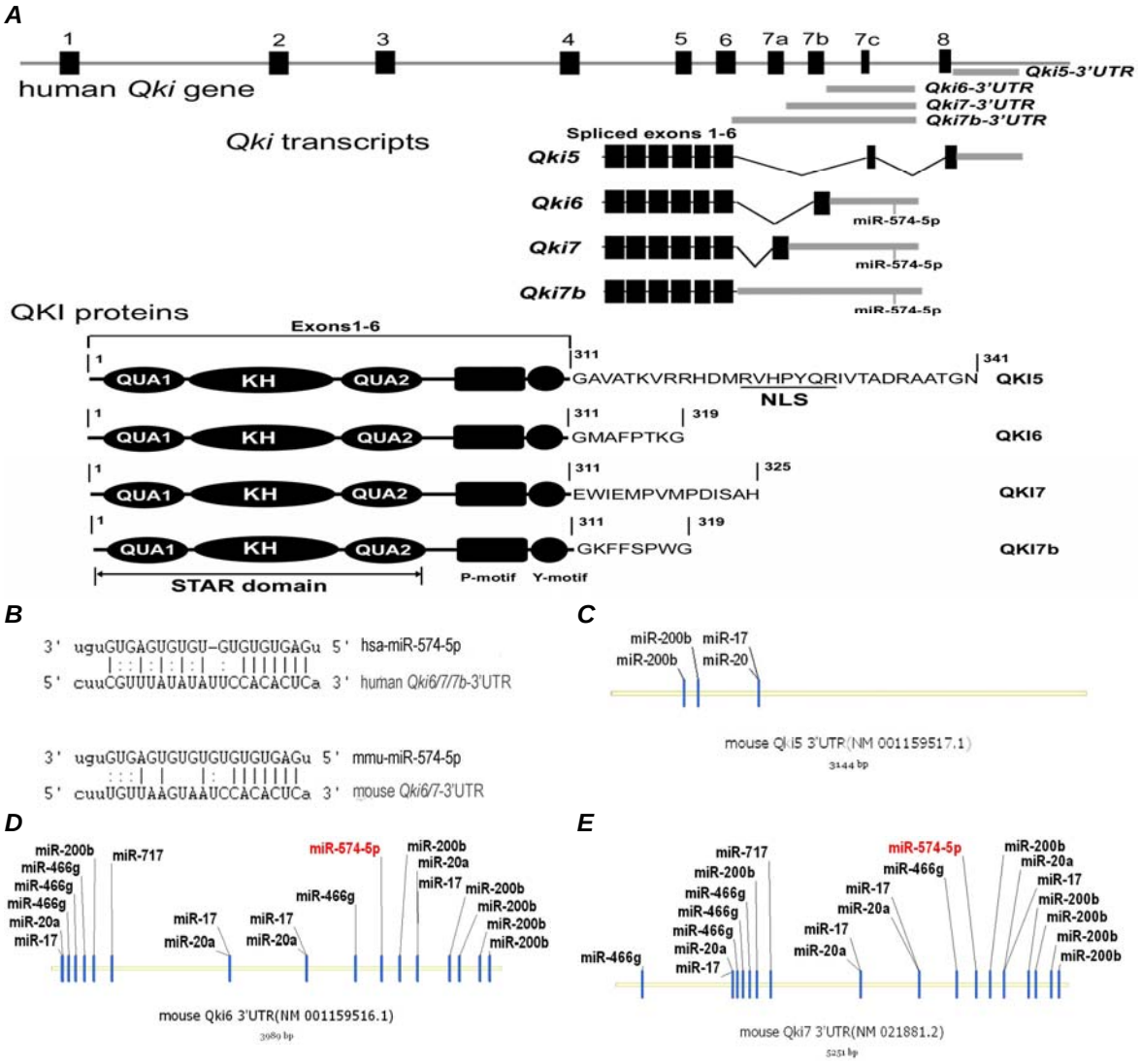
A
human Qki gene
Qki5-3'UTR
Qki6-3'UTR
Qki7-3'UTR
Qki7b-3'UTR
Qki transcripts
Spliced exons 1-6
Qki5
Qki6
Qki7
Qki7b
miR-574-5p
QKI proteins
Exons1-6
QUA1
KH
QUA2
GAVATKVRRHDMRVHPYQRIVTADRAATGN
NLS
QKI5
GMAFPTKG
QKI6
EWIEMPVMPDISAH
QKI7
GKFFSPWG
QKI7b
STAR domain
P-motif
Y-motif
B
hsa-miR-574-5p
human Qki6/7/7b-3'UTR
mmu-miR-574-5p
mouse Qki6/7-3'UTR
C
mouse Qki5 3'UTR(NM 001159517.1)
D
mouse Qki6 3'UTR(NM 001159516.1)
E
mouse Qki7 3'UTR(NM 021881.2)

Fig. S2

A

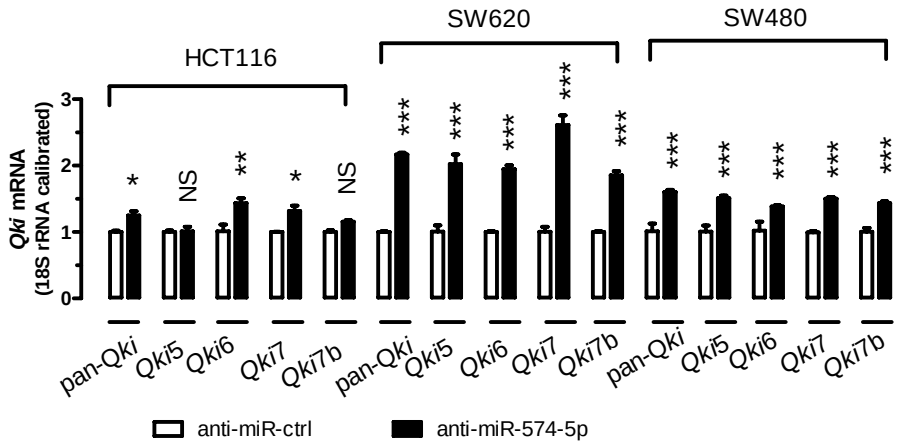
HCT116
SW620
SW480
Qki mRNA (18S rRNA calibrated)
pan-Qki
Qki5
Qki6
Qki7
Qki7b
anti-miR-ctrl
anti-miR-574-5p

B

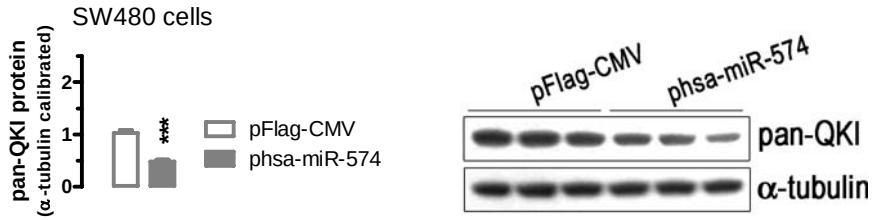
SW480 cells
pan-QKI protein (α-tubulin calibrated)
pFlag-CMV
phsa-miR-574
pan-QKI
α-tubulin

C

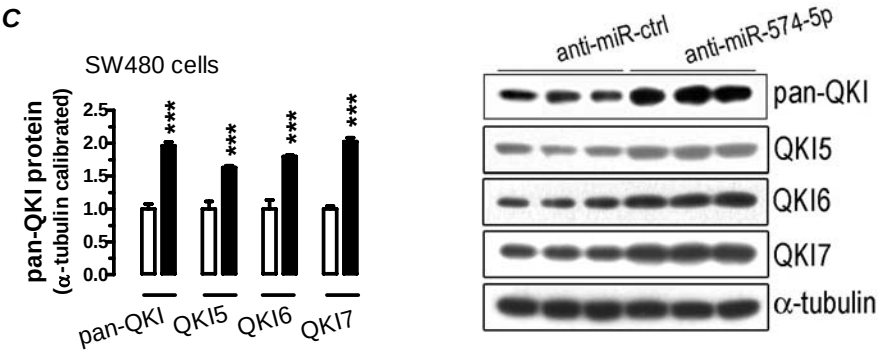
SW480 cells
pan-QKI protein (α-tubulin calibrated)
anti-miR-ctrl
anti-miR-574-5p
pan-QKI
QKI5
QKI6
QKI7
α-tubulin

Fig. S3

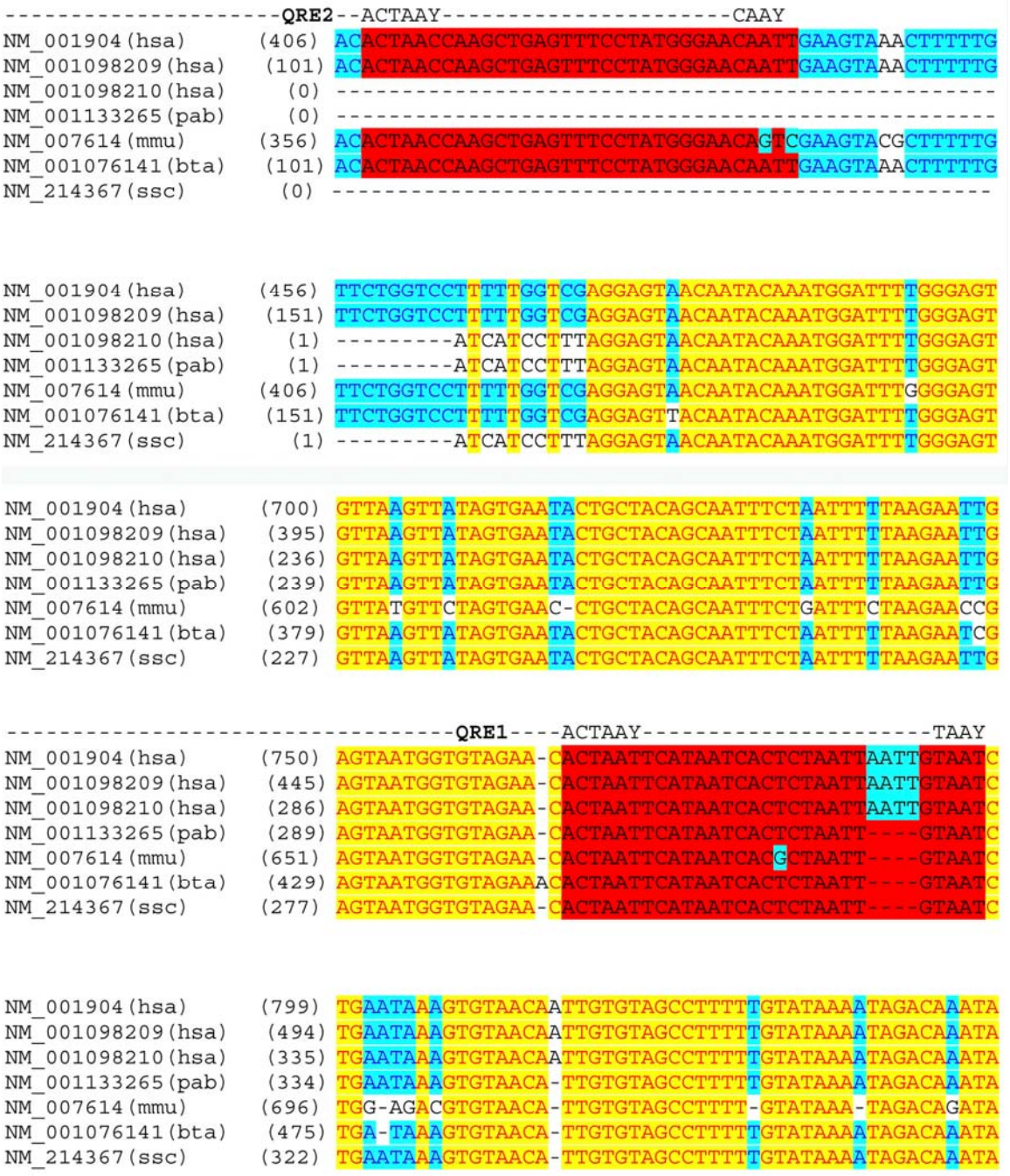
----------QRE2--ACTAAY----------CAAY
NM_001904(hsa) (406) ACACTAACCAAGCTGAGTTTCCTATGGGAACAATTGAAGTAAACTTTTTG
NM_001098209(hsa) (101) ACACTAACCAAGCTGAGTTTCCTATGGGAACAATTGAAGTAAACTTTTTG
NM_001098210(hsa) (0) ----------
NM_001133265(pab) (0) ----------
NM_007614(mmu) (356) ACACTAACCAAGCTGAGTTTCCTATGGGAACAGTCGAAGTACGCTTTTTG
NM_001076141(bta) (101) ACACTAACCAAGCTGAGTTTCCTATGGGAACAATTGAAGTAAACTTTTTG
NM_214367(ssc) (0) ----------
NM_001904(hsa) (456) TTCTGGTCCTTTTTGGTCGAGGAGTAACAATACAAATGGATTTTGGGAGT
NM_001098209(hsa) (151) TTCTGGTCCTTTTTGGTCGAGGAGTAACAATACAAATGGATTTTGGGAGT
NM_001098210(hsa) (1) ---------ATCATCCTTTAGGAGTAACAATACAAATGGATTTTGGGAGT
NM_001133265(pab) (1) ---------ATCATCCTTTAGGAGTAACAATACAAATGGATTTTGGGAGT
NM_007614(mmu) (406) TTCTGGTCCTTTTTGGTCGAGGAGTAACAATACAAATGGATTTGGGGAGT
NM_001076141(bta) (151) TTCTGGTCCTTTTTGGTCGAGGAGTTACAATACAAATGGATTTTGGGAGT
NM_214367(ssc) (1) ---------ATCATCCTTTAGGAGTAACAATACAAATGGATTTTGGGAGT
NM_001904(hsa) (700) GTTAAGTTATAGTGAATACTGCTACAGCAATTTCTAATTTTTAAGAATTG
NM_001098209(hsa) (395) GTTAAGTTATAGTGAATACTGCTACAGCAATTTCTAATTTTTAAGAATTG
NM_001098210(hsa) (236) GTTAAGTTATAGTGAATACTGCTACAGCAATTTCTAATTTTTAAGAATTG
NM_001133265(pab) (239) GTTAAGTTATAGTGAATACTGCTACAGCAATTTCTAATTTTTAAGAATTG
NM_007614(mmu) (602) GTTATGTTCTAGTGAAC-CTGCTACAGCAATTTCTGATTTCTAAGAACCG
NM_001076141(bta) (379) GTTAAGTTATAGTGAATACTGCTACAGCAATTTCTAATTTTTAAGAATCG
NM_214367(ssc) (227) GTTAAGTTATAGTGAATACTGCTACAGCAATTTCTAATTTTTAAGAATTG
----------QRE1----ACTAAY----------TAAY
NM_001904(hsa) (750) AGTAATGGTGTAGAA-CACTAATTCATAATCACTCTAATTAATTGTAATC
NM_001098209(hsa) (445) AGTAATGGTGTAGAA-CACTAATTCATAATCACTCTAATTAATTGTAATC
NM_001098210(hsa) (286) AGTAATGGTGTAGAA-CACTAATTCATAATCACTCTAATTAATTGTAATC
NM_001133265(pab) (289) AGTAATGGTGTAGAA-CACTAATTCATAATCACTCTAATT----GTAATC
NM_007614(mmu) (651) AGTAATGGTGTAGAA-CACTAATTCATAATCAGCTAATT----GTAATC
NM_001076141(bta) (429) AGTAATGGTGTAGAAACACTAATTCATAATCACTCTAATT----GTAATC
NM_214367(ssc) (277) AGTAATGGTGTAGAA-CACTAATTCATAATCACTCTAATT----GTAATC
NM_001904(hsa) (799) TGAATAAAGTGTAACAATTGTGTAGCCTTTTTGTATAAAATAGACAAATA
NM_001098209(hsa) (494) TGAATAAAGTGTAACAATTGTGTAGCCTTTTTGTATAAAATAGACAAATA
NM_001098210(hsa) (335) TGAATAAAGTGTAACAATTGTGTAGCCTTTTTGTATAAAATAGACAAATA
NM_001133265(pab) (334) TGAATAAAGTGTAACA-TTGTGTAGCCTTTTTGTATAAAATAGACAAATA
NM_007614(mmu) (696) TGG-AGACGTGTAACA-TTGTGTAGCCTTTT-GTATAAA-TAGACAGATA
NM_001076141(bta) (475) TGA-TAAAGTGTAACA-TTGTGTAGCCTTTTTGTATAAAATAGACAAATA
NM_214367(ssc) (322) TGAATAAAGTGTAACA-TTGTGTAGCCTTTTTGTATAAAATAGACAAATA

Fig. S4

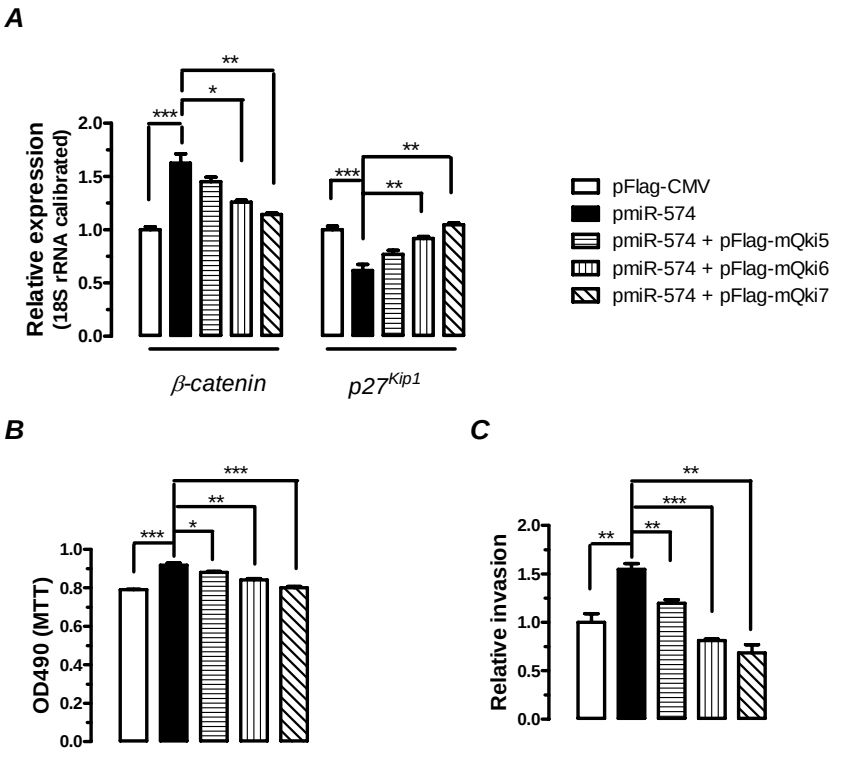
A
Relative expression (18S rRNA calibrated)
2.0
1.5
1.0
0.5
0.0
***
*
**
***
**
**
β-catenin
p27Kip1
pFlag-CMV
pmiR-574
pmiR-574 + pFlag-mQki5
pmiR-574 + pFlag-mQki6
pmiR-574 + pFlag-mQki7
B
OD490 (MTT)
1.0
0.8
0.6
0.4
0.2
0.0
***
**
*
***
C
Relative invasion
2.0
1.5
1.0
0.5
0.0
**
**
***
**

Fig. S5

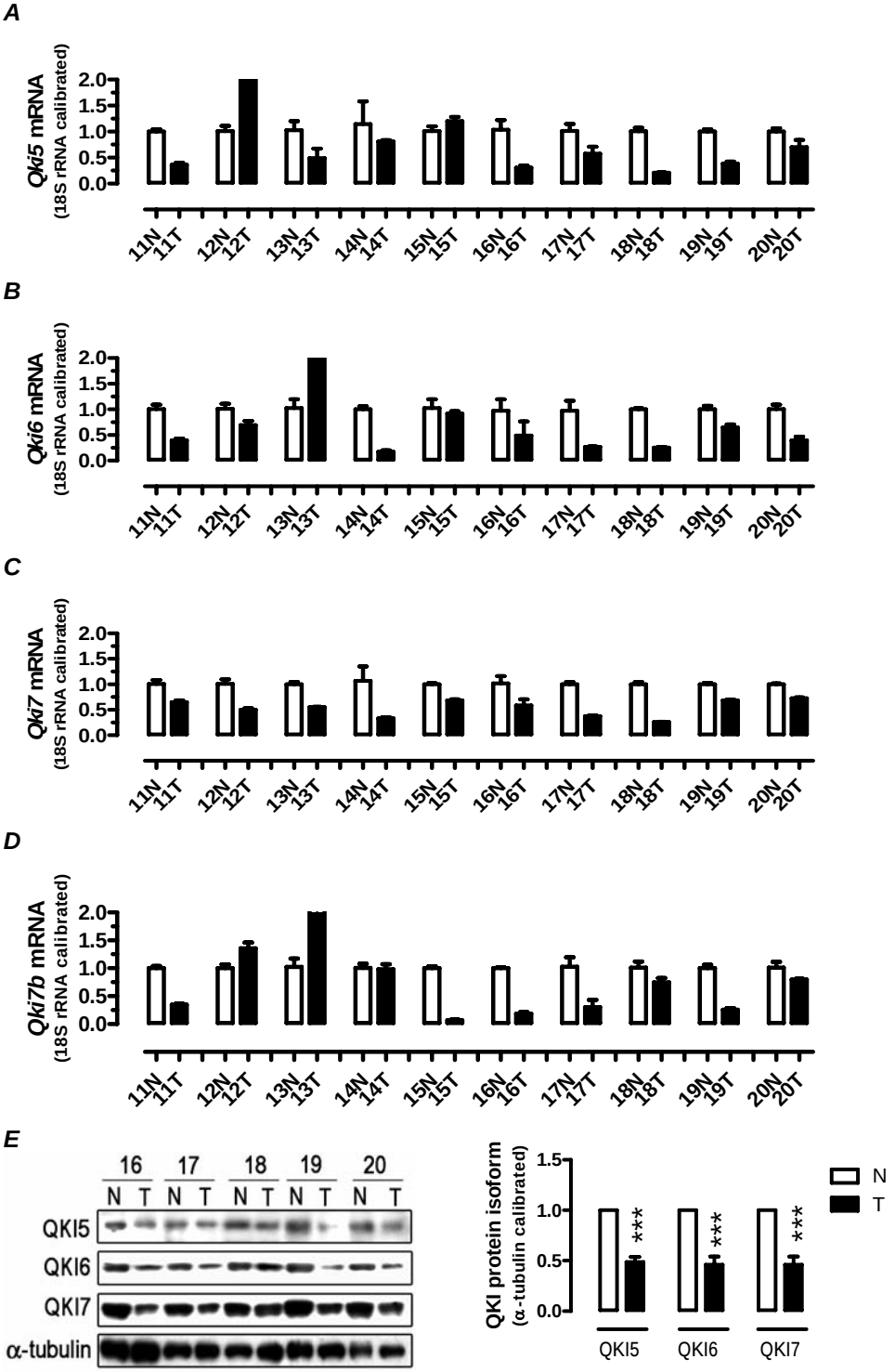
A
Qki5 mRNA
(18S rRNA calibrated)
B
Qki6 mRNA
(18S rRNA calibrated)
C
Qki7 mRNA
(18S rRNA calibrated)
D
Qki7b mRNA
(18S rRNA calibrated)
2.0
1.5
1.0
0.5
0.0
11N 11T 12N 12T 13N 13T 14N 14T 15N 15T 16N 16T 17N 17T 18N 18T 19N 19T 20N 20T
E
16 17 18 19 20
N T N T N T N T N T
QKI5
QKI6
QKI7
α-tubulin
QKI protein isoform
(α-tubulin calibrated)
***
N
T
QKI5 QKI6 QKI7

Fig. S6

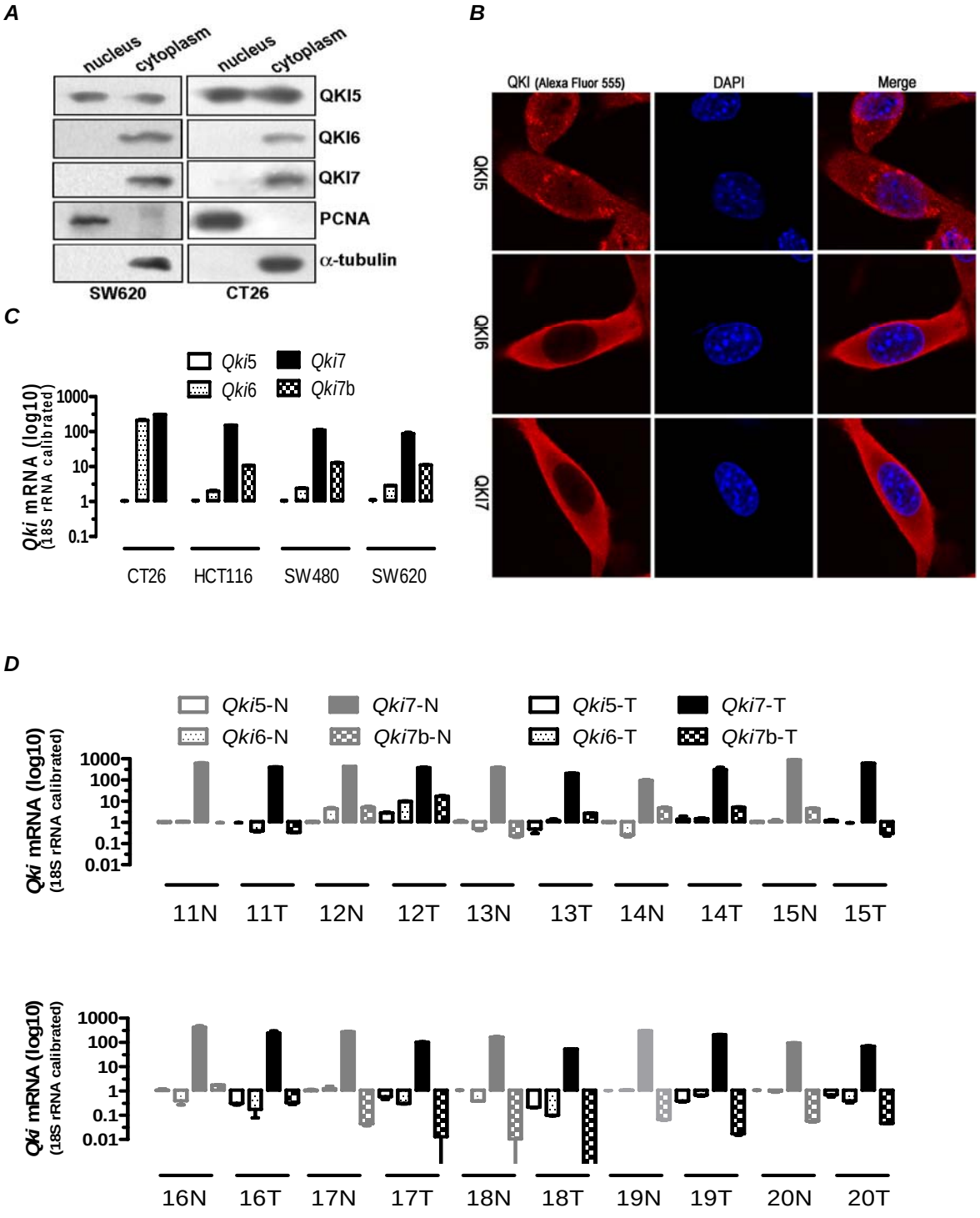
A
nucleus
cytoplasm
nucleus
cytoplasm
QKI5
QKI6
QKI7
PCNA
α-tubulin
SW620
CT26
B
QKI (Alexa Fluor 555)
DAPI
Merge
QKI5
QKI6
QKI7
C
Qki5
Qki7
Qki6
Qki7b
Qki mRNA (log10)
(18S rRNA calibrated)
1000
100
10
1
0.1
CT26
HCT116
SW480
SW620
D
Qki5-N
Qki7-N
Qki5-T
Qki7-T
Qki6-N
Qki7b-N
Qki6-T
Qki7b-T
Qki mRNA (log10)
(18S rRNA calibrated)
1000
100
10
1
0.1
0.01
11N
11T
12N
12T
13N
13T
14N
14T
15N
15T
16N
16T
17N
17T
18N
18T
19N
19T
20N
20T

Fig. S7

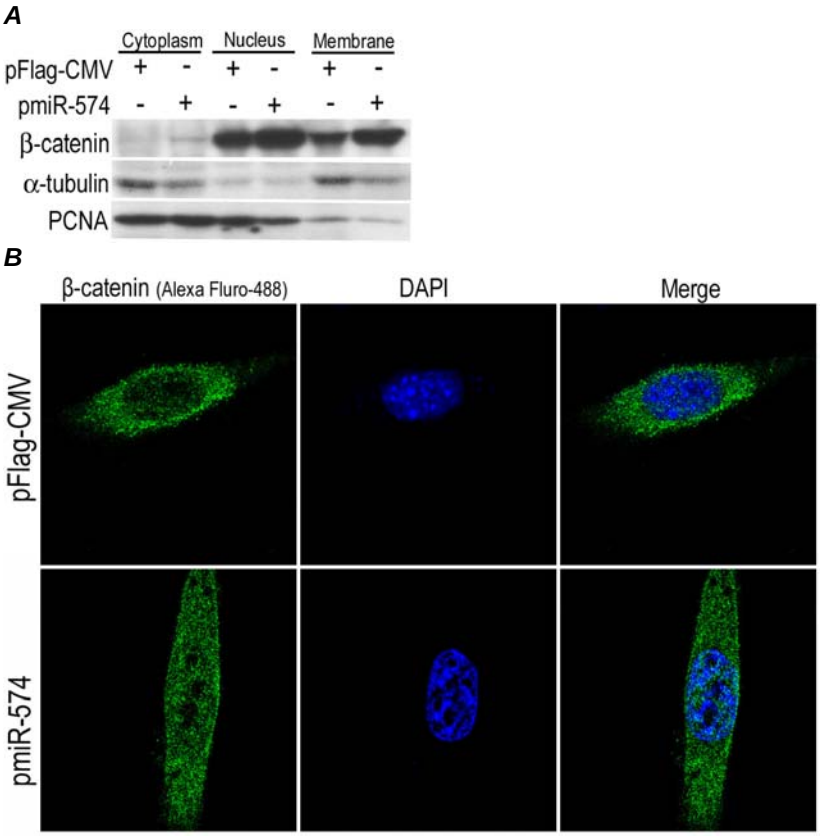
A
Cytoplasm
Nucleus
Membrane
pFlag-CMV + - + - + -
pmiR-574 - + - + - +
β-catenin
α-tubulin
PCNA
B
β-catenin (Alexa Fluro-488)
DAPI
Merge
pFlag-CMV
pmiR-574

Fig. S8

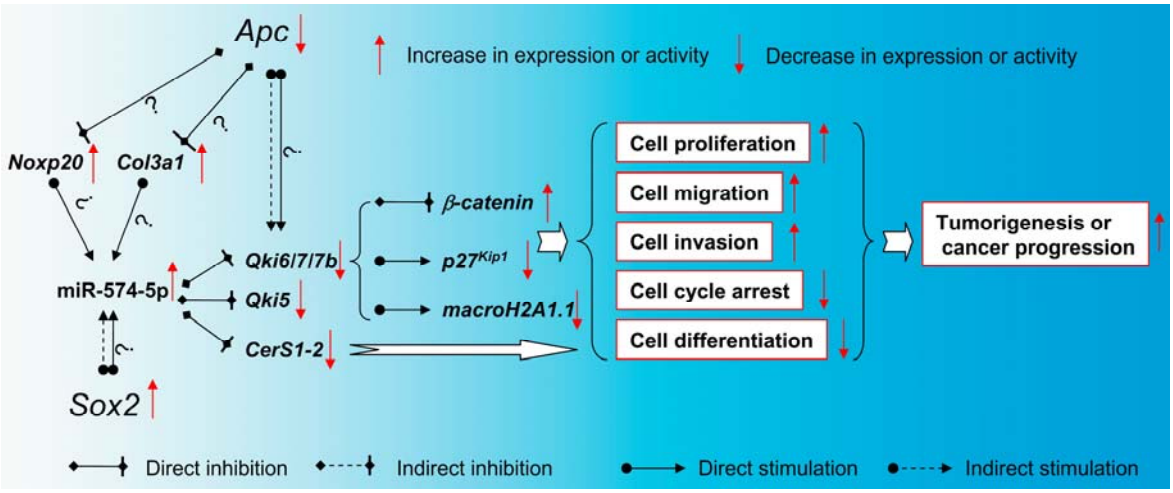
Apc
Increase in expression or activity
Decrease in expression or activity
Noxp20
Col3a1
miR-574-5p
Qki6/7/7b
Qki5
CerS1-2
Sox2
β-catenin
p27Kip1
macroH2A1.1
Cell proliferation
Cell migration
Cell invasion
Cell cycle arrest
Cell differentiation
Tumorigenesis or cancer progression
Direct inhibition
Indirect inhibition
Direct stimulation
Indirect stimulation

Fig. S9

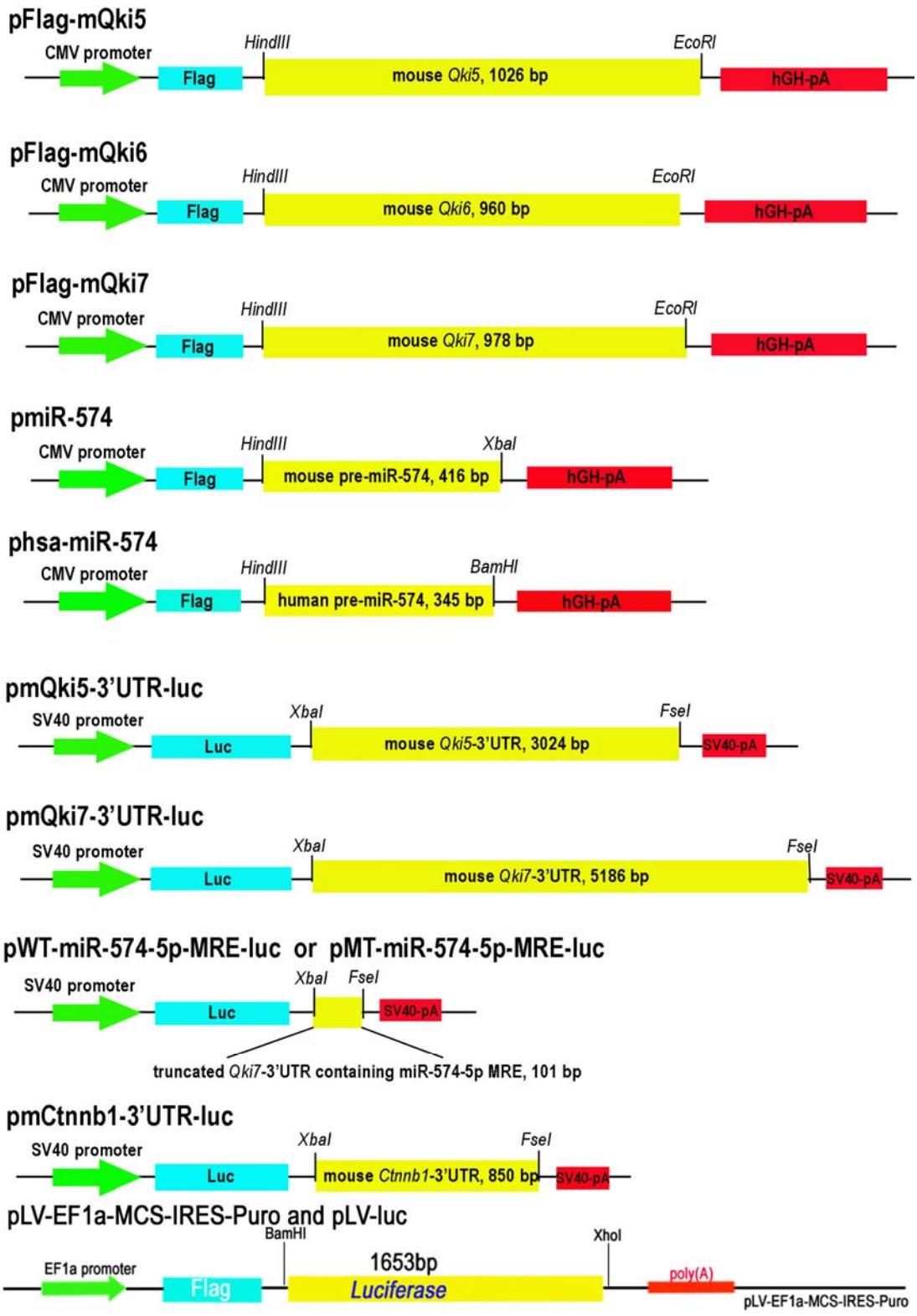
pFlag-mQki5
CMV promoter
Flag
HindIII
mouse Qki5, 1026 bp
EcoRI
hGH-pA
pFlag-mQki6
CMV promoter
Flag
HindIII
mouse Qki6, 960 bp
EcoRI
hGH-pA
pFlag-mQki7
CMV promoter
Flag
HindIII
mouse Qki7, 978 bp
EcoRI
hGH-pA
pmiR-574
CMV promoter
Flag
HindIII
mouse pre-miR-574, 416 bp
XbaI
hGH-pA
phsa-miR-574
CMV promoter
Flag
HindIII
human pre-miR-574, 345 bp
BamHI
hGH-pA
pmQki5-3'UTR-luc
SV40 promoter
Luc
XbaI
mouse Qki5-3'UTR, 3024 bp
FseI
SV40-pA
pmQki7-3'UTR-luc
SV40 promoter
Luc
XbaI
mouse Qki7-3'UTR, 5186 bp
FseI
SV40-pA
pWT-miR-574-5p-MRE-luc or pMT-miR-574-5p-MRE-luc
SV40 promoter
Luc
XbaI
FseI
SV40-pA
truncated Qki7-3'UTR containing miR-574-5p MRE, 101 bp
pmCtnnb1-3'UTR-luc
SV40 promoter
Luc
XbaI
mouse Ctnnb1-3'UTR, 850 bp
FseI
SV40-pA
pLV-EF1a-MCS-IRES-Puro and pLV-luc
EF1a promoter
Flag
BamHI
1653bp
Luciferase
XhoI
poly(A)
pLV-EF1a-MCS-IRES-Puro

Table S1

		n	**%**	**miR-574-5p (Normalized)**	**Pan-*Qki* mRNA (Normalized)**	**Pan-QKI protein (Normalized)**
Gender	M	40	67.7	3.136 ± 0.5718	0.8483 ± 0.1774	0.7554 ± 0.0977
	F	20	33.3	2.793 ± 0.532	0.7278 ± 0.1335	0.7882 ± 0.0929
Age	≤60	28	46.7	3.238 ± 0.8269	0.9206 ± 0.2304	0.7509 ± 0.094
	>60	32	53.3	2.843 ± 0.3409	0.7134 ± 0.1315	0.7789 ± 0.1097
TNM stage	I	8	13.3	5.737 ± 2.546	0.9503 ± 0.4494	0.8613 ± 0.3316
	II	15	25	2.666 ± 0.5652	1.115 ± 0.412	0.8046 ± 0.1773
	III	36	60	2.593 ± 0.3291	0.6608 ± 0.082	0.7292 ± 0.0674
	IV	1	1.7	2.415	0.4825	0.74
Lymph node status	N0	23	38.4	3.734 ± 0.9734	1.058 ± 0.3051	0.8243 ± 0.1589
	N1	17	28.3	2.549 ± 0.5684	0.7131 ± 0.1462	0.7564 ± 0.0935
	N2	20	33.3	2.621 ± 0.3574	0.6075 ± 0.0828	0.7066 ± 0.0935
	N3	0				

Table S2

Organism	Condition	miR-574-5p expression	Affected cells or tissues	Fold change	References
Human	CRC	Up	Colorectal cells	Very significant	Current study
Human	Pituitary adenomas	Up	Pituitary tissue	2.89	[23]
Human	Systemic lupus erythematosus	Up	T lymphocyte	> 2	[24]
Human	Pancreatic cancer	Up	Pancreatic tissue	51	[25]
Human	Lymphoma	Altered	Lymphocyte	?	[26]
Human	Myocardial infarction	Up	Heart	Very significant	[27]
Human	Non-small cell lung cancer	Up	Lung	2.17	[20]
Human	Small cell lung cancer	Altered	Lung	?	[21]
Human	Eosphageal squamous cell carcinoma	Up	Eosphageal squamous cells	1.72	[22]
Human	Alzheimer's	Up	Gray matter	?	[28]
Human	Schizophrenia	Altered	Brain tissue	?	[29]
Human	Mitral stenosis	Up	Right atrial appendage	1.96	[30]
Human	Ovarian cancer	Up	Ovary tissue	1.24	[31]
Mouse	CRC	Up	Colorectal cells	3.7	Current study
Mouse	Vesicular stomatitis virus infection	Up	Macrophage	?	[32]
Mouse	Asthma	Up	Lung cells	13	[33]
Mouse	SARS infection	Altered	Bronchoalveolar stem cells	?	[34]
Mouse	Liver injury	Up	Liver/plasma	3.4/1.49	[35]

2. SUPPLEMENTAL MATERIALS AND METHODS

Plasmids.TOP/FOP-Flash plasmids and the Wnt1-overexpressing (Wnt1) plasmid were kind gifts from Prof. Qiao Wu, Xiamen University.

For *Qki* overexpression plasmids, primers were designed based on the genomic sequences from the NCBI databases, with the forward primer carrying a *HindIII* site and the reverse primer carrying an *EcoRI* respectively. Mouse *Qki5*, *Qki6*, *Qki7* were individually PCR-amplified using mouse brain tissue cDNA and appropriate primers (see List of primers used for miRNA or *Qki* overexpression plasmids), with the LA Taq DNA Polymerase (TaKaRa, Dalian). The resultant DNA fragments were subcloned into pFlag-CMV (Sigma Aldrich, St. Louis, MO, USA) using the *HindIII* and *EcoRI* sites.

For mouse miRNA overexpressing plasmids, primers were designed based on the genomic sequences from the miRBase (microrna.sanger.ac.uk), with the forward primers carrying a *HindIII* site and the reverse primers carrying a *XbaI* site respectively. Pre-miRNA gene fragments were individually PCR-amplified using genomic DNA prepared from mouse inner medullary collecting duct epithelial mIMCD3 cells (mmu-miR-574) or human CRC SW480 cells (hsa-miR-574) and appropriate primers (see List of primers used for miRNA or *Qki* overexpression plasmids), with Pyrobest DNA Polymerase (TaKaRa). The resultant DNA fragments were subcloned into pFlag-CMV, using the *HindIII* and *XbaI* (mmu-miR-574) or *HindIII* and *BamHI* (hsa-miR-574) sites. The insertion sequences of the resultant plasmids were confirmed by sequencing.

For the construction of mouse *Qki5*-3'UTR, wildtype *Qki7*-3'UTR miR-574-5p MRE, mutant *Qki7*-3'UTR miR-574-5p MRE and *Ctnnb1* luciferase reporters, mouse 3'UTR regions were amplified from mouse brain tissue cDNA through PCR amplification with the LA Taq DNA Polymerase (TaKaRa) and appropriate primers (see List of primers used for the construction of five luciferase reporters). The resultant PCR fragments carrying a *NheI* site and a *FseI* site was subcloned into the pGL3-control vector (Promega), using the *XbaI* and *FseI* sites immediately downstream of the stop codon of the luciferase cDNA, generating pmQki5-3'UTR-luc, pmQki7-3'UTR-luc, pWT-miR574-5p-MRE-luc, pMT-miR574-5p-MRE-luc and pmCtnnb1-3'UTR-luc respectively.

For the construction of lentiviral plasmid carrying a luciferase gene, the luciferase reporter gene on pladmid pGL3 (Promega, USA) was PCR amplified and a *BamHI-XhoI* insert gene cassette was inserted

into a lentiviral vector pLV-EF1a-MCS-IRES-Puro (A gift from Prof. Jiahuai Han) to obtain a plasmid pLV-luc.

The resulting twelve plasmids are shown in Fig. S9 in the previous section.

Cell culture and transient transfections. Mouse CT26, human SW480 and SW620 CRC cells were obtained from ATCC (Manassas, VA, USA), human HCT116 CRC cells was obtained from the Chinese Academy of Sciences (Shanghai, China). CT26 cells and HCT116 cells were normally cultured in RPMI 1640 with 10% fetal bovine serum (FBS). SW480 and SW620 cells were cultured in DMEM supplemented with 10% FBS. Plasmids, miRNA mimics and inhibitor transfections were performed with Lipofectamine 2000 reagent (Invitrogen, Carlsbad, CA, USA) according to the manufacturer's protocols.

Western blot, immunohistochemistry, immunofluorescence and in situ hybridization analyses. Western blots were performed according to standard protocols. The detection was achieved using the Immobilon Western Chemiluminescent HRP Substrate kit (Millipore, Billerica, MA, USA). Antibodies and the dilutions are anti-α-tubulin (sc-5286, Santa Cruz, 1:10000); anti-β-actin (sc-47778, Santa Cruz, 1:20000); anti-pan-QKI (sc-103851, Santa Cruz, 1:2000); anti-QKI5 (AB9904, Millipore, 1:2000); anti-QKI6 (AB9906, , Millipore, 1:2000); anti-QKI7 (AB9908, Millipore, 1:2000); anti-$p27^{Kip1}$ (sc-528, Santa Cruz, 1:2000); anti-β-catenin (sc-7199, Santa Cruz, 1:2000); anti-PCNA (sc-7907, Santa Cruz, 1:2000); Alexa Fluor 555-labeled goat Anti-Rabbit IgG (H+L) (A0452, Beyotime Institute of Biotechnology, 1:500) respectively.

Immunohistochemistry was performed with an instant-type SABC immunohistochemistry kit purchased from the Boster Bioengineering Company (Wuhan, China) as instructed. Briefly, 5 um fixed tissue sections were microwave-heated for 10 min for antigen retrieval. Slides were washed and incubated with primary antibody for 1 hour followed by incubation with instant-type secondary antibody for 30 minutes at room temperature. After being thoroughly washed with PBS (pH 7.5), the tissues were incubated with SABC (Strept-Avidin-Biotin Complex) for 20 minutes at room temperature. After washing thoroughly, 100-200 μl freshly-made diaminobenzidine (DAB) solution was added to each slide. After incubation for ~10 minutes, sections were lightly counter-stained with hematoxylin.

For immunofluorescence analyses, cells seeded on cover glass overnight were fixed in 4% paraformaldehyde. Fixed cells were incubated with anti-QKI5, QKI6 or QKI7 primary antibody

respectively, followed by incubation with Alexa Fluor® 555-conjugated secondary antibody or Alexa Fluor® 488-conjugated secondary antibody (Beyotime Institute of Biotechnology, Jiangsu, China). Cell nuclei were stained by DAPI (Beyotime Institute of Biotechnology). Stained cells were visualized and photographed with a Leica-TCS-SP2-SE confocal microscope.

In situ hybridization of miRNAs was performed as described [36]. miRCURY^{TM} LNA miRNA probes (hsa-miR-574-5p, 5'-ACACACTCA-CACACACACACTCA-3'; hsa-miR-200b, 5'-TCATCATTACCAGGCAGTATTA-3'; U6, 5'-CACGAATTTGCGTGTCATCCTT-3'; Scramble-miR, 5'-GTGTAACACGTCTATACGCCCA-3') were purchased from Exiqon (Copenhagen, Denmark).

qPCR analyses of mRNAs and miRNAs. For qPCR mRNA quantification, reverse transcription was performed with TRIzol (Invitrogen)-extracted total RNAs using a ReverTra Ace-α-® Kit as instructed (TOYOBO, Shanghai). qPCR was performed by using the SYBR Green qPCR Master Mix (TOYOBO) and the StepOne Plus qPCR system (Applied Biosystems Inc., Foster City, CA) according to the manufacturer's protocols and with the primer pairs listed below.

For miRNAs, qPCR was performed with the stem-loop primers as described previously [37] using the miRNA-specific reverse transcription primers, the universal primer and the miRNA-specific reverse locked nucleic acid (LNA)-primers as described below.

Cell cycle, proliferation, migration, invasion and colony formation assays. For cell cycle analysis, 5×10^5 cells were synchronized by serum starvation for 24 hours and induced to re-enter the cell cycle by replacing old media with a fresh media containing 10% fetal bovine serum (FBS) for 24 hours. Cells were harvested and fixed in 75% ethanol at 4 ºC overnight. Cells were incubated with RNase A at 37 ºC for 30 min, and then stained with propidium iodide. The cell cycle phases were measured by flow cytometry.

Cell proliferation was analyzed by the MTT assay. A total of 4×10^3 cells was seeded in 96-well plates and MTT was added to each well every 24 hours. The plates were incubated for 4 hours before the addition of 10% SDS (in 0.01M HCl) (Sigma Aldrich, St. Louis, MO, USA). The absorbance was measured at 490 nm using a microplate reader.

Cell migration was analyzed by the wound-healing assays. SW480 cells were seeded onto 6-well plates. After transfection, a wound was incised in the center of the confluent culture, followed by careful washing to remove detached cells and the addition of fresh medium. Phase contrast images of the wounded

area were recorded using an inverted microscope at indicated time points.

Matrigel invasion assays were performed using Millicell inserts coated with matrigel (BD Biosciences, Sparks, MD, USA). 5×10^4 CT26 cells were seeded per upper chambers in serum-free RPMI1640 whereas the lower chambers were loaded with RPMI1640 containing 5% FBS. After 48 hours, the non-migrating cells on the upper chambers were removed by a cotton swab, and cells invaded through the matrigel layer to the underside of the membrane were stained with a 0.1% crystal violet solution and counted manually in eight random microscopic fields.

For colony formation assays, control and miRNA inhibitor or LV-miR-shRNA (Supplemental Materials and Methods section, Supplementary Information) transfected SW480 cells were seeded on six-well plates and maintained in DMEM containing 10% FBS for 2 weeks. Cells were fixed with methanol and stained with 0.5% crystal violet in 50% methanol for 1 hour and colonies larger than 100 μm in diameter were counted.

Luciferase reporter assays and IAP enzyme activity assays. Luciferase reporter activities were determined using a Luciferase Reporter Gene Assay System (Promega, Madison, WI, USA) as instructed. For all luciferase assays, β-galactosidase activities were determined to calibrate the transfection efficiency. The calibrated value for a proper control was used to normalize all other values to obtain the normalized relative luciferase units (RLU) representing the activities of 3'UTRs.

The enzyme activity of IAP was measured by an IAP kit (Jiancheng, Nanjing, China) according to the manufacturer's instructions. Protein concentration was measured by the Pierce BCA kit (Pierce Biotechnology, Rockford, USA).

Bioluminescence imaging of tumor growth in live animals. Briefly, CT26 cells were transfected with a luciferase-overexpressing plasmid or its control vector (pLV-luc or pLV-EF1a-MCS-IRES-Puro). Stable clones of cells overexpressing luciferase were selected with the addition of 8-10 μg/ml puromycin in the media for 3 weeks (Invitrogen, Carlsbad, CA, USA). Luciferase-overexpressing cells or its controls were subsequently injected into the nude mice intraperitoneally (5×10^5 cells/mouse). Starting from the third day after CT26 cell inoculation, each mouse was injected with 2×10^7 transducing units of control lentiviruses or lentiviruses carrying shRNA for miR-574-5p once a week for 2 weeks. Three days after lentiviral injection, the mice were subjected to bioluminescence imaging under an IVIS Lunina II *in vivo* imaging system

(Xenogen, Hopkinton, MA, USA) as described by Lan et al. [38] every other three days. Ten minutes prior to imaging, each mouse was injected with 100 ul D-luciferin solution (15 mg/ml in PBS, Promega #E1602) by i.p. injection. Immediately before imaging taking, the experimental mice were anesthetized using an XGI-8 Gas Anesthesia System (Xenogen). Images and amount of bioluminescent signals were analyzed using Living Image software (Xenogen).

Serum miRNA preparations and analyses. Total RNA from serum was extracted using a miRVana miRNA isolation kit (Ambion, Austin, TX, USA) according to the manufacturer's protocol. RNA was eluted in nuclease free water at 95°C. Five microliters of total RNA was reverse transcribed using the ReverTra Ace-α-® Kit as instructed (TOYOBO, Shanghai) and miRNA-specific stem-loop primersas shown in the Materials and Mathods section. has-miR-16-5p served as an internal control. Visible and dissectable peritoneal tumors were dissected and weighted.

Bioinformatics, data acquisition, image processing and statistical analyses. Mature and pre-miRNA sequences were based on miRBase (microrna.sanger.ac.uk). miRNA target predictions were performed with the miRanda (www.microrna.org) algorithm. Western blot images were captured by Biosense SC8108 Gel Documentation System with GeneScope V1.73 software (Shanghai BioTech, Shanghai, China). Gel images were imported into Photoshop for orientation and cropping. The digital density values were acquired by Image-Pro Plus software (Media Cybernetics) and analyzed by Graphpad Prism 5.0. Data are the means ± SEM. One-way ANOVA with Bonferonni's post-test was used for multiple comparisons and the Student's *t*-test (two-tailed) for pair-wise comparisons. The correlation analyses were performed with Pearson's test.

List of primers used for the construction of miRNA or Qki overexpression plasmids

Plasmid	Primer sequence (from 5'→3')	Gene ID	Amplicon (bp)
pFlag-mQki5 (mouse)	Forward:CCCAAGCTTATGGTCGGGGAAATGGAAAC Reverse:CCGGAATTCTTAGTTGCCGGTGGCGGCTC	NM_001159517 (Genbank)	1026
pFlag-mQki6 (mouse)	Forward:CCCAAGCTTATGGTCGGGGAAATGGAAAC Reverse:CCGGAATTCTTAGCCTTTCGTTGGGAAAG	NM_001159516 (Genbank)	960
pFlag-mQki7 (mouse)	Forward:CCCAAGCTTATGGTCGGGGAAATGGAAAC Reverse:CCGGAATTCTCAATGGGCTGAAATATCAG	NM_021881 (Genbank)	978
pmiR-574 (mouse)	Forward: CCCAAGCTTTGTCCGCTGTAGGGTGTGAGAA Reverse: TGCTCTAGAATCAGGATGGAGGTCAAGGCCT	MI0005518 (miRBase)	416
phsa-miR-574 (human)	Forward： CCCAAGCTTCCTCTGCGTTAGTGAGAAGCAG Reverse： GCGGGATCCTCTGTCTTACAGGGACCTGCTC	MI0003581 (miRBase)	345

List of primers used for the construction of six luciferase reporters.

Plasmid	Primer sequence (from 5'→3')	Gene ID	Amplicon length and location
pmQki5-3'UTR-luc	Forward: TGCGCTAGCTATGACCTTCTGACCTCTGAACTCT Reverse: ACTGGCCGGCCTATGGGTTAATAGAAACAGCAAAGA	*mQki5* NM_001159517	(NTs 1517-4540) 3024 bp
pmQki7-3'UTR-luc	Forward: TGCGCTAGCCTTGCTGGATGAAGGACTAGA Reverse: ACTGGCCGGCCTTGGCCTCATGATACAAAGCAATAC	*mQki7* NM_021881	(NTs 1467-6652) 5186 bp
pWT-miR574-5p-MRE-luc	Forward: TGCTCTAGACTTTGTTAAGTAATCCACACTC Reverse: ACTGGCCGGCCAACGGTTGTCCCATAGTCTTAA	*mQki7* NM_021881	(NTs 5650-5750) 101bp
pMT-miR574-5p-MRE-luc	Forward: TGCTCTAGACTTTGTTAAGTAATCCGCACGC Reverse: ACTGGCCGGCCAACGGTTGTCCCATAGTCTTAA	*mQki7* NM_021881	(NTs 5650-5750) 101 bp
pmCnnb1-3'UTR-luc	Forward: TGATCTAGAAAGACTTGGTAGGGTGGGAATGG Reverse: ACTGGCCGGCCGCAGGTTACAACAACTTTGGGAT	Mouse β-catenin NM_001904	(NTs 2707-3557) 850 bp
pLV-luc	Forward: AGAGAATTCGGATCCATGGAAGACGCCAAAAACATAA Reverse: CCATGGCTCGAGCCCTTACACGGCGATCTTTCCG	pGL3 (Promega)	1365 bp

List of miR-mimics, anti-miRs, lentiviral miR-shRNAs and LNA-probes for miRNA in situ hybridization.

Name	Sequence or target (5'→3')	Catalog #	Supplier
mimics-ctrl	Scrambled		GenePharma, Shanghai
miR-574-5p mimics	UGAGUGUGUGUGUGAGUGUGU ACACUCACACACACACACUCAUU		GenePharma, Shanghai
anti-miR-ctrl	Scrambled		GenePharma, Shanghai
anti-miR-574-5p	UGAGUGUGUGUGUGAGUGUGU	AM17000	Ambion
LV-miR-shRNA-ctrl	TTCTCCGAACGTGTCACGT	pLVT4	Sunbio, Shanghai
LV-miR-574-5p-shRNA	ACACACTCACACACACACACTCA	pLVT278	Sunbio, Shanghai
Scrambled miRNA	GTGTAACACGTCTATACGCCCA/3Dig	99004-05	Exiqon, Copenhagen
U6 probe	CACGAATTTGCGTGTCATCCTT/3Dig	99002-05	Exiqon, Copenhagen
hsa-miR-574-5p probe	ACACACTCACACACACACACTCA//3Dig	38674-05	Exiqon, Copenhagen

List of primers used for qPCR analyses of mRNAs.

Organism	Gene	Gene ID	Primer sequence (5'→3')	Amplicon (bp)
Human	pan-*Qki*	NM_006775 NM_206853 NM_206854 NM_206855	Forward:CATCAGCTGCATCTTCTTCAG Reverse:CACTGTGGAAGATGCTCAGAA	121
	Qki5	NM_006775	Forward:GCCCTACCATAATGCCTTTGA Reverse:AACTTTAGTAGCCACCGCAACC	211
	Qki6	NM_206853	Forward:GCCCGAAGCTGGTTTAATCTATA Reverse:TCGTTGGGAAAGCCATACCTAAT	118
	Qki7	NM_206854	Forward:GCTGGTTTAATCTATACACCCTATGA Reverse:GACTGGCATTTCAATCCACTCTA	113
	Qki7b	NM_206855	Forward:AATGCCTTTGATCAGACAAATACAG Reverse:TGGGGAGAAGAACTTACCTAATACA	198
	β-catenin	NM_001904	Forward:AGCCACAAGATTACAAGAAACGG Reverse:ATCCACCAGAGTGAAAAGAACGA	173
	$p27^{Kip1}$	NM_004064	Forward:GGGGCTCCGGCTAACTCTGA Reverse:AGGCTTCTTGGGCGTCTGCT	215
	18S rRNA	NR_003286.2	Forward:CGACGACCCATTCGAACGTCT Reverse:CTCTCCGGAATCGAACCCTGA	102
Mouse	pan-*Qki*	NM_001159517 NM_001159516 NM_021881	Forward:TAGAGGACTTACAGCTAAACAACT Reverse:ATTCAGAATTGCAAGCTCCATCA	288
	Qki5	NM_001159517	Forward:GCCCTACCATAATGCCTTTGA Reverse:AACTTTAGTAGCCACCGCAACC	211
	Qki6	NM_001159516	Forward:GCCTGAAGCTGGGTTAATCTACA Reverse:TCGTTGGGAAAGCCATACCTAAC	118
	Qki7	NM_021881	Forward:GCTGGGTTAATCTACACACCCTATGA Reverse:GACTGGCATTTCAATCCACTCTA	113
	β-catenin	NM_007614	Forward:TGGACCCCAAGCCTTAGTAAACA Reverse:GTCTGTCAGATGAAGCCCCAGTG	159

	Lactase	NM_001081078	Forward:GAGACCCAGAACTCAATGACACC Reverse:GGTCAGAGCGGTTCACAAAGT	165
	p27^{Kip1}	NM_009875	Forward:GCGGTGCCTTTAATTGGGTCT Reverse:TCTTGGGCGTCTGCTCCACA	225
	Col3a1	NM_009930	Forward:GTTTCTTCTCACCCTTCTTCATCCC Reverse:GCAGTCTAGTGGCTCCTCATCACA G	196
	Noxp20	NM_026667	Forward:AGGGAGACACCGGATCTGAAATA Reverse:GAATTGGCAGTGTGGATTCGTAG	199
	Sox2	NM_011443	Forward: GCGGAGTGGAAACTTTTGTCC Reverse: GGGAAGCGTGTACTTATCCTTCT	156

List of conventional or LNA-primers for qPCR analyses of U6 and miRNAs.

RNA or miRNA	Genbank or miRBase seq#	Primer sequence (5'→3')
Mouse and human U6	NR_004394.1	Reverse transcription: CGCTTCACGAATTTGCGTGTCAT Forward: GCTTCGGCAGCACATATACTAAAAT Reverse: CGCTTCACGAATTTGCGTGTCAT (LNA)
hsa-miR-16-5p	MI0000070	Reverse transcription: GTCGTATCCAGTGCGTGTCGTGGAGTCGGCAATTGCA CTGGATACGACTCGCCAA Forward: GGGGTAGCAGCACGTAAA Reverse: TGCGTGTCGTGGAGTC (LNA)
mmu-miR-574-5p	MI0005518	Reverse transcription: GTCGTATCCAGTGCGTGTCGTGGAGTCGGCAATTGC ACTGGATACGACTACACAC Forward: GGGGTGAGTGTGTGTGTG Reverse: TGCGTGTCGTGGAGTC (LNA)
hsa-miR-574-5p	MI0003581	Reverse transcription: GTCGTATCCAGTGCGTGTCGTGGAGTCGGCAATTGC ACTGGATACGACTACACAC Forward： GGGGTGAGTGTGTGTGTG Reverse： TGCGTGTCGTGGAGTC (LNA)
mmu-miR-200b	MI0000243	See Huang et al. [37]
mmu-miR-717	MI0004704	See Huang et al. [37]
mmu-miR-466g	MI0005510	Reverse transcription: GTCGTATCCAGTGCGTGTCGTGGAGTCGGCAATTGC ACTGGATACGACTGTGTGT Forward： GGGGATACAGACACATGC Reverse：TGCGTGTCGTGGAGTC (LNA)
mmu-miR-17	MI0000687	Reverse transcription: GTCGTATCCAGTGCGTGTCGTGGAGTCGGCAATTGC ACTGGATACGACTCTACCT Forward：GGGGCAAAGTGCTTACAG Reverse：TGCGTGTCGTGGAGTC (LNA)
mmu-miR-20a	MI0000568	Reverse transcription: GTCGTATCCAGTGCGTGTCGTGGAGTCGGCAATTGC ACTGGATACGACTCTACCT

	Forward：GGGGTAAAGTGCTTATAG
	Reverse：TGCGTGTCGTGGAGTC (LNA)

3. SUPPLEMENTAL REFERENCES

1 Bockbrader K, Feng Y. Essential function, sophisticated regulation and pathological impact of the selective RNA-binding protein QKI in CNS myelin development. *Future Neurol* 2008;**3**(6):655-68.

2 Klempan TA, Ernst C, Deleva V *et al*. Characterization of QKI gene expression, genetics, and epigenetics in suicide victims with major depressive disorder. *Biol Psychiatry* 2009;**66**(9):824-31.

3 Li ZZ, Kondo T, Murata T *et al*. Expression of Hqk encoding a KH RNA binding protein is altered in human glioma. *Jpn J Cancer Res* 2002;**93**(2):167-77.

4 Yang G, Fu H, Zhang J *et al*. RNA-binding protein quaking, a critical regulator of colon epithelial differentiation and a suppressor of colon cancer. *Gastroenterology* 2010;**138**(1):231-40.

5 Meyers-Needham M, Ponnusamy S, Gencer S *et al*. Concerted functions of HDAC1 and microRNA-574-5p repress alternatively spliced ceramide synthase 1 expression in human cancer cells. *EMBO Mol Med* 2011.

6 Novikov L, Park JW, Chen H *et al*. QKI-mediated alternative splicing of the histone variant MacroH2A1 regulates cancer cell proliferation. *Mol Cell Biol* 2011;**31**(20):4244-55.

7 Takahashi K, Tanabe K, Ohnuki M *et al*. Induction of pluripotent stem cells from adult human fibroblasts by defined factors. *Cell* 2007;**131**(5):861-72.

8 Takahashi K, Yamanaka S. Induction of pluripotent stem cells from mouse embryonic and adult fibroblast cultures by defined factors. *Cell* 2006;**126**(4):663-76.

9 Yu J, Vodyanik MA, Smuga-Otto K *et al*. Induced pluripotent stem cell lines derived from human somatic cells. *Science* 2007;**318**(5858):1917-20.

10 Ferri AL, Cavallaro M, Braida D *et al*. Sox2 deficiency causes neurodegeneration and impaired neurogenesis in the adult mouse brain. *Development* 2004;**131**(15):3805-19.

11 Archer TC, Jin J, Casey ES. Interaction of Sox1, Sox2, Sox3 and Oct4 during primary neurogenesis. *Dev Biol* 2011;**350**(2):429-40.

12 Episkopou V. SOX2 functions in adult neural stem cells. *Trends Neurosci* 2005;**28**(5):219-21.

13 Bylund M, Andersson E, Novitch BG *et al*. Vertebrate neurogenesis is counteracted by Sox1-3 activity. *Nat Neurosci* 2003;**6**(11):1162-8.

14 Saigusa S, Tanaka K, Toiyama Y *et al*. Correlation of CD133, OCT4, and SOX2 in rectal cancer and their association with distant recurrence after chemoradiotherapy. *Ann Surg Oncol* 2009;**16**(12):3488-98.

15 Fang X, Yu W, Li L *et al*. ChIP-seq and functional analysis of the SOX2 gene in colorectal cancers. *OMICS* 2010;**14**(4):369-84.

16 Wang Q, He W, Lu C *et al*. Oct3/4 and Sox2 are significantly associated with an unfavorable clinical outcome in human esophageal squamous cell carcinoma. *Anticancer Res* 2009;**29**(4):1233-41.

17 Sanada Y, Yoshida K, Ohara M *et al*. Histopathologic evaluation of stepwise progression of pancreatic carcinoma with immunohistochemical analysis of gastric epithelial transcription factor SOX2: comparison of expression patterns between invasive components and cancerous or nonneoplastic intraductal components. *Pancreas* 2006;**32**(2):164-70.

18 Fang X, Yoon JG, Li L *et al*. The SOX2 response program in glioblastoma multiforme: an integrated ChIP-seq, expression microarray, and microRNA analysis. *BMC Genomics* 2011;**12**:11.

19 Sholl LM, Barletta JA, Yeap BY *et al*. Sox2 protein expression is an independent poor prognostic indicator in stage I lung adenocarcinoma. *Am J Surg Pathol* 2010;**34**(8):1193-8.

20 Foss KM, Sima C, Ugolini D *et al*. miR-1254 and miR-574-5p: Serum-Based microRNA Biomarkers for Early-Stage Non-small Cell Lung Cancer. *J Thorac Oncol* 2011;**6**(3):482-8.

21 Ranade AR, Cherba D, Sridhar S *et al*. MicroRNA 92a-2*: a biomarker predictive for chemoresistance and prognostic for survival in patients with small cell lung cancer. *J Thorac Oncol* 2010;**5**(8):1273-8.

22 Liu H, Liu R, Su Y *et al*. [A pilot study of differentially expressed microRNAs between esophageal squamous cell carcinoma and adjacent tissues in Huai'an population]. *Carcinogenesis,Teratogenesis & Mutagenesis (Chinese)* 2010;**22**(6):418-22.

23 Mao ZG, He DS, Zhou J *et al*. Differential expression of microRNAs in GH-secreting pituitary adenomas. *Diagn Pathol* 2010;**5**:79.

24 Zhao S, Wang Y, Liang Y *et al*. MicroRNA-126 regulates DNA methylation in CD4+ T cells and contributes to systemic lupus erythematosus by targeting DNA methyltransferase 1. *Arthritis Rheum* 2011;**63**(5):1376-86.

25 Ali S, Almhanna K, Chen W *et al*. Differentially expressed miRNAs in the plasma may provide a molecular signature for aggressive pancreatic cancer. *Am J Transl Res* 2010;**3**(1):28-47.

26 Malumbres R, Sarosiek KA, Cubedo E *et al*. Differentiation stage-specific expression of microRNAs in B lymphocytes and diffuse large B-cell lymphomas. *Blood* 2009;**113**(16):3754-64.

27 Bostjancic E, Zidar N, Glavac D. MicroRNA microarray expression profiling in human myocardial infarction. *Dis Markers* 2009;**27**(6):255-68.

28 Wang WX, Huang Q, Hu Y *et al*. Patterns of microRNA expression in normal and early Alzheimer's disease human temporal cortex: white matter versus gray matter. *Acta Neuropathol* 2011;**121**(2):193-205.

29 Moreau MP. Altered microRNA regulatory networks in individuals with schizophrenia. Rutgers, The State University of New Jersey and The Graduate School of Biomedical Sciences University of Medicine and Dentistry of New Jersey, 2009.

30 Xiao J, Liang D, Zhang Y *et al*. MicroRNA expression signature in atrial fibrillation with mitral stenosis. *Physiol Genomics* 2011;**43**(11):655-64.

31 Eitan R, Kushnir M, Lithwick-Yanai G *et al*. Tumor microRNA expression patterns associated with resistance to platinum based chemotherapy and survival in ovarian cancer patients. *Gynecol Oncol* 2009;**114**(2):253-9.

32 Hou J, Wang P, Lin L *et al*. MicroRNA-146a feedback inhibits RIG-I-dependent Type I IFN production in macrophages by targeting TRAF6, IRAK1, and IRAK2. *J Immunol* 2009;**183**(3):2150-8.

33 Garbacki N, Di VE, Huynh-Thu VA *et al*. MicroRNAs Profiling in Murine Models of Acute and Chronic Asthma: A Relationship with mRNAs Targets. *PLoS One* 2011;**6**(1):e16509.

34 Mallick B, Ghosh Z, Chakrabarti J. MicroRNome analysis unravels the molecular basis of SARS infection in bronchoalveolar stem cells. *PLoS One* 2009;**4**(11):e7837.

35 Wang K, Zhang S, Marzolf B *et al*. Circulating microRNAs, potential biomarkers for drug-induced liver

injury. *Proc Natl Acad Sci U S A* 2009;**106**(11):4402-7.

36 Hu SJ, Ren G, Liu JL *et al*. MicroRNA expression and regulation in mouse uterus during embryo implantation. *J Biol Chem* 2008;**283**(34):23473-84.

37 Huang W, Liu H, Wang T *et al*. Tonicity-responsive microRNAs contribute to the maximal induction of osmoregulatory transcription factor OREBP in response to high-NaCl hypertonicity. *Nucleic Acids Res* 2011;**39**(2):475-85.

38 Lan KL, Yen SH, Liu RS *et al*. Mutant Bik gene transferred by cationic liposome inhibits peritoneal disseminated murine colon cancer. *Clin Exp Metastasis* 2007;**24**(6):461-70.

SUPPLEMENTARY INFORMATION

1. SUPPLEMENTAL DATA

Fig. S1 miR-574-5p MREs on human *Qki6/7/7b* mRNAs (related to Fig. 1). ***A***, Human *Qki* gene structure, major transcripts, protein isoforms and 3'UTRs. Located at 6q26-q27, the human *Qki* gene contains eight exons. Due to alternative splicing, at least 4 major transcripts, namely *Qki5*/*6*/*7*/*7b*, can be produced. Each of these transcript isoforms has its own unique 3'UTR derived from the alternatively-spliced exons. However, a long stretch of overlapping sequences is found in the 3'UTRs for *Qki6*/*7*/*7b* respectively. Furthermore, a putative MRE for miR-574-5p was found in the 3'UTRs of *Qki6/7*/*7b* but not that of *Qki5* mRNA. Four major QKI proteins (QKI5/6/7/7b) can be produced from the four mRNA isoforms, which differ in their carboxyl termini encoded for by the alternatively spliced exons. A common N-terminal 311amino acid peptide fragment encoded by the first six exons is shared by all four protein isoforms. This region contains a KH domain flanked by the QUA1 and the QUA2 motifs respectively. QUA1 is involved in protein homodimerization or heterodimerization while the KH and QUA2 domains might be responsible for RNA binding. The Y-motif is a tyrosine-rich region that serves as a site for tyrosine phosphorylation. In addition, there is a P-motif for the proline–rich region. The C-terminal of QKI5 (but not of the other three isoforms) contains a nuclear localization signal (NLS) that directs its entry into the nucleus. The figure was redrawn based on previous reports[1-3]. The putative MREs for miR-574-5p were indicated on the 3'UTRs for *Qki6/7/7b* respectively. ***B***, Alignment of putative miR-574-5p seed-binding sites of mouse *Qki6/7*-3'UTR and human *Qki6/7/7b*-3'UTR. Mature human miR-574-5p (hsa-miR-574-5p) and mouse miR-574-5p (mmu-miR-574-5p) share 100% sequence similarity, with the sequence being 5'-ugagugugugugugagugugu-3'. ***C***, MREs for miR-17, miR-20a and miR-200b on mouse *Qki5*-3'UTR as predicted by the miRanda algorithm (www.microrna.org). Data sets on www.microrna.org so far contain more complete 3'UTRs for specific genes and the miRanda algorithm distinguishes the 3'UTRs. ***D*** & ***E***, MREs for miR-17, miR-20a, miR-200b, miR-466g, miR-574-5p and miR-717 on mouse *Qki6/7*-3'UTRs as predicted by the miRanda algorithm. Surprisingly, no MRE for miR-574-3p was predicted in the 3'UTRs for mouse or human *Qki5* or *Qki6/7/7b* mRNA.

Fig. S2 Effects of miR-574-5p on *Qki* expression in human HCT116, SW480 and SW620 cells (related to Fig. 2). Human CRC cells were transfected with a miR-574 overexpressing plasmid, a miR-574-5p inhibitor. Cells were harvested for qPCR or western blot assays 24 hours after the transfections (n = 3-4). Statistical comparisons were made between a control (pFlag-CMV or inhibitor control)-transfected cells and a particular treatment. NS, not significant; **, $\boldsymbol{p} < 0.01$; ***, $\boldsymbol{p} < 0.001$. ***A***, Inhibition of miR-574-5p significantly increased the levels of *Qki5/6/7/7b* mRNA isoforms in SW480 and SW620 cells, but only *Qki6/7* were increased in HCT116 cells. ***B***, Overexpression of miR-574-5p significantly reduced the level of total QKI protein in SW480 cells. ***C,*** Inhibition of miR-574-5p significantly increased the levels of total QKI and QKI5/6/7 proteins in SW480 cells.

Fig. S3 Putative QREs on *β-catenin* mRNAs from a few mammals (related to Fig. 3). hsa, *Homo sapiens*; pab, *Pongo abelii*; mmu, *Mus, musculus*; bta, *Bos taurus*; ssc, *Sus scrofa*. Two putative QREs were indicated by QRE1 and QRE2 respectively. The distal QRE1 for *β-catenin* mRNAs from orangutans, mice, cows and pigs completely satisfies the bipartite consensus sequence of NACUAAY-N_{1-20}-UAAY (Galarneau and Richard, 2005; Hafner et al., 2010). With human *β-catenin* mRNAs, however, the number of the intervening nucleotides in the QRE1 between the core site NACUAAY and the half site UAAY is 22 rather than smaller than or equal to 20. Similarly, the proximal QRE2 might also be functional [4]. However, this putative QRE is also slightly different from the consensus sequence, with the half-site being "CAAY" rather than "TAAY" and 22 intervening nucleotides between the putative core site and the putative half site.

Fig. S4 Co-overexpression of *Qki5/6/7* significantly attenuated the oncogenic effects of miR-574-5p. CT26 cells were grown and transfected with pmiR-574 or pFlag-CMV in the presence or absence of pFlag-Qki5/6/7 for 24 hours. Cells were subsequently harvested for mRNA or MTT analyses. For invasion analysis, similar transfection was performed with CT26 cells for 12 hours. Subsequently, 5×10^4 transfected cells were seeded per upper chambers in serum-free RPMI 1640 medium whereas the lower chambers were loaded with RPMI 1640 medium containing 5% FBS. After 48 hours of incubation, cells were harvested for analysis. *, $\boldsymbol{p} < 0.05$; *, $\boldsymbol{p} < 0.01$; ****, $\boldsymbol{p} < 0.001$. ***A,*** Re-introduction of *Qki5/6/7* significantly decreased *β-catenin* and increased $p27^{kip1}$ mRNA expression in miR-574-5p-overexpressing cells (n = 3-4). ***B*** and ***C,*** Re-introduction of *Qki5/6/7* significantly reduced cell viability and cell invasion in miR-574-5p-overexpressing cells (n = 3-4).

Fig. S5 Expression levels of *Qki5/6/7/7b* mRNA and protein isoforms in the human CRC tissues and the adjacent normal epithelial tissues. T, tumor tissue； N, normal adjacent epithelial tissue. ***A***, *Qki5* expression from ten pairs of clinical samples (#11-20) as determined by qPCR. ***B***, *Qki6* expression from ten pairs of clinical samples (#11-20) as determined by qPCR. ***C***, *Qki7* expression from ten pairs of clinical samples (#11-20) as determined by qPCR. ***D***, *Qki7b* expression from ten pairs of clinical samples (#11-20) as determined by qPCR. ***E***, QKI5/6/7/7b protein isoform expression in five pairs of clinical samples (#16-20) as determined by western blotting. $n = 5$, ***, $\boldsymbol{p} < 0.001$.

Fig. S6 Subcellular localization of QKI5/6/7 proteins in human SW620 or mouse CT26 cells and the relative expression of *Qki5/6/7/7b* mRNAs in CRC cells, clinical CRC tissue samples and normal adjacent epithelial tissue samples. ***A***, Subcellular localization of QKI5/6/7 proteins in SW620 or CT26 cells as determined by western blotting. ***B***, Subcellular localization of QKI5/6/7 proteins in CT26 cells as determined by immunofluorescence assays. Original magnification, ×1,000. ***C***, Relative expression of *Qki* mRNA isoforms in CT26, HCT116, SW480 and SW620 cells. Total RNA samples were isolated and qPCR was performed (n = 3-4). All values were normalized with *Qki*5 expression. ***D***, Relative expression of *Qki* mRNA isoforms in clinical CRC and normal adjacent epithelial samples from 10 patients. Both the values for tumor tissues (T, black-colored) and corresponding adjacent noncancerous epithelial tissues from a particular patient (N, grey-colored) were normalized with the expression of *Qki*5 mRNA in normal adjacent epithelial tissue from the same patient.

Fig. S7 Effects of miR-574-5p overexpression on β-catenin subcellular localization as determined by western blots and immunofluorescent staining. For western blots, CT26 cells were transfected with a miR-574-5p overexpressing plasmid (pmiR-574) or its control (pFlag-CMV) for 24 hours and harvested for western blot analyses. For immunofluorescent staining, CT26 cells were seed on the coverslips and transfected with pmiR-574 or pFlag-CMV for 24 hours. Cells were then fixed for immunofluorescence analyses. ***A***, Subcellular distribution of β-catenin protein as determined by western blots; ***B***, Subcellular distribution of β-catenin protein as determined by immunofluorescent staining. Original magnification, ×1000.

Fig. S8 The miR-574-5p-QKI-β-catenin/$p27^{Kip1}$ axis of signal transduction in the development of CRC. miR-574-5p derived from the first intron of either *Col3a1* or *Noxp20* regulates the expression of *Qki6/7/7b*

directly and negatively. *Qki5* may also be regulated by miR-574-5p indirectly. Down-regulation of QKIs will cause the overactivation of β-catenin and the suppression of $p27^{Kip1}$. As a result, activities in colorectal epithelial cell proliferation, migration and invasion will be enhanced, whereas cell cycle arrest and differentiation will be suppressed. Additionally, miR-574-5p might also repress the expression of tumor suppressor ceramide synthase-1 isoform 2 (*CerS1-2*) posttranscriptionally.[5] QKIs, on the other hand, might also control the expression of macroH1A1.1 to impact tumorigenesis.[6] miR-574-5p thus appears to be oncogenic and may contribute to the dysregulation of colorectal epithelial cell differentiation and tumorigenesis or cancer progression through the suppression of tumor-suppressive QKIs. miR-574-5p expression might be co-regulated with its hosting-genes (either *Noxp20* or *Col3a1*), although this needs to be verified with further study. Additionally, Sox2 is a transcriptional factor implicated in the maintenance of the pluripotency of stem cells[7-9], neurogenesis[10-13] and development of cancers.[14-17] In glioblastoma multiforme cells, the knockdown of *Sox2* caused significant down-regulation of miR-574-5p.[18] Coincidentally or not, aberrant Sox2 up-regulation and miR-574-5p up-regulation are often co-detected in diseases such as CRC ([15] and current study), glioblastoma,[18] lung cancer,[19-21] esophageal squamous carcinoma [16;22] etc. Together these observations suggest that Sox2 might regulate miR-574-5p positively. The possible regulation of *Noxp20*, *Col3a1* and miR-574-5p and *Qki*s by Apc, however, is not clear and warrant further research. *Apc*, adenomatous polyposis coli; *Col3a1*, procollagen Type III, alpha-1; *Noxp20*, nervous system overexpressed protein-20; *Sox2*, SRY-like HMG box-2.

Fig. S9 Schematic graphs for twelve plasmids used in the current study. See the Materials and Methods section for more details. hGH-pA, poly-A for human growth hormone gene; Luc, luciferase; SV40-pA, SV40 poly-A.

Table S1 The expression of miR-574-5p and pan-*Qki* mRNA and protein and the clinicopathological features of 60 CRC patients.

Table S2 Alterations of miR-574-5p expression in diseases.

Fig. S1

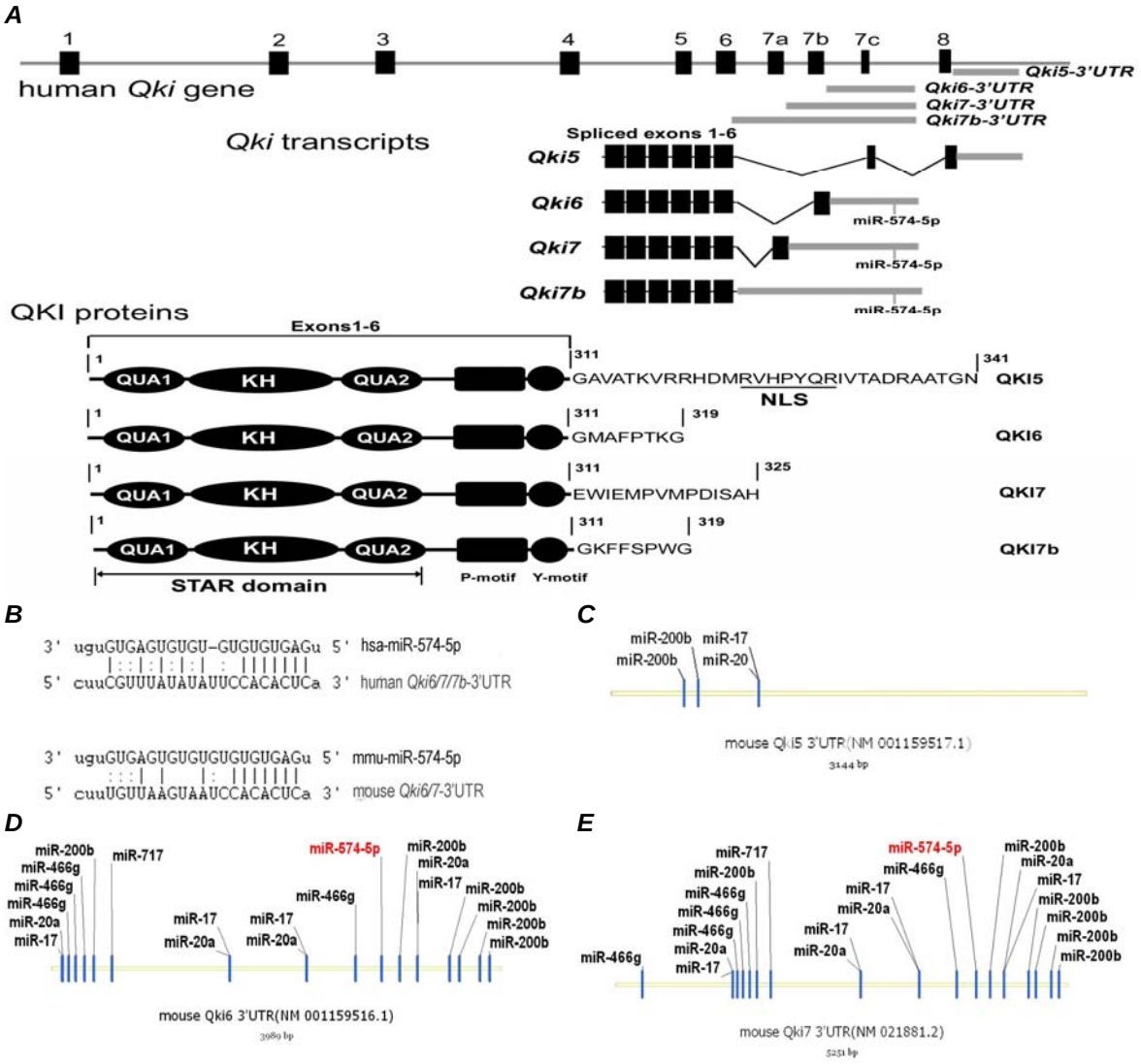
A
human Qki gene
Qki5-3'UTR
Qki6-3'UTR
Qki7-3'UTR
Qki7b-3'UTR
Qki transcripts
Spliced exons 1-6
Qki5
Qki6
Qki7
Qki7b
miR-574-5p
QKI proteins
Exons1-6
QUA1
KH
QUA2
GAVATKVRRHDMRVHPYQRIVTADRAATGN
NLS
QKI5
GMAFPTKG
QKI6
EWIEMPVMPDISAH
QKI7
GKFFSPWG
QKI7b
STAR domain
P-motif
Y-motif
B
hsa-miR-574-5p
human Qki6/7/7b-3'UTR
mmu-miR-574-5p
mouse Qki6/7-3'UTR
C
mouse Qki5 3'UTR(NM 001159517.1)
D
mouse Qki6 3'UTR(NM 001159516.1)
E
mouse Qki7 3'UTR(NM 021881.2)

Fig. S2

A

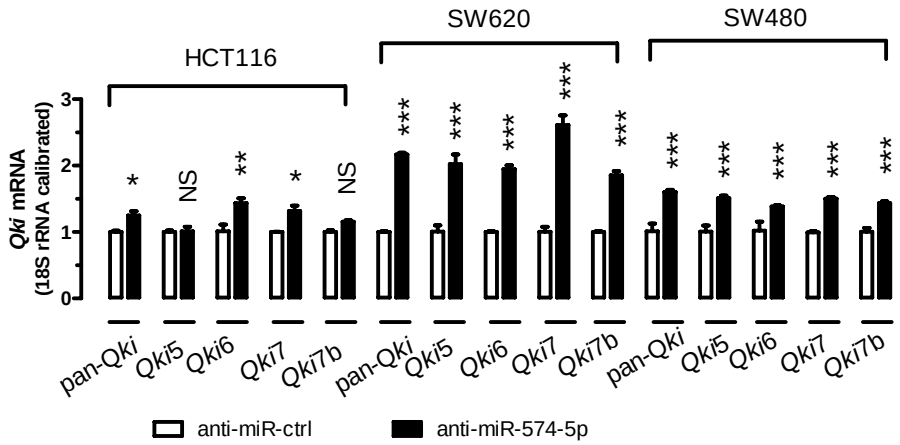
HCT116
SW620
SW480
Qki mRNA (18S rRNA calibrated)
pan-Qki
Qki5
Qki6
Qki7
Qki7b
anti-miR-ctrl
anti-miR-574-5p

B

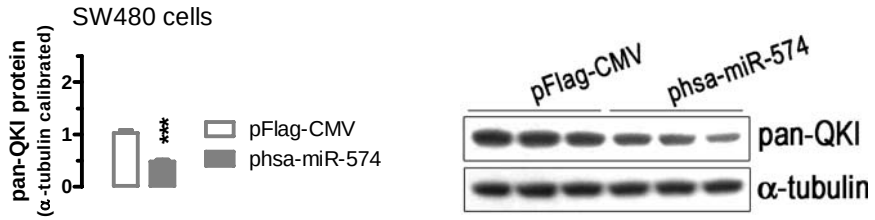
SW480 cells
pan-QKI protein (α-tubulin calibrated)
pFlag-CMV
phsa-miR-574
pan-QKI
α-tubulin

C

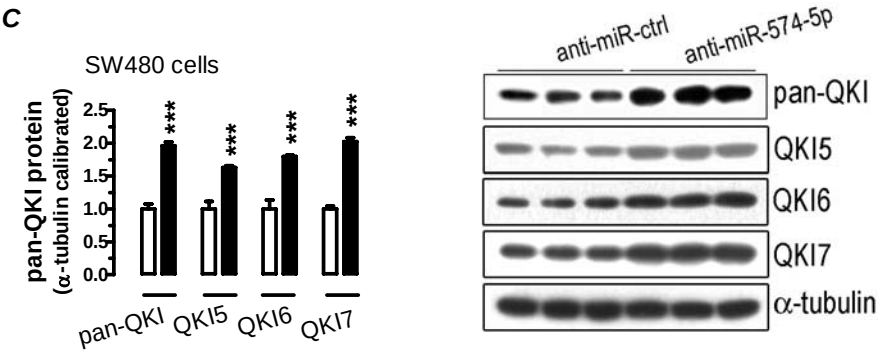
SW480 cells
pan-QKI protein (α-tubulin calibrated)
anti-miR-ctrl
anti-miR-574-5p
pan-QKI
QKI5
QKI6
QKI7
α-tubulin

Fig. S3

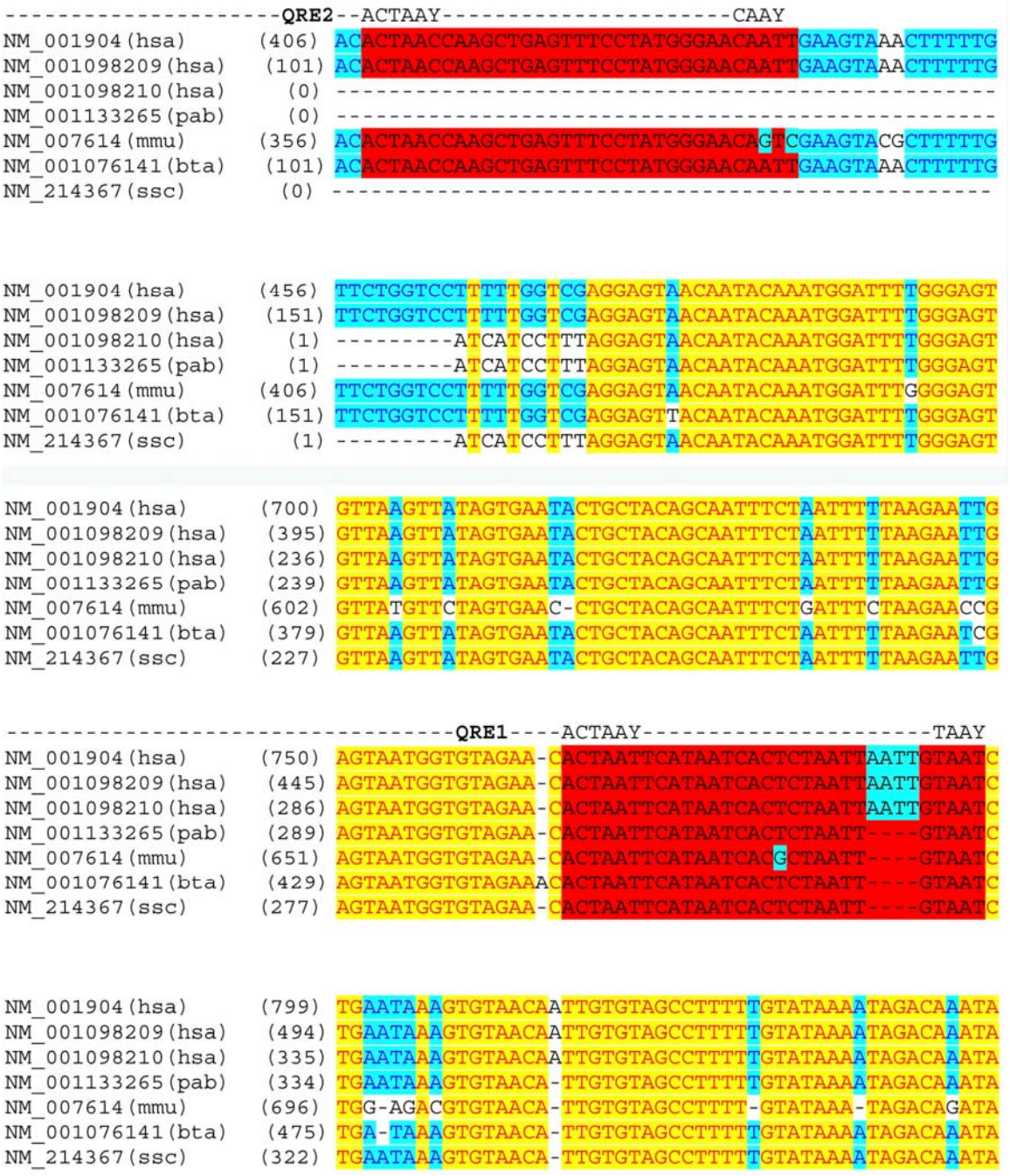
----------QRE2--ACTAAY----------CAAY
NM_001904(hsa) (406) ACACTAACCAAGCTGAGTTTCCTATGGGAACAATTGAAGTAAACTTTTTG
NM_001098209(hsa) (101) ACACTAACCAAGCTGAGTTTCCTATGGGAACAATTGAAGTAAACTTTTTG
NM_001098210(hsa) (0) ----------
NM_001133265(pab) (0) ----------
NM_007614(mmu) (356) ACACTAACCAAGCTGAGTTTCCTATGGGAACAGTCGAAGTACGCTTTTTG
NM_001076141(bta) (101) ACACTAACCAAGCTGAGTTTCCTATGGGAACAATTGAAGTAAACTTTTTG
NM_214367(ssc) (0) ----------
NM_001904(hsa) (456) TTCTGGTCCTTTTTGGTCGAGGAGTAACAATACAAATGGATTTTGGGAGT
NM_001098209(hsa) (151) TTCTGGTCCTTTTTGGTCGAGGAGTAACAATACAAATGGATTTTGGGAGT
NM_001098210(hsa) (1) ---------ATCATCCTTTAGGAGTAACAATACAAATGGATTTTGGGAGT
NM_001133265(pab) (1) ---------ATCATCCTTTAGGAGTAACAATACAAATGGATTTTGGGAGT
NM_007614(mmu) (406) TTCTGGTCCTTTTTGGTCGAGGAGTAACAATACAAATGGATTTGGGGAGT
NM_001076141(bta) (151) TTCTGGTCCTTTTTGGTCGAGGAGTTACAATACAAATGGATTTTGGGAGT
NM_214367(ssc) (1) ---------ATCATCCTTTAGGAGTAACAATACAAATGGATTTTGGGAGT
NM_001904(hsa) (700) GTTAAGTTATAGTGAATACTGCTACAGCAATTTCTAATTTTTAAGAATTG
NM_001098209(hsa) (395) GTTAAGTTATAGTGAATACTGCTACAGCAATTTCTAATTTTTAAGAATTG
NM_001098210(hsa) (236) GTTAAGTTATAGTGAATACTGCTACAGCAATTTCTAATTTTTAAGAATTG
NM_001133265(pab) (239) GTTAAGTTATAGTGAATACTGCTACAGCAATTTCTAATTTTTAAGAATTG
NM_007614(mmu) (602) GTTATGTTCTAGTGAAC-CTGCTACAGCAATTTCTGATTTCTAAGAACCG
NM_001076141(bta) (379) GTTAAGTTATAGTGAATACTGCTACAGCAATTTCTAATTTTTAAGAATCG
NM_214367(ssc) (227) GTTAAGTTATAGTGAATACTGCTACAGCAATTTCTAATTTTTAAGAATTG
----------QRE1----ACTAAY----------TAAY
NM_001904(hsa) (750) AGTAATGGTGTAGAA-CACTAATTCATAATCACTCTAATTAATTGTAATC
NM_001098209(hsa) (445) AGTAATGGTGTAGAA-CACTAATTCATAATCACTCTAATTAATTGTAATC
NM_001098210(hsa) (286) AGTAATGGTGTAGAA-CACTAATTCATAATCACTCTAATTAATTGTAATC
NM_001133265(pab) (289) AGTAATGGTGTAGAA-CACTAATTCATAATCACTCTAATT----GTAATC
NM_007614(mmu) (651) AGTAATGGTGTAGAA-CACTAATTCATAATCAGCTAATT----GTAATC
NM_001076141(bta) (429) AGTAATGGTGTAGAAACACTAATTCATAATCACTCTAATT----GTAATC
NM_214367(ssc) (277) AGTAATGGTGTAGAA-CACTAATTCATAATCACTCTAATT----GTAATC
NM_001904(hsa) (799) TGAATAAAGTGTAACAATTGTGTAGCCTTTTTGTATAAAATAGACAAATA
NM_001098209(hsa) (494) TGAATAAAGTGTAACAATTGTGTAGCCTTTTTGTATAAAATAGACAAATA
NM_001098210(hsa) (335) TGAATAAAGTGTAACAATTGTGTAGCCTTTTTGTATAAAATAGACAAATA
NM_001133265(pab) (334) TGAATAAAGTGTAACA-TTGTGTAGCCTTTTTGTATAAAATAGACAAATA
NM_007614(mmu) (696) TGG-AGACGTGTAACA-TTGTGTAGCCTTTT-GTATAAA-TAGACAGATA
NM_001076141(bta) (475) TGA-TAAAGTGTAACA-TTGTGTAGCCTTTTTGTATAAAATAGACAAATA
NM_214367(ssc) (322) TGAATAAAGTGTAACA-TTGTGTAGCCTTTTTGTATAAAATAGACAAATA

Fig. S4

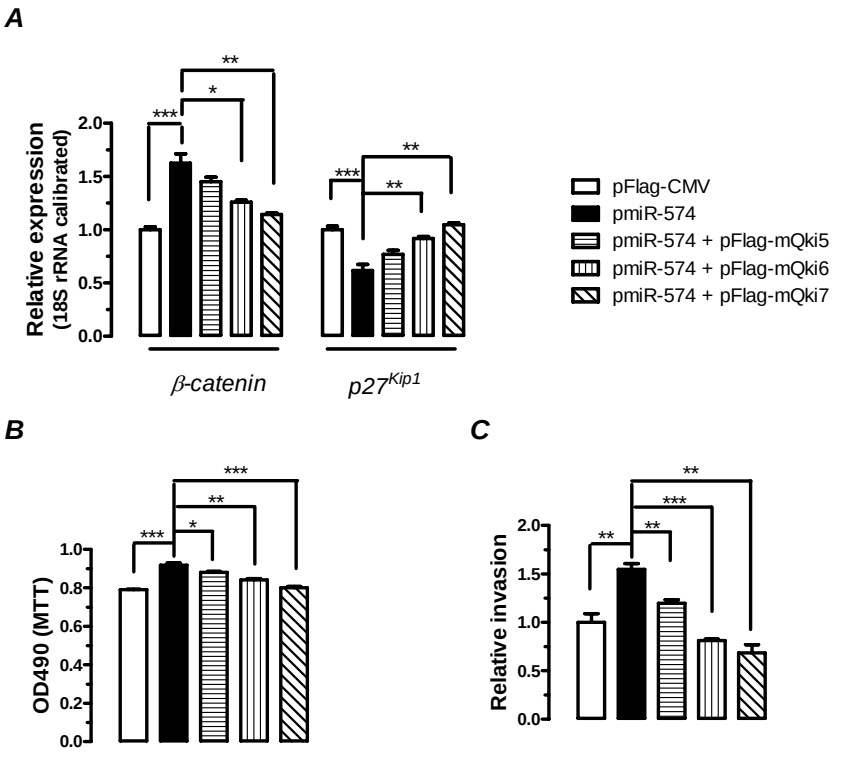
A
Relative expression (18S rRNA calibrated)
2.0
1.5
1.0
0.5
0.0
***
*
**
***
**
**
β-catenin
p27Kip1
pFlag-CMV
pmiR-574
pmiR-574 + pFlag-mQki5
pmiR-574 + pFlag-mQki6
pmiR-574 + pFlag-mQki7
B
OD490 (MTT)
1.0
0.8
0.6
0.4
0.2
0.0
***
**
*
***
C
Relative invasion
2.0
1.5
1.0
0.5
0.0
**
**
***
**

Fig. S5

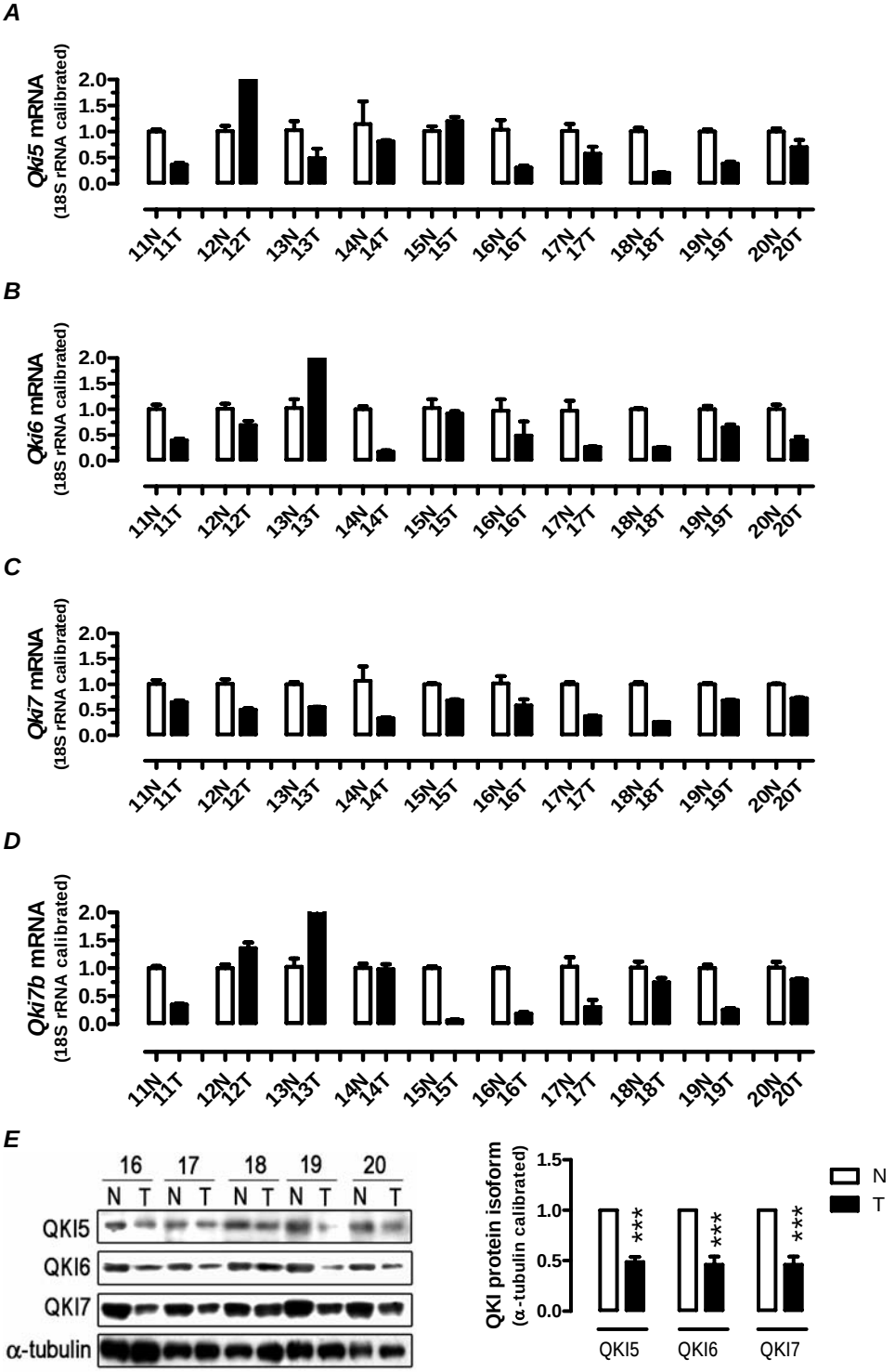
A
Qki5 mRNA
(18S rRNA calibrated)
B
Qki6 mRNA
(18S rRNA calibrated)
C
Qki7 mRNA
(18S rRNA calibrated)
D
Qki7b mRNA
(18S rRNA calibrated)
2.0
1.5
1.0
0.5
0.0
11N 11T 12N 12T 13N 13T 14N 14T 15N 15T 16N 16T 17N 17T 18N 18T 19N 19T 20N 20T
E
16 17 18 19 20
N T N T N T N T N T
QKI5
QKI6
QKI7
α-tubulin
QKI protein isoform
(α-tubulin calibrated)
***
N
T
QKI5 QKI6 QKI7

Fig. S6

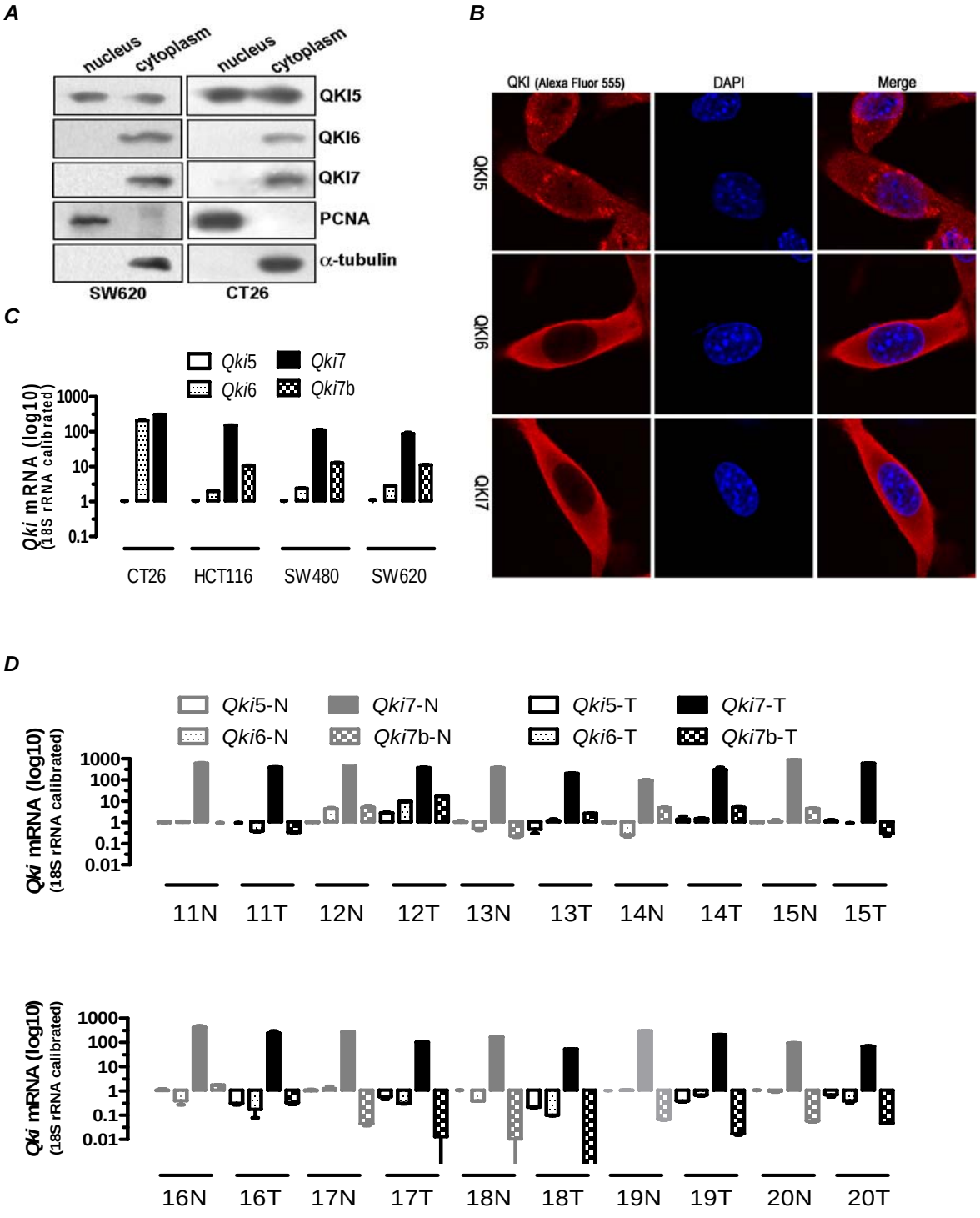
A
nucleus
cytoplasm
nucleus
cytoplasm
QKI5
QKI6
QKI7
PCNA
α-tubulin
SW620
CT26
B
QKI (Alexa Fluor 555)
DAPI
Merge
QKI5
QKI6
QKI7
C
Qki5
Qki7
Qki6
Qki7b
Qki mRNA (log10)
(18S rRNA calibrated)
1000
100
10
1
0.1
CT26
HCT116
SW480
SW620
D
Qki5-N
Qki7-N
Qki5-T
Qki7-T
Qki6-N
Qki7b-N
Qki6-T
Qki7b-T
Qki mRNA (log10)
(18S rRNA calibrated)
1000
100
10
1
0.1
0.01
11N
11T
12N
12T
13N
13T
14N
14T
15N
15T
16N
16T
17N
17T
18N
18T
19N
19T
20N
20T

Fig. S7

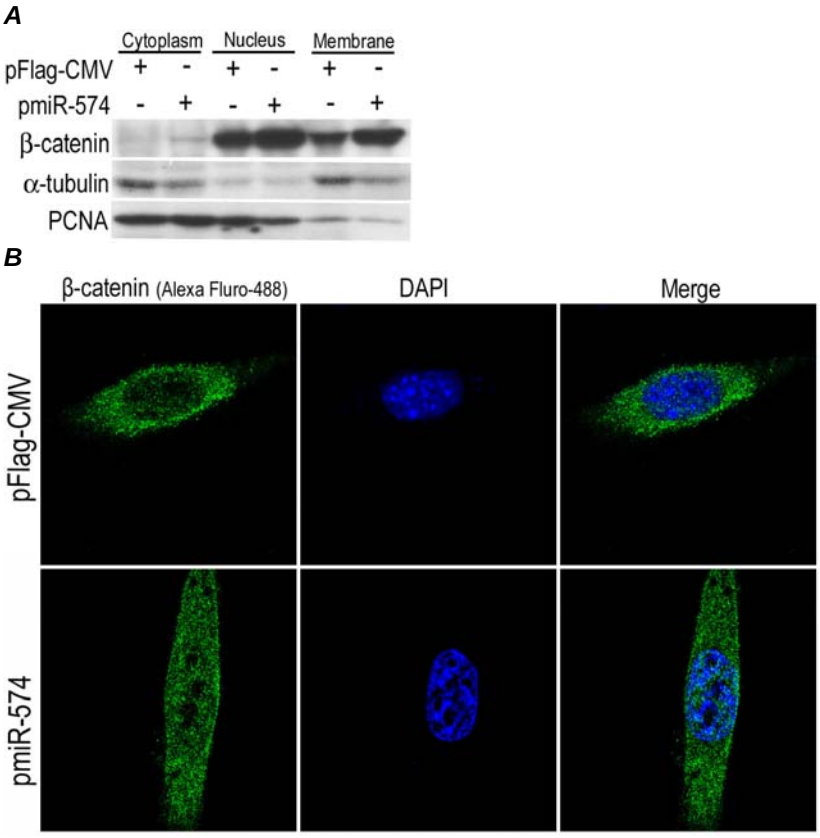
A
Cytoplasm
Nucleus
Membrane
pFlag-CMV + - + - + -
pmiR-574 - + - + - +
β-catenin
α-tubulin
PCNA
B
β-catenin (Alexa Fluro-488)
DAPI
Merge
pFlag-CMV
pmiR-574

Fig. S8

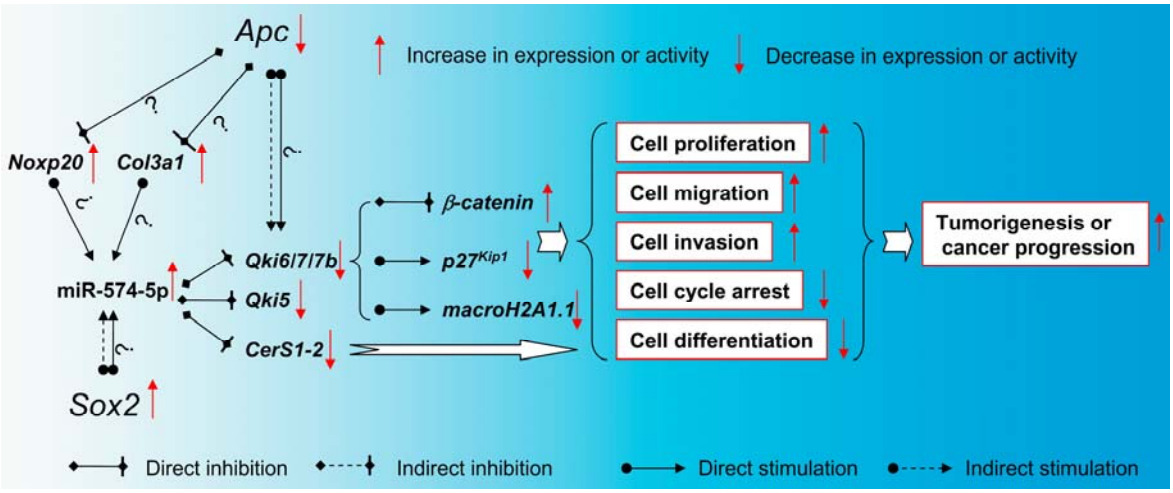
Apc
Increase in expression or activity
Decrease in expression or activity
Noxp20
Col3a1
miR-574-5p
Qki6/7/7b
Qki5
CerS1-2
Sox2
β-catenin
p27Kip1
macroH2A1.1
Cell proliferation
Cell migration
Cell invasion
Cell cycle arrest
Cell differentiation
Tumorigenesis or cancer progression
Direct inhibition
Indirect inhibition
Direct stimulation
Indirect stimulation

Fig. S9

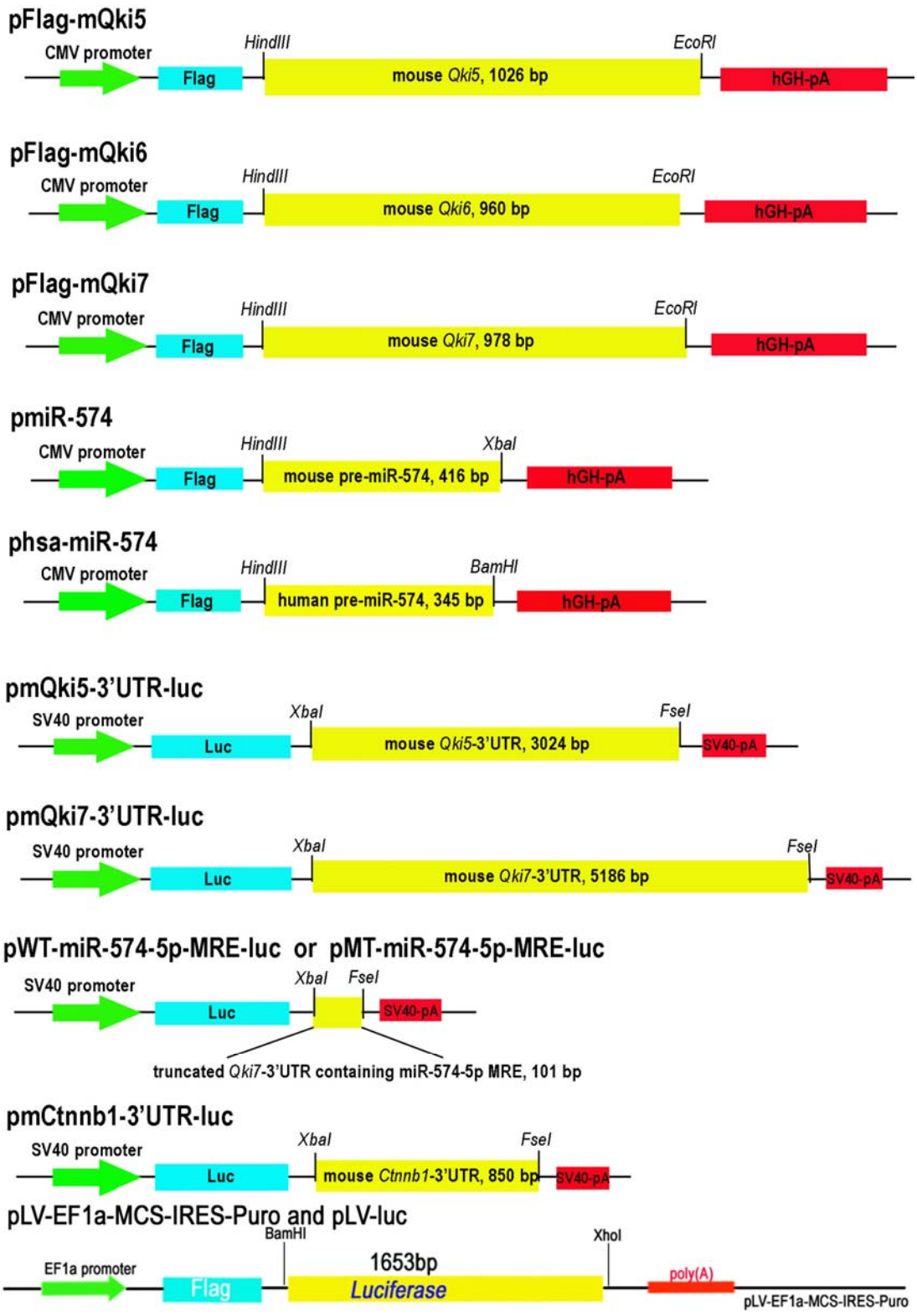
pFlag-mQki5
CMV promoter
Flag
HindIII
mouse Qki5, 1026 bp
EcoRI
hGH-pA
pFlag-mQki6
CMV promoter
Flag
HindIII
mouse Qki6, 960 bp
EcoRI
hGH-pA
pFlag-mQki7
CMV promoter
Flag
HindIII
mouse Qki7, 978 bp
EcoRI
hGH-pA
pmiR-574
CMV promoter
Flag
HindIII
mouse pre-miR-574, 416 bp
XbaI
hGH-pA
phsa-miR-574
CMV promoter
Flag
HindIII
human pre-miR-574, 345 bp
BamHI
hGH-pA
pmQki5-3'UTR-luc
SV40 promoter
Luc
XbaI
mouse Qki5-3'UTR, 3024 bp
FseI
SV40-pA
pmQki7-3'UTR-luc
SV40 promoter
Luc
XbaI
mouse Qki7-3'UTR, 5186 bp
FseI
SV40-pA
pWT-miR-574-5p-MRE-luc or pMT-miR-574-5p-MRE-luc
SV40 promoter
Luc
XbaI
FseI
SV40-pA
truncated Qki7-3'UTR containing miR-574-5p MRE, 101 bp
pmCtnnb1-3'UTR-luc
SV40 promoter
Luc
XbaI
mouse Ctnnb1-3'UTR, 850 bp
FseI
SV40-pA
pLV-EF1a-MCS-IRES-Puro and pLV-luc
EF1a promoter
Flag
BamHI
1653bp
Luciferase
XhoI
poly(A)
pLV-EF1a-MCS-IRES-Puro

Table S1

		n	**%**	**miR-574-5p (Normalized)**	**Pan-*Qki* mRNA (Normalized)**	**Pan-QKI protein (Normalized)**
Gender	M	40	67.7	3.136 ± 0.5718	0.8483 ± 0.1774	0.7554 ± 0.0977
	F	20	33.3	2.793 ± 0.532	0.7278 ± 0.1335	0.7882 ± 0.0929
Age	≤60	28	46.7	3.238 ± 0.8269	0.9206 ± 0.2304	0.7509 ± 0.094
	>60	32	53.3	2.843 ± 0.3409	0.7134 ± 0.1315	0.7789 ± 0.1097
TNM stage	I	8	13.3	5.737 ± 2.546	0.9503 ± 0.4494	0.8613 ± 0.3316
	II	15	25	2.666 ± 0.5652	1.115 ± 0.412	0.8046 ± 0.1773
	III	36	60	2.593 ± 0.3291	0.6608 ± 0.082	0.7292 ± 0.0674
	IV	1	1.7	2.415	0.4825	0.74
Lymph node status	N0	23	38.4	3.734 ± 0.9734	1.058 ± 0.3051	0.8243 ± 0.1589
	N1	17	28.3	2.549 ± 0.5684	0.7131 ± 0.1462	0.7564 ± 0.0935
	N2	20	33.3	2.621 ± 0.3574	0.6075 ± 0.0828	0.7066 ± 0.0935
	N3	0				

Table S2

Organism	Condition	miR-574-5p expression	Affected cells or tissues	Fold change	References
Human	CRC	Up	Colorectal cells	Very significant	Current study
Human	Pituitary adenomas	Up	Pituitary tissue	2.89	[23]
Human	Systemic lupus erythematosus	Up	T lymphocyte	> 2	[24]
Human	Pancreatic cancer	Up	Pancreatic tissue	51	[25]
Human	Lymphoma	Altered	Lymphocyte	?	[26]
Human	Myocardial infarction	Up	Heart	Very significant	[27]
Human	Non-small cell lung cancer	Up	Lung	2.17	[20]
Human	Small cell lung cancer	Altered	Lung	?	[21]
Human	Eosphageal squamous cell carcinoma	Up	Eosphageal squamous cells	1.72	[22]
Human	Alzheimer's	Up	Gray matter	?	[28]
Human	Schizophrenia	Altered	Brain tissue	?	[29]
Human	Mitral stenosis	Up	Right atrial appendage	1.96	[30]
Human	Ovarian cancer	Up	Ovary tissue	1.24	[31]
Mouse	CRC	Up	Colorectal cells	3.7	Current study
Mouse	Vesicular stomatitis virus infection	Up	Macrophage	?	[32]
Mouse	Asthma	Up	Lung cells	13	[33]
Mouse	SARS infection	Altered	Bronchoalveolar stem cells	?	[34]
Mouse	Liver injury	Up	Liver/plasma	3.4/1.49	[35]

2. SUPPLEMENTAL MATERIALS AND METHODS

Plasmids.TOP/FOP-Flash plasmids and the Wnt1-overexpressing (Wnt1) plasmid were kind gifts from Prof. Qiao Wu, Xiamen University.

For *Qki* overexpression plasmids, primers were designed based on the genomic sequences from the NCBI databases, with the forward primer carrying a *HindIII* site and the reverse primer carrying an *EcoRI* respectively. Mouse *Qki5*, *Qki6*, *Qki7* were individually PCR-amplified using mouse brain tissue cDNA and appropriate primers (see List of primers used for miRNA or *Qki* overexpression plasmids), with the LA Taq DNA Polymerase (TaKaRa, Dalian). The resultant DNA fragments were subcloned into pFlag-CMV (Sigma Aldrich, St. Louis, MO, USA) using the *HindIII* and *EcoRI* sites.

For mouse miRNA overexpressing plasmids, primers were designed based on the genomic sequences from the miRBase (microrna.sanger.ac.uk), with the forward primers carrying a *HindIII* site and the reverse primers carrying a *XbaI* site respectively. Pre-miRNA gene fragments were individually PCR-amplified using genomic DNA prepared from mouse inner medullary collecting duct epithelial mIMCD3 cells (mmu-miR-574) or human CRC SW480 cells (hsa-miR-574) and appropriate primers (see List of primers used for miRNA or *Qki* overexpression plasmids), with Pyrobest DNA Polymerase (TaKaRa). The resultant DNA fragments were subcloned into pFlag-CMV, using the *HindIII* and *XbaI* (mmu-miR-574) or *HindIII* and *BamHI* (hsa-miR-574) sites. The insertion sequences of the resultant plasmids were confirmed by sequencing.

For the construction of mouse *Qki5*-3'UTR, wildtype *Qki7*-3'UTR miR-574-5p MRE, mutant *Qki7*-3'UTR miR-574-5p MRE and *Ctnnb1* luciferase reporters, mouse 3'UTR regions were amplified from mouse brain tissue cDNA through PCR amplification with the LA Taq DNA Polymerase (TaKaRa) and appropriate primers (see List of primers used for the construction of five luciferase reporters). The resultant PCR fragments carrying a *NheI* site and a *FseI* site was subcloned into the pGL3-control vector (Promega), using the *XbaI* and *FseI* sites immediately downstream of the stop codon of the luciferase cDNA, generating pmQki5-3'UTR-luc, pmQki7-3'UTR-luc, pWT-miR574-5p-MRE-luc, pMT-miR574-5p-MRE-luc and pmCtnnb1-3'UTR-luc respectively.

For the construction of lentiviral plasmid carrying a luciferase gene, the luciferase reporter gene on pladmid pGL3 (Promega, USA) was PCR amplified and a *BamHI-XhoI* insert gene cassette was inserted

into a lentiviral vector pLV-EF1a-MCS-IRES-Puro (A gift from Prof. Jiahuai Han) to obtain a plasmid pLV-luc.

The resulting twelve plasmids are shown in Fig. S9 in the previous section.

Cell culture and transient transfections. Mouse CT26, human SW480 and SW620 CRC cells were obtained from ATCC (Manassas, VA, USA), human HCT116 CRC cells was obtained from the Chinese Academy of Sciences (Shanghai, China). CT26 cells and HCT116 cells were normally cultured in RPMI 1640 with 10% fetal bovine serum (FBS). SW480 and SW620 cells were cultured in DMEM supplemented with 10% FBS. Plasmids, miRNA mimics and inhibitor transfections were performed with Lipofectamine 2000 reagent (Invitrogen, Carlsbad, CA, USA) according to the manufacturer's protocols.

Western blot, immunohistochemistry, immunofluorescence and in situ hybridization analyses. Western blots were performed according to standard protocols. The detection was achieved using the Immobilon Western Chemiluminescent HRP Substrate kit (Millipore, Billerica, MA, USA). Antibodies and the dilutions are anti-α-tubulin (sc-5286, Santa Cruz, 1:10000); anti-β-actin (sc-47778, Santa Cruz, 1:20000); anti-pan-QKI (sc-103851, Santa Cruz, 1:2000); anti-QKI5 (AB9904, Millipore, 1:2000); anti-QKI6 (AB9906, , Millipore, 1:2000); anti-QKI7 (AB9908, Millipore, 1:2000); anti-$p27^{Kip1}$ (sc-528, Santa Cruz, 1:2000); anti-β-catenin (sc-7199, Santa Cruz, 1:2000); anti-PCNA (sc-7907, Santa Cruz, 1:2000); Alexa Fluor 555-labeled goat Anti-Rabbit IgG (H+L) (A0452, Beyotime Institute of Biotechnology, 1:500) respectively.

Immunohistochemistry was performed with an instant-type SABC immunohistochemistry kit purchased from the Boster Bioengineering Company (Wuhan, China) as instructed. Briefly, 5 um fixed tissue sections were microwave-heated for 10 min for antigen retrieval. Slides were washed and incubated with primary antibody for 1 hour followed by incubation with instant-type secondary antibody for 30 minutes at room temperature. After being thoroughly washed with PBS (pH 7.5), the tissues were incubated with SABC (Strept-Avidin-Biotin Complex) for 20 minutes at room temperature. After washing thoroughly, 100-200 μl freshly-made diaminobenzidine (DAB) solution was added to each slide. After incubation for ~10 minutes, sections were lightly counter-stained with hematoxylin.

For immunofluorescence analyses, cells seeded on cover glass overnight were fixed in 4% paraformaldehyde. Fixed cells were incubated with anti-QKI5, QKI6 or QKI7 primary antibody

respectively, followed by incubation with Alexa Fluor® 555-conjugated secondary antibody or Alexa Fluor® 488-conjugated secondary antibody (Beyotime Institute of Biotechnology, Jiangsu, China). Cell nuclei were stained by DAPI (Beyotime Institute of Biotechnology). Stained cells were visualized and photographed with a Leica-TCS-SP2-SE confocal microscope.

In situ hybridization of miRNAs was performed as described [36]. miRCURY^{TM} LNA miRNA probes (hsa-miR-574-5p, 5'-ACACACTCA-CACACACACACTCA-3'; hsa-miR-200b, 5'-TCATCATTACCAGGCAGTATTA-3'; U6, 5'-CACGAATTTGCGTGTCATCCTT-3'; Scramble-miR, 5'-GTGTAACACGTCTATACGCCCA-3') were purchased from Exiqon (Copenhagen, Denmark).

qPCR analyses of mRNAs and miRNAs. For qPCR mRNA quantification, reverse transcription was performed with TRIzol (Invitrogen)-extracted total RNAs using a ReverTra Ace-α-® Kit as instructed (TOYOBO, Shanghai). qPCR was performed by using the SYBR Green qPCR Master Mix (TOYOBO) and the StepOne Plus qPCR system (Applied Biosystems Inc., Foster City, CA) according to the manufacturer's protocols and with the primer pairs listed below.

For miRNAs, qPCR was performed with the stem-loop primers as described previously [37] using the miRNA-specific reverse transcription primers, the universal primer and the miRNA-specific reverse locked nucleic acid (LNA)-primers as described below.

Cell cycle, proliferation, migration, invasion and colony formation assays. For cell cycle analysis, 5×10^5 cells were synchronized by serum starvation for 24 hours and induced to re-enter the cell cycle by replacing old media with a fresh media containing 10% fetal bovine serum (FBS) for 24 hours. Cells were harvested and fixed in 75% ethanol at 4 ºC overnight. Cells were incubated with RNase A at 37 ºC for 30 min, and then stained with propidium iodide. The cell cycle phases were measured by flow cytometry.

Cell proliferation was analyzed by the MTT assay. A total of 4×10^3 cells was seeded in 96-well plates and MTT was added to each well every 24 hours. The plates were incubated for 4 hours before the addition of 10% SDS (in 0.01M HCl) (Sigma Aldrich, St. Louis, MO, USA). The absorbance was measured at 490 nm using a microplate reader.

Cell migration was analyzed by the wound-healing assays. SW480 cells were seeded onto 6-well plates. After transfection, a wound was incised in the center of the confluent culture, followed by careful washing to remove detached cells and the addition of fresh medium. Phase contrast images of the wounded

area were recorded using an inverted microscope at indicated time points.

Matrigel invasion assays were performed using Millicell inserts coated with matrigel (BD Biosciences, Sparks, MD, USA). 5×10^4 CT26 cells were seeded per upper chambers in serum-free RPMI1640 whereas the lower chambers were loaded with RPMI1640 containing 5% FBS. After 48 hours, the non-migrating cells on the upper chambers were removed by a cotton swab, and cells invaded through the matrigel layer to the underside of the membrane were stained with a 0.1% crystal violet solution and counted manually in eight random microscopic fields.

For colony formation assays, control and miRNA inhibitor or LV-miR-shRNA (Supplemental Materials and Methods section, Supplementary Information) transfected SW480 cells were seeded on six-well plates and maintained in DMEM containing 10% FBS for 2 weeks. Cells were fixed with methanol and stained with 0.5% crystal violet in 50% methanol for 1 hour and colonies larger than 100 μm in diameter were counted.

Luciferase reporter assays and IAP enzyme activity assays. Luciferase reporter activities were determined using a Luciferase Reporter Gene Assay System (Promega, Madison, WI, USA) as instructed. For all luciferase assays, β-galactosidase activities were determined to calibrate the transfection efficiency. The calibrated value for a proper control was used to normalize all other values to obtain the normalized relative luciferase units (RLU) representing the activities of 3'UTRs.

The enzyme activity of IAP was measured by an IAP kit (Jiancheng, Nanjing, China) according to the manufacturer's instructions. Protein concentration was measured by the Pierce BCA kit (Pierce Biotechnology, Rockford, USA).

Bioluminescence imaging of tumor growth in live animals. Briefly, CT26 cells were transfected with a luciferase-overexpressing plasmid or its control vector (pLV-luc or pLV-EF1a-MCS-IRES-Puro). Stable clones of cells overexpressing luciferase were selected with the addition of 8-10 μg/ml puromycin in the media for 3 weeks (Invitrogen, Carlsbad, CA, USA). Luciferase-overexpressing cells or its controls were subsequently injected into the nude mice intraperitoneally (5×10^5 cells/mouse). Starting from the third day after CT26 cell inoculation, each mouse was injected with 2×10^7 transducing units of control lentiviruses or lentiviruses carrying shRNA for miR-574-5p once a week for 2 weeks. Three days after lentiviral injection, the mice were subjected to bioluminescence imaging under an IVIS Lunina II *in vivo* imaging system

(Xenogen, Hopkinton, MA, USA) as described by Lan et al. [38] every other three days. Ten minutes prior to imaging, each mouse was injected with 100 ul D-luciferin solution (15 mg/ml in PBS, Promega #E1602) by i.p. injection. Immediately before imaging taking, the experimental mice were anesthetized using an XGI-8 Gas Anesthesia System (Xenogen). Images and amount of bioluminescent signals were analyzed using Living Image software (Xenogen).

Serum miRNA preparations and analyses. Total RNA from serum was extracted using a miRVana miRNA isolation kit (Ambion, Austin, TX, USA) according to the manufacturer's protocol. RNA was eluted in nuclease free water at 95°C. Five microliters of total RNA was reverse transcribed using the ReverTra Ace-α-® Kit as instructed (TOYOBO, Shanghai) and miRNA-specific stem-loop primersas shown in the Materials and Mathods section. has-miR-16-5p served as an internal control. Visible and dissectable peritoneal tumors were dissected and weighted.

Bioinformatics, data acquisition, image processing and statistical analyses. Mature and pre-miRNA sequences were based on miRBase (microrna.sanger.ac.uk). miRNA target predictions were performed with the miRanda (www.microrna.org) algorithm. Western blot images were captured by Biosense SC8108 Gel Documentation System with GeneScope V1.73 software (Shanghai BioTech, Shanghai, China). Gel images were imported into Photoshop for orientation and cropping. The digital density values were acquired by Image-Pro Plus software (Media Cybernetics) and analyzed by Graphpad Prism 5.0. Data are the means ± SEM. One-way ANOVA with Bonferonni's post-test was used for multiple comparisons and the Student's *t*-test (two-tailed) for pair-wise comparisons. The correlation analyses were performed with Pearson's test.

List of primers used for the construction of miRNA or Qki overexpression plasmids

Plasmid	Primer sequence (from 5'→3')	Gene ID	Amplicon (bp)
pFlag-mQki5 (mouse)	Forward:CCCAAGCTTATGGTCGGGGAAATGGAAAC Reverse:CCGGAATTCTTAGTTGCCGGTGGCGGCTC	NM_001159517 (Genbank)	1026
pFlag-mQki6 (mouse)	Forward:CCCAAGCTTATGGTCGGGGAAATGGAAAC Reverse:CCGGAATTCTTAGCCTTTCGTTGGGAAAG	NM_001159516 (Genbank)	960
pFlag-mQki7 (mouse)	Forward:CCCAAGCTTATGGTCGGGGAAATGGAAAC Reverse:CCGGAATTCTCAATGGGCTGAAATATCAG	NM_021881 (Genbank)	978
pmiR-574 (mouse)	Forward: CCCAAGCTTTGTCCGCTGTAGGGTGTGAGAA Reverse: TGCTCTAGAATCAGGATGGAGGTCAAGGCCT	MI0005518 (miRBase)	416
phsa-miR-574 (human)	Forward： CCCAAGCTTCCTCTGCGTTAGTGAGAAGCAG Reverse： GCGGGATCCTCTGTCTTACAGGGACCTGCTC	MI0003581 (miRBase)	345

List of primers used for the construction of six luciferase reporters.

Plasmid	Primer sequence (from 5'→3')	Gene ID	Amplicon length and location
pmQki5-3'UTR-luc	Forward: TGCGCTAGCTATGACCTTCTGACCTCTGAACTCT Reverse: ACTGGCCGGCCTATGGGTTAATAGAAACAGCAAAGA	*mQki5* NM_001159517	(NTs 1517-4540) 3024 bp
pmQki7-3'UTR-luc	Forward: TGCGCTAGCCTTGCTGGATGAAGGACTAGA Reverse: ACTGGCCGGCCTTGGCCTCATGATACAAAGCAATAC	*mQki7* NM_021881	(NTs 1467-6652) 5186 bp
pWT-miR574-5p-MRE-luc	Forward: TGCTCTAGACTTTGTTAAGTAATCCACACTC Reverse: ACTGGCCGGCCAACGGTTGTCCCATAGTCTTAA	*mQki7* NM_021881	(NTs 5650-5750) 101bp
pMT-miR574-5p-MRE-luc	Forward: TGCTCTAGACTTTGTTAAGTAATCCGCACGC Reverse: ACTGGCCGGCCAACGGTTGTCCCATAGTCTTAA	*mQki7* NM_021881	(NTs 5650-5750) 101 bp
pmCnnb1-3'UTR-luc	Forward: TGATCTAGAAAGACTTGGTAGGGTGGGAATGG Reverse: ACTGGCCGGCCGCAGGTTACAACAACTTTGGGAT	Mouse β-catenin NM_001904	(NTs 2707-3557) 850 bp
pLV-luc	Forward: AGAGAATTCGGATCCATGGAAGACGCCAAAAACATAA Reverse: CCATGGCTCGAGCCCTTACACGGCGATCTTTCCG	pGL3 (Promega)	1365 bp

List of miR-mimics, anti-miRs, lentiviral miR-shRNAs and LNA-probes for miRNA in situ hybridization.

Name	Sequence or target (5'→3')	Catalog #	Supplier
mimics-ctrl	Scrambled		GenePharma, Shanghai
miR-574-5p mimics	UGAGUGUGUGUGUGAGUGUGU ACACUCACACACACACACUCAUU		GenePharma, Shanghai
anti-miR-ctrl	Scrambled		GenePharma, Shanghai
anti-miR-574-5p	UGAGUGUGUGUGUGAGUGUGU	AM17000	Ambion
LV-miR-shRNA-ctrl	TTCTCCGAACGTGTCACGT	pLVT4	Sunbio, Shanghai
LV-miR-574-5p-shRNA	ACACACTCACACACACACACTCA	pLVT278	Sunbio, Shanghai
Scrambled miRNA	GTGTAACACGTCTATACGCCCA/3Dig	99004-05	Exiqon, Copenhagen
U6 probe	CACGAATTTGCGTGTCATCCTT/3Dig	99002-05	Exiqon, Copenhagen
hsa-miR-574-5p probe	ACACACTCACACACACACACTCA//3Dig	38674-05	Exiqon, Copenhagen

List of primers used for qPCR analyses of mRNAs.

Organism	Gene	Gene ID	Primer sequence (5'→3')	Amplicon (bp)
Human	pan-*Qki*	NM_006775 NM_206853 NM_206854 NM_206855	Forward:CATCAGCTGCATCTTCTTCAG Reverse:CACTGTGGAAGATGCTCAGAA	121
	Qki5	NM_006775	Forward:GCCCTACCATAATGCCTTTGA Reverse:AACTTTAGTAGCCACCGCAACC	211
	Qki6	NM_206853	Forward:GCCCGAAGCTGGTTTAATCTATA Reverse:TCGTTGGGAAAGCCATACCTAAT	118
	Qki7	NM_206854	Forward:GCTGGTTTAATCTATACACCCTATGA Reverse:GACTGGCATTTCAATCCACTCTA	113
	Qki7b	NM_206855	Forward:AATGCCTTTGATCAGACAAATACAG Reverse:TGGGGAGAAGAACTTACCTAATACA	198
	β-catenin	NM_001904	Forward:AGCCACAAGATTACAAGAAACGG Reverse:ATCCACCAGAGTGAAAAGAACGA	173
	$p27^{Kip1}$	NM_004064	Forward:GGGGCTCCGGCTAACTCTGA Reverse:AGGCTTCTTGGGCGTCTGCT	215
	18S rRNA	NR_003286.2	Forward:CGACGACCCATTCGAACGTCT Reverse:CTCTCCGGAATCGAACCCTGA	102
Mouse	pan-*Qki*	NM_001159517 NM_001159516 NM_021881	Forward:TAGAGGACTTACAGCTAAACAACT Reverse:ATTCAGAATTGCAAGCTCCATCA	288
	Qki5	NM_001159517	Forward:GCCCTACCATAATGCCTTTGA Reverse:AACTTTAGTAGCCACCGCAACC	211
	Qki6	NM_001159516	Forward:GCCTGAAGCTGGGTTAATCTACA Reverse:TCGTTGGGAAAGCCATACCTAAC	118
	Qki7	NM_021881	Forward:GCTGGGTTAATCTACACACCCTATGA Reverse:GACTGGCATTTCAATCCACTCTA	113
	β-catenin	NM_007614	Forward:TGGACCCCAAGCCTTAGTAAACA Reverse:GTCTGTCAGATGAAGCCCCAGTG	159

	Lactase	NM_001081078	Forward:GAGACCCAGAACTCAATGACACC Reverse:GGTCAGAGCGGTTCACAAAGT	165
	p27^{Kip1}	NM_009875	Forward:GCGGTGCCTTTAATTGGGTCT Reverse:TCTTGGGCGTCTGCTCCACA	225
	Col3a1	NM_009930	Forward:GTTTCTTCTCACCCTTCTTCATCCC Reverse:GCAGTCTAGTGGCTCCTCATCACA G	196
	Noxp20	NM_026667	Forward:AGGGAGACACCGGATCTGAAATA Reverse:GAATTGGCAGTGTGGATTCGTAG	199
	Sox2	NM_011443	Forward: GCGGAGTGGAAACTTTTGTCC Reverse: GGGAAGCGTGTACTTATCCTTCT	156

List of conventional or LNA-primers for qPCR analyses of U6 and miRNAs.

RNA or miRNA	Genbank or miRBase seq#	Primer sequence (5'→3')
Mouse and human U6	NR_004394.1	Reverse transcription: CGCTTCACGAATTTGCGTGTCAT Forward: GCTTCGGCAGCACATATACTAAAAT Reverse: CGCTTCACGAATTTGCGTGTCAT (LNA)
hsa-miR-16-5p	MI0000070	Reverse transcription: GTCGTATCCAGTGCGTGTCGTGGAGTCGGCAATTGCA CTGGATACGACTCGCCAA Forward: GGGGTAGCAGCACGTAAA Reverse: TGCGTGTCGTGGAGTC (LNA)
mmu-miR-574-5p	MI0005518	Reverse transcription: GTCGTATCCAGTGCGTGTCGTGGAGTCGGCAATTGC ACTGGATACGACTACACAC Forward: GGGGTGAGTGTGTGTGTG Reverse: TGCGTGTCGTGGAGTC (LNA)
hsa-miR-574-5p	MI0003581	Reverse transcription: GTCGTATCCAGTGCGTGTCGTGGAGTCGGCAATTGC ACTGGATACGACTACACAC Forward： GGGGTGAGTGTGTGTGTG Reverse： TGCGTGTCGTGGAGTC (LNA)
mmu-miR-200b	MI0000243	See Huang et al. [37]
mmu-miR-717	MI0004704	See Huang et al. [37]
mmu-miR-466g	MI0005510	Reverse transcription: GTCGTATCCAGTGCGTGTCGTGGAGTCGGCAATTGC ACTGGATACGACTGTGTGT Forward： GGGGATACAGACACATGC Reverse：TGCGTGTCGTGGAGTC (LNA)
mmu-miR-17	MI0000687	Reverse transcription: GTCGTATCCAGTGCGTGTCGTGGAGTCGGCAATTGC ACTGGATACGACTCTACCT Forward：GGGGCAAAGTGCTTACAG Reverse：TGCGTGTCGTGGAGTC (LNA)
mmu-miR-20a	MI0000568	Reverse transcription: GTCGTATCCAGTGCGTGTCGTGGAGTCGGCAATTGC ACTGGATACGACTCTACCT

	Forward：GGGGTAAAGTGCTTATAG
	Reverse：TGCGTGTCGTGGAGTC (LNA)

3. SUPPLEMENTAL REFERENCES

1 Bockbrader K, Feng Y. Essential function, sophisticated regulation and pathological impact of the selective RNA-binding protein QKI in CNS myelin development. *Future Neurol* 2008;**3**(6):655-68.

2 Klempan TA, Ernst C, Deleva V *et al*. Characterization of QKI gene expression, genetics, and epigenetics in suicide victims with major depressive disorder. *Biol Psychiatry* 2009;**66**(9):824-31.

3 Li ZZ, Kondo T, Murata T *et al*. Expression of Hqk encoding a KH RNA binding protein is altered in human glioma. *Jpn J Cancer Res* 2002;**93**(2):167-77.

4 Yang G, Fu H, Zhang J *et al*. RNA-binding protein quaking, a critical regulator of colon epithelial differentiation and a suppressor of colon cancer. *Gastroenterology* 2010;**138**(1):231-40.

5 Meyers-Needham M, Ponnusamy S, Gencer S *et al*. Concerted functions of HDAC1 and microRNA-574-5p repress alternatively spliced ceramide synthase 1 expression in human cancer cells. *EMBO Mol Med* 2011.

6 Novikov L, Park JW, Chen H *et al*. QKI-mediated alternative splicing of the histone variant MacroH2A1 regulates cancer cell proliferation. *Mol Cell Biol* 2011;**31**(20):4244-55.

7 Takahashi K, Tanabe K, Ohnuki M *et al*. Induction of pluripotent stem cells from adult human fibroblasts by defined factors. *Cell* 2007;**131**(5):861-72.

8 Takahashi K, Yamanaka S. Induction of pluripotent stem cells from mouse embryonic and adult fibroblast cultures by defined factors. *Cell* 2006;**126**(4):663-76.

9 Yu J, Vodyanik MA, Smuga-Otto K *et al*. Induced pluripotent stem cell lines derived from human somatic cells. *Science* 2007;**318**(5858):1917-20.

10 Ferri AL, Cavallaro M, Braida D *et al*. Sox2 deficiency causes neurodegeneration and impaired neurogenesis in the adult mouse brain. *Development* 2004;**131**(15):3805-19.

11 Archer TC, Jin J, Casey ES. Interaction of Sox1, Sox2, Sox3 and Oct4 during primary neurogenesis. *Dev Biol* 2011;**350**(2):429-40.

12 Episkopou V. SOX2 functions in adult neural stem cells. *Trends Neurosci* 2005;**28**(5):219-21.

13 Bylund M, Andersson E, Novitch BG *et al*. Vertebrate neurogenesis is counteracted by Sox1-3 activity. *Nat Neurosci* 2003;**6**(11):1162-8.

14 Saigusa S, Tanaka K, Toiyama Y *et al*. Correlation of CD133, OCT4, and SOX2 in rectal cancer and their association with distant recurrence after chemoradiotherapy. *Ann Surg Oncol* 2009;**16**(12):3488-98.

15 Fang X, Yu W, Li L *et al*. ChIP-seq and functional analysis of the SOX2 gene in colorectal cancers. *OMICS* 2010;**14**(4):369-84.

16 Wang Q, He W, Lu C *et al*. Oct3/4 and Sox2 are significantly associated with an unfavorable clinical outcome in human esophageal squamous cell carcinoma. *Anticancer Res* 2009;**29**(4):1233-41.

17 Sanada Y, Yoshida K, Ohara M *et al*. Histopathologic evaluation of stepwise progression of pancreatic carcinoma with immunohistochemical analysis of gastric epithelial transcription factor SOX2: comparison of expression patterns between invasive components and cancerous or nonneoplastic intraductal components. *Pancreas* 2006;**32**(2):164-70.

18 Fang X, Yoon JG, Li L *et al*. The SOX2 response program in glioblastoma multiforme: an integrated ChIP-seq, expression microarray, and microRNA analysis. *BMC Genomics* 2011;**12**:11.

19 Sholl LM, Barletta JA, Yeap BY *et al*. Sox2 protein expression is an independent poor prognostic indicator in stage I lung adenocarcinoma. *Am J Surg Pathol* 2010;**34**(8):1193-8.

20 Foss KM, Sima C, Ugolini D *et al*. miR-1254 and miR-574-5p: Serum-Based microRNA Biomarkers for Early-Stage Non-small Cell Lung Cancer. *J Thorac Oncol* 2011;**6**(3):482-8.

21 Ranade AR, Cherba D, Sridhar S *et al*. MicroRNA 92a-2*: a biomarker predictive for chemoresistance and prognostic for survival in patients with small cell lung cancer. *J Thorac Oncol* 2010;**5**(8):1273-8.

22 Liu H, Liu R, Su Y *et al*. [A pilot study of differentially expressed microRNAs between esophageal squamous cell carcinoma and adjacent tissues in Huai'an population]. *Carcinogenesis,Teratogenesis & Mutagenesis (Chinese)* 2010;**22**(6):418-22.

23 Mao ZG, He DS, Zhou J *et al*. Differential expression of microRNAs in GH-secreting pituitary adenomas. *Diagn Pathol* 2010;**5**:79.

24 Zhao S, Wang Y, Liang Y *et al*. MicroRNA-126 regulates DNA methylation in CD4+ T cells and contributes to systemic lupus erythematosus by targeting DNA methyltransferase 1. *Arthritis Rheum* 2011;**63**(5):1376-86.

25 Ali S, Almhanna K, Chen W *et al*. Differentially expressed miRNAs in the plasma may provide a molecular signature for aggressive pancreatic cancer. *Am J Transl Res* 2010;**3**(1):28-47.

26 Malumbres R, Sarosiek KA, Cubedo E *et al*. Differentiation stage-specific expression of microRNAs in B lymphocytes and diffuse large B-cell lymphomas. *Blood* 2009;**113**(16):3754-64.

27 Bostjancic E, Zidar N, Glavac D. MicroRNA microarray expression profiling in human myocardial infarction. *Dis Markers* 2009;**27**(6):255-68.

28 Wang WX, Huang Q, Hu Y *et al*. Patterns of microRNA expression in normal and early Alzheimer's disease human temporal cortex: white matter versus gray matter. *Acta Neuropathol* 2011;**121**(2):193-205.

29 Moreau MP. Altered microRNA regulatory networks in individuals with schizophrenia. Rutgers, The State University of New Jersey and The Graduate School of Biomedical Sciences University of Medicine and Dentistry of New Jersey, 2009.

30 Xiao J, Liang D, Zhang Y *et al*. MicroRNA expression signature in atrial fibrillation with mitral stenosis. *Physiol Genomics* 2011;**43**(11):655-64.

31 Eitan R, Kushnir M, Lithwick-Yanai G *et al*. Tumor microRNA expression patterns associated with resistance to platinum based chemotherapy and survival in ovarian cancer patients. *Gynecol Oncol* 2009;**114**(2):253-9.

32 Hou J, Wang P, Lin L *et al*. MicroRNA-146a feedback inhibits RIG-I-dependent Type I IFN production in macrophages by targeting TRAF6, IRAK1, and IRAK2. *J Immunol* 2009;**183**(3):2150-8.

33 Garbacki N, Di VE, Huynh-Thu VA *et al*. MicroRNAs Profiling in Murine Models of Acute and Chronic Asthma: A Relationship with mRNAs Targets. *PLoS One* 2011;**6**(1):e16509.

34 Mallick B, Ghosh Z, Chakrabarti J. MicroRNome analysis unravels the molecular basis of SARS infection in bronchoalveolar stem cells. *PLoS One* 2009;**4**(11):e7837.

35 Wang K, Zhang S, Marzolf B *et al*. Circulating microRNAs, potential biomarkers for drug-induced liver

injury. *Proc Natl Acad Sci U S A* 2009;**106**(11):4402-7.

36 Hu SJ, Ren G, Liu JL *et al*. MicroRNA expression and regulation in mouse uterus during embryo implantation. *J Biol Chem* 2008;**283**(34):23473-84.

37 Huang W, Liu H, Wang T *et al*. Tonicity-responsive microRNAs contribute to the maximal induction of osmoregulatory transcription factor OREBP in response to high-NaCl hypertonicity. *Nucleic Acids Res* 2011;**39**(2):475-85.

38 Lan KL, Yen SH, Liu RS *et al*. Mutant Bik gene transferred by cationic liposome inhibits peritoneal disseminated murine colon cancer. *Clin Exp Metastasis* 2007;**24**(6):461-70.